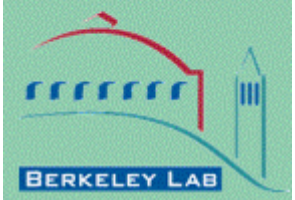

ERNEST ORLANDO LAWRENCE
BERKELEY NATIONAL LABORATORY

LBNL 4746E

Using Cool Roofs to Reduce Energy Use, Greenhouse Gas Emissions, and Urban Heat-island Effects: Findings from an India Experiment

Hashem Akbari, Tengfang Xu, Haider Taha, Craig Wray, and Jayant Sathaye

Environmental Energy Technologies Division
Lawrence Berkeley National Laboratory (LBNL)
Berkeley, CA 94720

Vishal Garg, Surekha Tetali, M. Hari Babu and K. Niranjan Reddy

International Institute for Information Technology (IIIT)
Hyderabad, India

May 2011

This work was supported by the U.S. Agency for International Development, through the U.S. Department of Energy under Contract No. DE-AC02-05CH11231.

ABSTRACT

Cool roofs, cool pavements, and urban vegetation reduce energy use in buildings, lower local air pollutant concentrations, and decrease greenhouse gas emissions from urban areas. This report summarizes the results of a detailed monitoring project in India and related simulations of meteorology and air quality in three developing countries. The field results quantified direct energy savings from installation of cool roofs on individual commercial buildings. The measured annual energy savings potential from roof-whitening of previously black roofs ranged from 20 – 22 kWh/m^2 of roof area, corresponding to an air-conditioning energy use reduction of 14 – 26% in commercial buildings. The study estimated that typical annual savings of 13 – 14 kWh/m^2 of roof area could be achieved by applying white coating to uncoated concrete roofs on commercial buildings in the Metropolitan Hyderabad region, corresponding to cooling energy savings of 10 – 19%.

With the assumption of an annual increase of 100,000 square meters of new roof construction for the next 10 years in the Metropolitan Hyderabad region, the annual cooling energy savings due to whitening concrete roof would be 13 -14 GWh of electricity in year ten alone, with cumulative 10-year cooling energy savings of 73 – 79 GWh for the region. The estimated savings for the entire country would be at least 10 times the savings in Hyderabad, i.e., more than 730 – 790 GWh. We estimated that annual direct CO_2 reduction associated with reduced energy use would be 11 – 12 kg CO_2/m^2 of flat concrete roof area whitened, and the cumulative 10-year CO_2 reduction would be approximately 0.60 – 0.65 million tons in India. With the price of electricity estimated at seven Rupees per kWh, the annual electricity savings on air-conditioning would be approximately 93 – 101 Rupees per m^2 of roof. This would translate into annual national savings of approximately one billion Rupees in year ten, and cumulative 10-year savings of over five billion Rupees for cooling energy in India.

Meteorological simulations in this study indicated that a reduction of 2°C in air temperature in the Hyderabad area would be likely if a combination of increased surface albedo and vegetative cover are used as urban heat-island control strategies. In addition, air-temperature reductions on the order of 2.5 – 3.5°C could be achieved if moderate and aggressive heat-island mitigation measures are adopted, respectively. A large-scale deployment of mitigation measures can bring additional indirect benefit to the urban area. For example, cooling outside air can improve the efficiency of cooling systems, reduce smog and greenhouse gas (GHG) emissions, and indirectly reduce pollution from power plants — all improving environmental health quality.

This study has demonstrated the effectiveness of cool-roof technology as one of the urban heat-island control strategies for the Indian industrial and scientific communities and has provided an estimate of the national energy savings potential of cool roofs in India. These outcomes can be used for developing cool-roof building standards and related policies in India. Additional field studies, built upon the successes and lessons learned from this project, may be helpful to further confirm the scale of potential energy savings from the application of cooler roofs in various regions of India. In the future, a more rigorous meteorological simulation using urbanized (meso-urban) meteorological models should be conducted, which may produce a more accurate estimate of the air-temperature reductions for the entire urban area.

Key Words: Urban heat island, mitigation measure, cool roof, cool pavement, vegetation, energy savings, urban environmental impact, India.

Please use the following citation for this report

Akbari, Hashem, Tengfang Xu, Haider Taha, Craig Wray, Jayant Sathaye, Vishal Garg, Surekha Tetali, M. Hari Babu, and K. Niranjan Reddy, 2011. Using Cool Roofs to Reduce Energy Use, Greenhouse Gas Emissions, and Urban Heat-island Effects: Findings from an India Experiment. Lawrence Berkeley National Laboratory Report.

TABLE OF CONTENTS

ABSTRACT i
TABLE OF CONTENTS iii
TABLE OF FIGURES iii
TABLE OF TABLES v
EXECUTIVE SUMMARY 1
1 Introduction 2
2 Project Goals and Tasks 3
3 Methodologies 3
4 Field Study of Cool-Roof Effects in India 4
4.1 Demonstration site selection 4
4.2 Monitoring plan and instrumentation 5
4.3 Pre- and post-coating monitoring 6
4.4 Pre- and post-coating comparisons 7
4.5 Comparative analysis to quantify energy savings from cool roofs 9
5 Discussion and Estimate of Energy Savings and GHG Reduction 13
6 Meteorological Simulations 14
7 Outreach and Training 15
8 Conclusions 15
9 References 16
Attachment 1. Demonstration Site Selection 18
Attachment 2. Field Measurement Details 24
A2.1Buildings and Systems Characteristics 24
A2.2 Measurement Equipment 24
2.2.1. Data Logger and Communication 25
2.2.2. Air Temperatures 26
2.2.3. Surface Temperature 27
2.2.4. Outdoor Air Relative Humidity 27
2.2.5. Horizontal Insolation 27
2.2.6. Roof Heat Fluxes 27
2.2.7. Electric Power Consumption 28
A2.3 Data Collection and Analysis 28
A2.4 Field Measurement Results 29
2.4.1. Temperature data 29
2.4.2. Heat flux data 45
2.4.3 Energy Use 58
Attachment 3. Meteorological Simulations for Hyderabad, India 70
Attachment 4. Summary of Training Materials 77

TABLE OF FIGURES

Figure 1. Methodology for energy, air-quality, and GHG analysis 4
Figure 2. Installation of white coating on the concrete roof 7
Figure 3. Pre- and post-coating comparison of air-conditioning energy usage for both buildings (three phases). 10

Figure 4. Hourly plots of West Building roof surface temperature, under-roof temperature, plenum temperature, heat flux, and air conditioning electricity use for a few days before and after installing cool roofs. 12
Figure 5. West building, Location 1, hourly temperature. Concrete to White. 30
Figure 6. West building, Location 2, hourly temperature. Concrete to White. 31
Figure 7. East building, Location 1, hourly temperature. Concrete to Black. 32
Figure 8. East building, Location 2, hourly temperature. Concrete to Black. 33
Figure 9. East building, Location 1, hourly temperature. Black to White. 34
Figure 10. East building, Location 2, hourly temperature. Black to White. 35
Figure 11. West building, Location 1, Daily temperature. Concrete to White. 37
Figure 12. West building, Location 2, Daily temperature. Concrete to White. 38
Figure 13. East building, Location 1, daily temperature. Concrete to Black. 39
Figure 14. East building, Location 2, daily temperature. Concrete to Black. 40
Figure 15. East building, Location 1, daily temperature. Black to White. 41
Figure 16. East building, Location 2, daily temperature. Black to White. 42
Figure 17. Comparison of hourly temperatures for East and West buildings. 43
Figure 18. Comparison of daily temperatures for East and West buildings. 44
Figure 19. Comparison of average hourly and daily temperatures for East and West buildings. 45
Figure 20. West building, Hourly heat flux. Concrete to White. 46
Figure 21. East building, Hourly heat flux. Concrete to Black 46
Figure 22. East building, Hourly heat flux. Black to White. 47
Figure 23. West building, Daily heat flux. Concrete to White. 48
Figure 24. East building, Daily heat flux. Concrete to Black. 48
Figure 25. East building, Daily heat flux. Black to White 49
Figure 26. Comparison of roof heat flux for East and West buildings. 49
Figure 27. Roof heat flux vs. outside air temperature for the East building. (a) Hours 8-19. 50
Figure 28. Roof heat flux vs. outside air temperature for the East building. (b) Hours 1-7 and 20-24. 51
Figure 29. Roof heat flux vs. (Outside air - inside air) temperature for the East building. (a) Hours 8-19. 52
Figure 30. Roof heat flux vs. (Outside air - inside air) temperature for the East building. (b) Hours 1-7 and 20-24. 53
Figure 31. Roof heat flux vs. outside air temperature for the West building. (a) Hours 8-19. 54
Figure 32. Roof heat flux vs. outside air temperature for the West building. (b) Hours 1-7 and 20-24. 55
Figure 33. Roof heat flux vs. (Outside air - inside air) temperature for the West building. (a) Hours 8-19. 56
Figure 34. Roof heat flux vs. (Outside air - inside air) temperature for the West building. (b) Hours 1-7 and 20-24. 57
Figure 35. Daily roof heat flux vs. outside air temperature for the East building. 58
Figure 36. Daily roof heat flux vs. outside air temperature for the West building. 59
Figure 37. Daily roof heat flux vs. (outside air – inside air) temperature for the East building. 59
Figure 38. Daily roof heat flux vs. (outside air – inside air) temperature for the West building. 60
Figure 39. Hourly and daily heat flux for the East and West building vs. the outside temperature and the difference between the outside and inside temperatures. 61

Figure 40. Hourly time series of air conditioning and non-conditioning electricity use for the West building going from concrete roof to white roof. 62
Figure 41. Hourly time series of air conditioning and non-conditioning electricity use for the East building (a) going from concrete roof to black roof, (b) going from black roof to white roof. 63
Figure 42. Daily time series of air conditioning and non-conditioning electricity use for the West building going from concrete roof to white roof. 64
Figure 43. Hourly time series of air conditioning and non-conditioning electricity use for the East building (a) going from concrete roof to black roof, (b) going from black roof to white roof. 65
Figure 44. East hourly AC use vs. Tout 66
Figure 45. West hourly AC use vs. Tout 67
Figure 46. East hourly AC use vs. Tout – Tin 68
Figure 47. West hourly AC use vs. Tout – Tin 69
Figure 48. Left: 1-km (fourth) MM5 domain with the earthPRO analysis sub-domain shown with a blue rectangle. Right: an example detail from earthPRO data for Hyderabad (the thick white line is 1 km). 71
Figure 49. Sub-domain (dimensions: EW = 35 km, NS = 30 km) for 1-km LULC and surface characterization. 71
Figure 50. Base-case albedo (left) and soil moisture (right) on the 1-km MM5 grid. These fields were developed by meshing results from the earthPRO analysis with the background default MM5 LULC and properties input. 72
Figure 51. Urban air temperature in south Hyderabad on 2 days of three episodes. Results based on 1-km simulations. 74
Figure 52. Temperature difference from base case for case11 and case22 for episode 1 75
Figure 53. Temperature difference from base case for case11 and case22 for episode 2 75
Figure 54. Temperature difference from base case for case11 and case22 for episode3 75

TABLE OF TABLES

Table 1. Monitoring periods and roof conditions. 7
Table 2. Monitoring results for the west and east buildings in the Satyam Learning Center. 8
Table 3. Summary: Candidate study countries and criteria for evaluation 20
Table 4. Estimated energy savings due to cool roofs for the median climate in Brazil, India, and Mexico 21
Table 5. Estimates of Annual Cooling Energy Savings for Office Buildings in India. 22
Table 6. Measurement point summary 25
Table 7. Power meter assignments and scale factors. 28
Table 8. Monitoring periods and roof conditions. 29
Table 9. Assumed levels of albedo increase per surface type 73
Table 10. Scenarios for vegetation cover increase 73
Table 11. New values of surface albedo and soil moisture for perturbation scenarios 73
Table 12. Degree-hours (DH/48hours) resulting from heat island control 76

EXECUTIVE SUMMARY

Cool roofs, cool pavements, and urban vegetation reduce energy use in buildings, lower local air pollutant concentrations, and decrease greenhouse gas emissions from urban areas. This report summarizes the results of a detailed monitoring project in India and related simulations of meteorology and air quality in three developing countries. The field results quantified direct energy savings from installation of cool roofs on individual commercial buildings. The measured annual energy savings potential from roof-whitening of previously black roofs ranged from 20 – 22 kWh/m^2 of roof area, corresponding to an air-conditioning energy use reduction of 14 – 26% in commercial buildings. The study estimated that typical annual savings of 13 – 14 kWh/m^2 of roof area could be achieved by applying white coating to uncoated concrete roofs on commercial buildings in the Metropolitan Hyderabad region, corresponding to cooling energy savings of 10 – 19%.

With the assumption of an annual increase of 100,000 square meters of new roof construction for the next 10 years in the Metropolitan Hyderabad region, the annual cooling energy savings due to whitening concrete roof would be 13 -14 GWh of electricity in year ten alone, with cumulative 10-year cooling energy savings of 73 – 79 GWh for the region. The estimated savings for the entire country would be at least 10 times the savings in Hyderabad, i.e., more than 730 – 790 GWh. We estimated that annual direct CO_2 reduction associated with reduced energy use would be 11 – 12 kg CO_2/m^2 of flat concrete roof area whitened, and the cumulative 10-year CO_2 reduction would be approximately 0.60 – 0.65 million tons in India. With the price of electricity estimated at seven Rupees per kWh, the annual electricity savings on air-conditioning would be approximately 93 – 101 Rupees per m^2 of roof. This would translate into annual national savings of approximately one billion Rupees in year ten, and cumulative 10-year savings of over five billion Rupees for cooling energy in India.

Meteorological simulations in this study indicated that a reduction of 2°C in air temperature in the Hyderabad area would be likely if a combination of increased surface albedo and vegetative cover are used as urban heat-island control strategies. In addition, air-temperature reductions on the order of 2.5 – 3.5°C could be achieved if moderate and aggressive heat-island mitigation measures are adopted, respectively. A large-scale deployment of mitigation measures can bring additional indirect benefit to the urban area. For example, cooling outside air can improve the efficiency of cooling systems, reduce smog and greenhouse gas (GHG) emissions, and indirectly reduce pollution from power plants — all improving environmental health quality.

This study has demonstrated the effectiveness of cool-roof technology as one of the urban heat-island control strategies for the Indian industrial and scientific communities and has provided an estimate of the national energy savings potential of cool roofs in India. These outcomes can be used for developing cool-roof building standards and related policies in India. Additional field studies, built upon the successes and lessons learned from this project, may be helpful to further confirm the scale of potential energy savings from the application of cooler roofs in various regions of India. In the future, a more rigorous meteorological simulation using urbanized (meso-urban) meteorological models should be conducted, which may produce a more accurate estimate of the air-temperature reductions for the entire urban area.

1 Introduction

Across the world, air temperatures in urban areas have increased faster than air temperatures in rural areas. For example, from 1930 to 1990, downtown Los Angeles recorded a growth of 0.5°C per decade (Akbari et al. 2001). It was estimated that an increase of 1°C would require the addition of about 500 megawatts (MW) for air conditioning for buildings in the Los Angeles Basin (Akbari et al. 2001). Similar increases are taxing the ability of developing countries to meet urban electricity demand while raising global GHG emissions. Local air pollution (e.g., particulates, volatile organic compounds, and nitrogen oxides that are precursors to ozone formation) are already a problem in most cities in developing countries. Higher temperatures mean increased ozone formation, with accompanying health impacts. Lawrence Berkeley National Laboratory (LBNL) conducted research on both the electricity costs and air pollution effects of higher air temperatures and devised methods to reduce both effects. In addition, LBNL has investigated tree-planting schemes and the use of reflective materials for building roofs and pavements to demonstrate potential cost-effective energy-use reductions of 10 – 40 %. Among energy-efficiency solutions, cool roofs and cool pavements are ideally suited to the hot climates that prevail in much of the developing world. Cool (e.g., light-colored) pavements also increase nighttime visibility and pavement durability.

When sunlight hits an opaque surface on the earth, a portion of the sunlight is reflected — the fraction known as the albedo — while the rest is absorbed by the surface. Low-albedo surfaces naturally become much hotter than high-albedo surfaces. High-albedo urban surfaces and tree planting are inexpensive measures that can reduce summertime air temperatures in urban areas. The effects of modifying the urban environment by planting trees and increasing albedo can be categorized as "direct" and "indirect" effects. The direct effects of planting trees around a building, or using reflective materials on roofs or walls, are to alter the energy balance and energy requirements for cooling that particular building. Direct effects bring immediate benefits to the building that applies them. Planting trees throughout a city would modify overall surface albedo and the energy balance of the entire city, producing a citywide reduction in air temperatures. Phenomena associated with citywide changes in local climate are referred to as indirect effects, because they indirectly affect the energy use in an individual building. Indirect effects or benefits become meaningful only with widespread deployment within a selected urban area. While direct effects are recognized and accounted for in current models of building-energy use, indirect effects are less understood or far less appreciated. Accounting for indirect effects is more difficult, and their quantifications are comparatively less certain. The goal of this research is to advance the understanding these effects and to incorporate them into accounts of energy use and air quality. Meanwhile, it is worth noting that the phenomenon of summer heat islands is an indirect effect of urbanization.

The issue of direct and indirect effects also enters into our discussion of atmospheric pollutants. Planting trees has the direct effect of reducing atmospheric CO_2, because each tree directly sequesters carbon from the atmosphere through photosynthesis. However, planting trees in cities also may have an indirect benefit in CO_2 reduction: By reducing the demand for cooling energy, urban trees indirectly reduce emission of CO_2 from power plants. Akbari et al. (1990) showed that the amount of CO_2 avoided via the indirect effect is considerably greater than the amount that is sequestered directly through photosynthesis. Similarly, trees directly trap ozone precursors by dry-deposition processes in which ozone is absorbed by tree leaves, and indirectly reduce the

emission of these precursors from power plants by reducing combustion of fossil fuels and reducing NO_x emissions from power plants (Taha 1996).

In order to promote the implementation of the mitigation measures for urban heat-island phenomenon in developing countries, there is a need to conduct evaluations on the effects of applying mitigation measures in developing countries and to document the outcomes, field experience, and lessons learned from such evaluations.

2 Project Goals and Tasks

The overarching goal of the project was to advance understanding of the benefits from extensive application of cool roofs, cool pavements, and tree planting in urban areas of developing countries. This was achieved through field evaluations, model simulations, and knowledge transfer. The project set out to document and demonstrate the benefits of heat-island mitigation measures in one selected developing country. The project enabled capacity building for continued monitoring after the end of the current cool-roof project.

The specific technical tasks were to:

- Perform analysis, develop selection criteria, and select a candidate country for cool-roof demonstration in buildings.
- Conduct field studies and develop comparative analyses to quantify and demonstrate the effect of cool roofs in reducing energy use in buildings.
- Perform meteorological simulations to estimate the effect of heat-island mitigation measures on urban climates (e.g., air-temperature reduction) in one selected region.
- Conduct outreach activities that include training programs, conference sessions, Web sites, and kiosks.

3 Methodologies

To advance our understanding of the benefits of applying mitigation measures for urban heat-islands in urban areas of developing countries, we performed analyses, field studies, and meteorological simulations. Our focus was on the potential benefits of lowering summertime urban air temperatures and reducing both energy use and GHGs. Figure 1 depicts the overall methodology used in analyzing the impact of heat-island mitigation measures on energy use and urban air pollution.

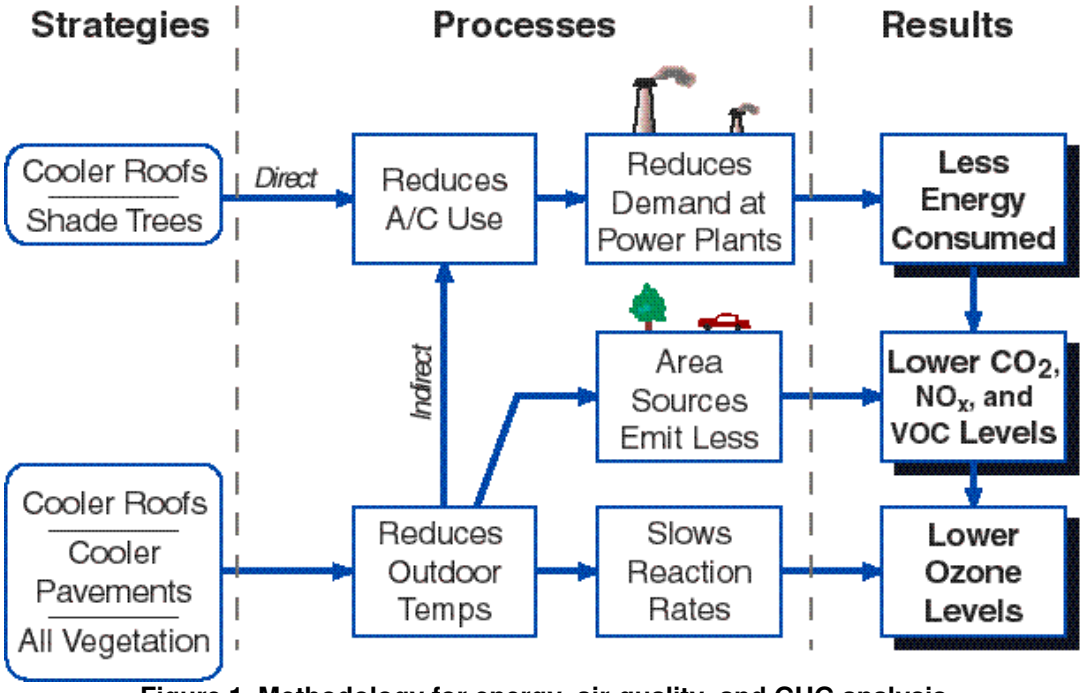

Figure 1. Methodology for energy, air-quality, and GHG analysis

For each of the technical tasks enlisted in the previous section, we have developed relevant technical approaches that were employed to accomplish them. Selected approaches used in the field investigations that quantified and demonstrated benefits of cool roofs on two commercial buildings are described here. Additional details about these approaches and results are included in the Attachment Section.

Capacity building and technology transfer have been cornerstones of the proposed project. LBNL provided training in the use of models and monitoring and measurement equipment. The Lab worked collaboratively with local stakeholders to develop a sustainable capacity to conduct both air-pollution modeling and cool-roofs demonstrations in selected countries. To the extent possible, LBNL built on existing U.S. Agency for International Development (USAID) climate change, energy efficiency, and urban development programs in India. Therefore, with resources available, we carried out the following relevant activities: (1) Laying out a process for the selection of cities/countries that would benefit from the use of heat-island-mitigation measures. (2) Developing an implementation approach to transfer this technology and knowledge to the selected countries.

4 Field Study of Cool-Roof Effects in India

In many previous experiments, LBNL has monitored the impact of reflective roofs on energy use of commercial and residential buildings in the United States. In this project, we emulated prior LBNL efforts by designing a field study to monitor and demonstrate the effect of cool roofs on two buildings at the Satyam Learning Center, in Hyderabad, India.

4.1 Demonstration site selection

With consultation with USAID's Global Climate Change team (GCC), three countries — Brazil, India, and Mexico — were initially selected as candidates for participation in the project. We

established the following key criteria for assessing the suitability of urban areas in the three countries for heat-island mitigation:

- Geographic site should have a hot summer climate; with available data on temperatures, air pollutant concentrations, and emissions sources; land use distribution maps; and available, ongoing, modeling work (e.g., on pollutant transport, climate change, urban air sheds, ozone, particulates) by local researchers.
- Buildings with operational air-conditioning systems to allow before- and after- roof retrofits that have potential for significant GHG-emissions reduction and availability to serve as a viable demonstration site.
- Preference to be given to the place where cooperation is appreciated among local governments, academic/research institutions, and industry and building associations.

We carried out a series of technical analyses and contacted various leads in order to select the focus country. The parameters used included (1) local climate, (2) potentials for electricity and GHG savings, (3) available data and resource capacity for climate simulations and local air-pollution modeling, (4) manufacturers as potential collaborators, and (5) government agencies and other institutions as partners. Details of the site selection are included in Attachment 1.

Based on the analyses of cooling degree-days, CO_2 and GHG emissions, and potential energy savings, LBNL recommended that the project be situated in India. Because of its high median temperature, cool roofs in India are expected to yield the highest electricity savings per unit of roof area for similar buildings. In addition, because of its high percentage of coal use for electricity generation, cool roofs are expected to yield the largest GHG reductions per kWh of electricity savings in India, compared with the other two countries. Based on the analysis and in consultation with local partners, we selected two similar buildings in Hyderabad for the buildings demonstration work.

4.2 Monitoring plan and instrumentation

For the selected buildings, LBNL developed a monitoring plan; specified monitoring equipment and sensors; purchased equipment; and commissioned and tested equipment in the lab before on-site installation. We specified data loggers capable of recording 30 single-ended 12-bit analog channels and five digital channels. The key parameters measured included indoor and outdoor air temperatures, outdoor air relative humidity, roof surface temperatures, roof heat fluxes, solar radiation, and electric power consumed by the building systems — including HVAC, UPS, and lighting systems.

In January 2006, we completed the installation and calibration of the monitoring system for both buildings. We also measured existing roof albedo; audited the buildings; and collected building and HVAC systems data. Researchers from IIIT accompanied LBNL during the installation of the monitoring system. We collaborated extensively with the local researchers and scientists for troubleshooting and maintenance of the equipment during the two-year period of the experiment. All sensors were continuously scanned, and averaged values were recorded every 30 seconds. Data were downloaded remotely via a modem about once a day. Out-of-range data were investigated to determine whether the sensors and monitoring equipment were functioning properly. Various research-grade sensors were used to measure indoor and outdoor air temperatures, outdoor-air relative humidity, roof surface temperatures, roof heat fluxes, solar

radiation, and electric power consumed by the HVAC, UPS, and lighting systems serving the test spaces.

In this report, we developed an analytical approach to evaluate the data gathered from the field and to quantify the direct cooling energy savings that resulted from installation of cooler roofs. Onsite measurement locations, sensor types, and detailed descriptions of the sensors and monitoring project can be found in Attachment 2, which also includes additional results on building and cool roof thermal performance.

4.3 Pre- and post-coating monitoring

Field monitoring of cool roof impacts included baseline characterization, applying various roof coatings, and post-coating characterizations. These tasks were carried out in sequence, with similar building occupancies and operation. The two adjacent buildings experienced the same weather conditions that were changing over the course of this study. Table 1 summarizes the coating installation, pre-retrofit monitoring (pre-coating), and post-retrofit monitoring (post-coating) in 2006. The instrumentation and data loggers were installed and commissioned in mid-January 2006.

For Phase I monitoring (i.e., from January to late March 2006), we monitored thermal environmental conditions for both buildings with the as-is roof exteriors (i.e., bare concrete roof with no coatings applied). For Phase II monitoring, we first applied coating to the roof to create a cool roof on the west building (white coating with an initial reflectivity of 0.80 and aged reflectivity of about 0.7) and a non-cool roof on the east building (black coating with an initial and aged reflectivity of 0.12). We then performed Phase II monitoring from late March 2006 through late July 2006. For Phase III monitoring, we applied the same white coating on the roof of the east building in July and continued monitoring for both buildings from August through December 2006.

Table 1. Monitoring periods and roof conditions.

Period	Dates	West Building Roof	East Building Roof
Monitoring Equipment Installation	01/13-01/15/2006	Monitoring equipment installed	Monitoring equipment installed*
Phase I Pre-coating Monitoring	01/16-03/22/2006	Concrete roof	Concrete roof
Phase II Coating Applied	03/23-03/26/2006	Applying white coating	Applying black coating
Phase II Post-coating Monitoring	03/27-07/22/2006	Cool white roof	Hot black roof
Phase III Additional Coating Applied	07/23-08/03/2006 3 August	No action	Applying white coating
Phase III - Post-coating Monitoring	08/04-12/16/2006	Cool white roof	Cool white roof

* Power meters for the two UPS systems in the east building were not installed until January 21, 2006

4.4 Pre- and post-coating comparisons

Figure 2 is a photo taken on the roof of the west building at the Satyam Learning Center (SLC). It illustrates the reflectance difference in roof surfaces before and after the white coating was applied to the roof. The solar reflectance of the original concrete roof without the coating was about 0.30. After installing three layers of a white coating, the initial solar reflectance of the new cool roof increased to 0.80, with aged solar reflectance of cool roof estimated as 0.70 for the west building.

Figure 2. Installation of white coating on the concrete roof

Table 2 is a comparison between the east and west buildings of performance metrics including roof surface temperatures, heat flux through ceiling, and air conditioning (AC) energy use. Results are compared before and after the white roof coating and black roof coating were applied to the west building and the east building, respectively.

For the west building, the maximum roof surface temperatures decreased from 54.7°C in Phase I to 41.2°C (a reduction of 13.5°C) in Phase II, after the white coating was applied to the original concrete roof; and further decreased to 38.3°C in Phase III, during which the white coating remained on the roof. For the east building, the maximum roof surface temperatures increased from 54.7°C in Phase I to 71.3°C in Phase II (an increase of 18.2°C), after the black coating was applied to the original concrete roof; and decreased to 39.6°C in Phase III after white coating was applied. In Phase III, after both roofs were painted white, the maximum roof temperatures of both roofs were similar.

For the west building, the peak heat flux through the ceiling decreased slightly from 12.8 W/m^2 in Phase I to 12.6 W/ m^2 in Phase II, after the white coating was applied to the original concrete roof, and further decreased to 7.6 W/m^2 in Phase III, during which the white coating remained on the roof. For the east building, the peak heat flux increased from 11.0 W/m^2 in Phase I to 21.9 W/m^2 in Phase II, after the black coating was applied to the original concrete roof, and decreased to 8.6 W/m^2 in in Phase III after the white coating was applied to the roof. In Phase III after both roofs were painted white, the peak heat flux through both roofs were again similar.

Table 2. Monitoring results for the west and east buildings in the Satyam Learning Center.

	West Building	East Building
Roof Area (m2)	700	700
Phase I - Initial roof reflectance	Concrete 0.30,	Concrete 0.30
Phase II - Modified roof reflectance	White 0.80 (fresh coating) 0.70 (aged coating)	Black 0.10
Phase III - Final roof reflectance	White 0.70	White 0.70
Phase I - Maximum roof surface temperature (°C)	54.7	54.7
Phase II - Maximum roof surface temperature (°C)	41.2	71.3
Phase III - Maximum roof surface temperature (°C)	38.3	39.6
Phase I - Peak roof heat flux (W/m^2)	12.8	11.0
Phase II - Peak roof heat flux (W/m^2)	12.6	21.9
Phase III - Peak roof heat flux (W/m^2)	7.6	8.6
Phase I – Average roof heat flux (W/m^2), 9AM to 5 PM	2.2	2.8
Phase II – Average roof heat flux (W/m^2), 9AM to 5 PM	3.6	9.7
Phase III – Average roof heat flux (W/m^2), 9AM to 5 PM	0.1	0.8
Phase I - Average daily AC use, (kWh/day), 9AM to 5 PM	219	200
Phase II - Average daily AC use (kWh/day), 9AM to 5 PM	285	280
Phase III – Average daily AC use (kWh/day), 9AM to 5 PM	215	187
Phase I – Average outdoor air temperature (°C) and solar radiation (W/m^2), 9AM to 5 PM	29.1°C, 653 W/m^2	
Phase II - Average outdoor air temperature (°C) and solar radiation (W/m^2), 9AM to 5 PM	32.4°C, 643 W/m^2	
Phase III - Average outdoor air temperature (°C) and solar radiation (W/m^2), 9AM to 5 PM	27.2°C, 529 W/m^2	

For the average heat flux between 9 a.m. and 5 p.m. in Phases I and III, both buildings exhibited similar magnitudes, with lower values happening in Phase III — during which the average outdoor air temperatures and solar radiation were lower. In Phase II, the west building, with its white roof, exhibited a higher average heat flux during the daytime than that in Phase I or Phase III, largely because outdoor air temperatures were higher in Phase II than they were in Phase I or Phase III. This implies that the impact of outdoor temperatures (and solar radiation) on average heat flux is more dominant than that of the white coating on the concrete roof (i.e., increase of reflectance by 0.4). By contrast, in Phase II, the east building with the black roof exhibited much higher average heat flux during daytime than that in Phase I or Phase III. This indicates that having both a higher outdoor temperature (and solar radiation) and a black roof (i.e., decrease of reflectance of 0.6) has a significant collective impact on increasing average heat flux through roofs.

Table 2 also shows average daily air-conditioning electricity use in each building with various roof coatings applied sequentially during the course of the study. For simplicity, we analyzed daily cooling energy use of each building from 9 a.m. to 5 p.m. on weekdays. One would expect that the average daily air-conditioning energy use in the buildings would tend to increase with the rise in outdoor temperatures and a decrease in roof-surface reflectance. From Phase I to Phase II, the average outdoor temperatures increased from 29.1°C to 32.4°C because of the seasonal change, corresponding to an increase of average energy use from 219 to 285 kWh/day, with an increase of average heat flux from 2.2 to 3.6 W/m^2 roof area. We also observed a reduction in the maximum roof surface temperature (by 12.5°C) of the west building as a result of its white roof, and a slight reduction in the peak roof heat flux (by 0.2 W/m^2).

While cooler roofs (i.e., those with a white coating) contributed to lowering the maximal roof surface temperatures and moderating the heat flux through the roofs into the buildings, the cooling energy savings attributed solely to reflectance changes was not apparent in the direct measurement results shown above. This is because actual cooling energy was also affected by other concurrent factors, such as outdoor air temperatures, occupancies, and operation. It remains a challenging task to quantify the reduction in cooling energy use attributable to roof reflectance changes. The following section describes the analytical approach we developed to estimate the effects of cool roofs on cooling energy use. It is based upon concurrently measured data from this field study in India.

4.5 Comparative analysis to quantify energy savings from cool roofs

For each building selected in this study, we anticipated that actual weather conditions would have a significant impact on the energy use of the air conditioning systems. The monitored results of average daily energy usage by air-conditioning systems during Phase I and Phase II confirmed such impacts. For example, for the west building, even though the concrete roof (in Phase I) was given a white coating (in Phase II), the cooling energy use increased slightly from Phase I (concrete roofs) to Phase II (white roofs). Notably, the weather was cooler during Phase I, and became warmer in Phase II. Therefore, given that weather conditions change by the day, month, and season over the course of the field monitoring, it would be prohibitively difficult to quantify the impacts of applying cool roofs by focusing on a single building.

Rather than trying to separate influence of weather conditions from that of roof coatings on the energy performance, we developed the following comparative analysis by evaluating the

correlations between the concurrently measured air-conditioning energy usages for each of the buildings.

While coating tasks were carried out in sequence with concurrent monitoring in both buildings, we assumed that each building maintained its own normal occupancies and that their operations were similar. Therefore, the impact analysis was performed by quantifying the correlations of the concurrent energy metrics between the two buildings, grouped by the three phases of the study — Phase I (both buildings with un-coated concrete roofs), Phase II (white roof on the west building, black roof on the east building), and Phase III (both buildings with white roofs).

Figure 3 shows the correlation of concurrent cooling energy use between the two buildings grouped on the bases of pre- and post-coating monitoring, i.e., Phases I through III. The quantification of the correlations between the two buildings using the west building as the reference case can then be used to predict the energy savings potentials attributable to roof-reflectance changes. The following describes the calculation method and analysis.

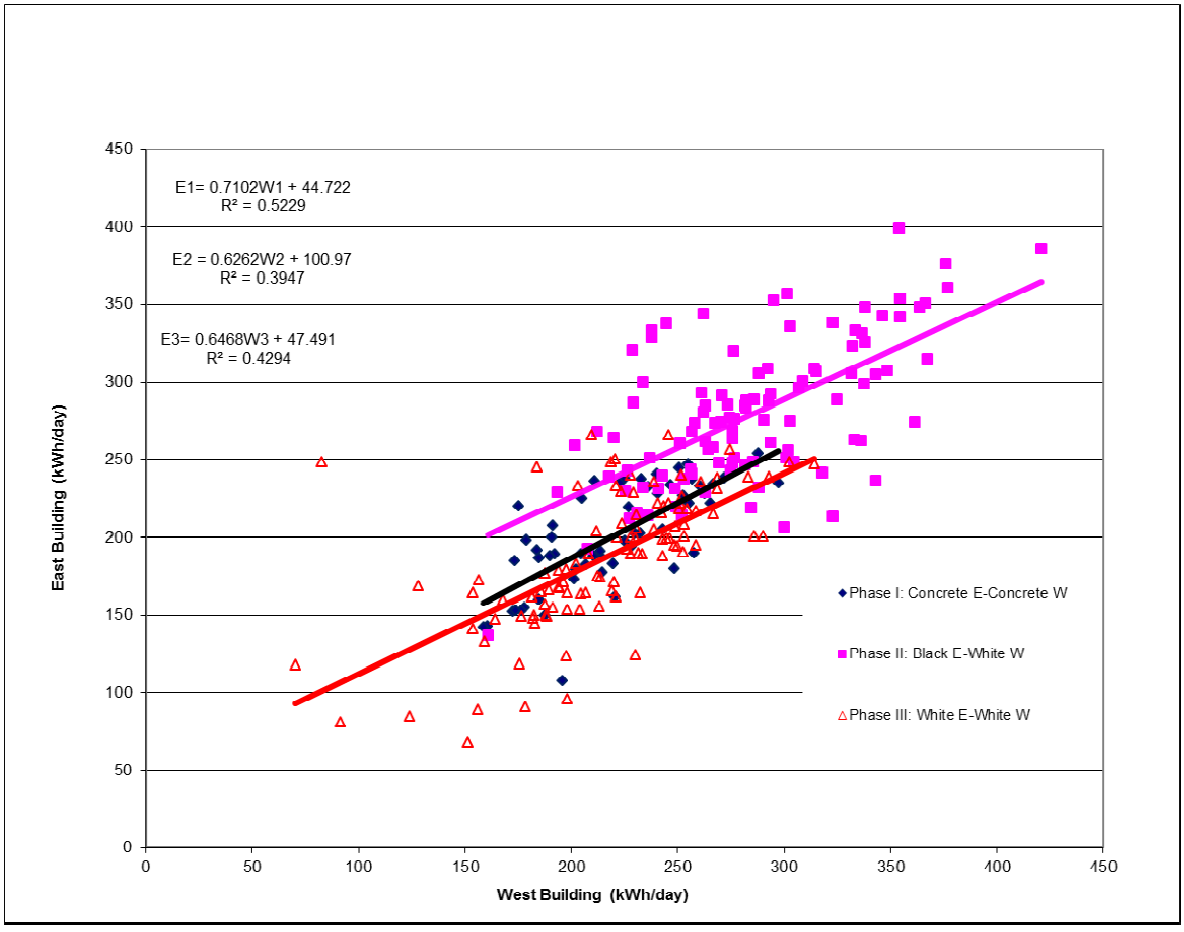

Figure 3. Pre- and post-coating comparison of air-conditioning energy usage for both buildings (three phases).

We established the following regression equations of air-conditioning energy use of the east building as it related to the air-conditioning energy use in the west building, with all p-values far lower than 10^{-3} indicating statistical significance.

Phase I: E1= 0.7102Wc + 44.722, in kWh/day (eq. 1)

Phase II: E2 = 0.6262Ww + 100.97, in kWh/day (eq. 2)

Phase III: E3 = 0.6468Ww + 47.491, in kWh/day (eq. 3)

Where

E1, E2 and E3 denote the daily cooling energy use in the east building in each of the three phases (concrete roof in Phase I, and black roof in Phase II, and white roof in Phase III), respectively;

Wc and Ww denote the daily cooling energy use in the west building with concrete roof in Phase I, and white roofs in Phases II and III, respectively;

In order to assess the difference in air-conditioning energy use with black and white roofs of the east building, we then calculate the difference between Phase II and Phase III as it corresponds to the same energy use in the reference case (i.e., west building. Therefore, the daily air-conditioning energy reduction due to the impact of changing a black roof to a white roof for the east building was:

$\Delta E = E2-E3 = -0.0206Ww+53.479$, in kWh/day (eq.4)

The percentage of daily air-conditioning energy reduction attributed to roof coating change from black to white was:

$\Delta E/E2 = (-0.0206Ww+53.479)/(0.6262Ww + 100.97)$ (eq.5)

Based upon the field observations that typical air-conditioning energy use of the west building ranged somewhere between 150 – 350 kWh/day (9 a.m.–5 p.m.), we can apply equations 4 and 5 to calculate the concurrent cooling energy use in the east building, and to quantify energy savings potential in the east building due to changes in roof reflectance.

Using the concurrent data of west and east buildings for equations 4 and 5, we calculated that cooling energy savings due to roof-whitening (compared to black roof) for the east building ranged from approximately 46 – 50kWh/day per 700 m^2 of roof area (i.e., 0.066 – 0.072 kWh/ m^2/day), representing a range of approximately 14 – 26% of energy savings attributed to cooler roofs, with surface reflectance changed from 0.10 (black roof) to 0.70 (white roof). The normalized energy savings per unit of reflectance reduction would therefore be 77 – 84 kWh/day, or approximately 0.11 – 0.12 kWh/ m^2/day.

Furthermore, given that the Satyam Learning Center operated 25 days per month throughout the year (i.e., 300 days per year), we can estimate that the annual energy savings potential from roof-whitening (from black roofs) ranged from 20 – 22 kWh/m^2 of roof area, which corresponds to an air-conditioning energy use reduction of 14 – 26% in commercial buildings. While these results showed that the real and substantial energy savings in cool-roof buildings were similar in both warm and cool seasons, the percentage reduction in air-conditioning energy use was nearly twice as high on the coolest days compared with the warmest. This is because air conditioning use is much higher to begin with on warmer days. In other words, a cool roof can significantly reduce

overall cooling energy use in commercial buildings, but the relative impact of roof-whitening on air conditioning is more pronounced on cooler, rather than warmer, days.

Additionally, Figure 4 shows hourly plots of roof surface temperature, under-roof temperature, plenum temperature, heat flux, and air conditioning electricity use during selected days. While it is premature to draw general conclusions from this small data set, the trend illustrates the changes of roof surface temperatures, heat flux, and cooling energy use corresponding to roof reflectance changes over time. For example, corresponding to a reduction of 20°C in the maximum roof surface temperature after installation of a cool roof in the west building, the drop in under-roof and plenum temperature was about 5°C and 4°C, respectively. The graph also shows a snapshot reduction of 8 W/m^2 in heat flux and 45 kWh/day in cooling energy use in the west building on the a short-term base, i.e., for a few days before and after applying white coatings to the west building's concrete roof. The reduction in heat flux and cooling energy use was expected to change on the daily basis throughout the year as a result of other concurrent factors, such as weather data (air temperatures, solar radiation, wind speeds, etc.), operational schedules, and occupant activities. Therefore, the numbers illustrated in the figure are not sufficient to derive average reduction in cooling energy use for the building.

Based upon the measured data gathered for all three phases of the field study, additional discussion and estimates of energy savings attributable to cool roofs are included in the next section.

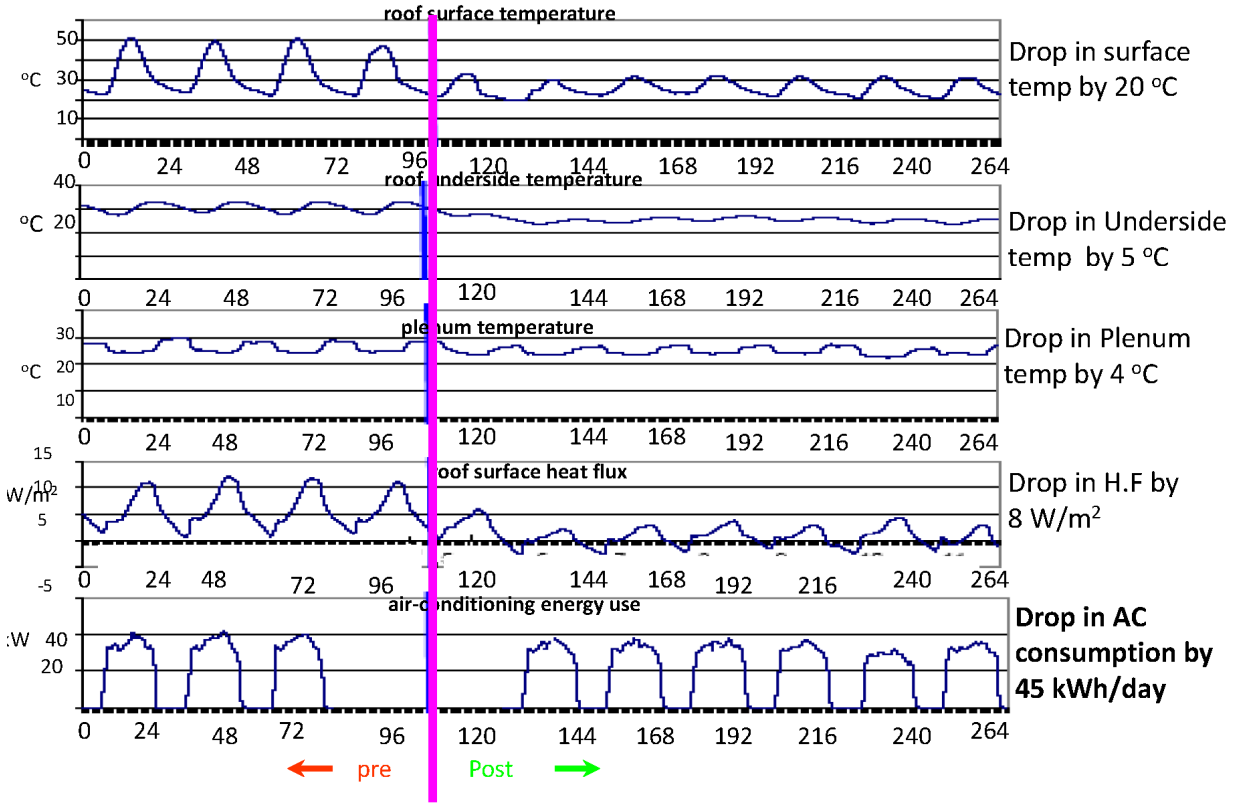

Figure 4. Hourly plots of West Building roof surface temperature, under-roof temperature, plenum temperature, heat flux, and air conditioning electricity use for a few days before and after installing cool roofs.

5 Discussion and Estimate of Energy Savings and GHG Reduction

From the analysis presented earlier for this study, using regression of concurrent cooling energy use data between two buildings can provide a valid quantification of the energy savings potential attributable to roofing reflectance changes. The analysis indicates that, while weather condition changes in the course of the field study would complicate the quantification of cool roof impacts on cooling energy use in buildings, a well-designed field study and the performance of experiments over an extended time period can lessen or eliminate the potential complications. For example, performing field tests in Phase II and Phase III over a period of time have allowed for evaluations of roof impact (black with 0.10 reflectance vs. white with 0.70 reflectance) on air-conditioning energy use, based on the results obtained from concurrent monitoring in the two buildings.

We have observed that the concurrent air-conditioning energy use of the two buildings selected for this study appeared to correlate very well with each other when they have the same roof reflectance (as illustrated by equations 1 and 3); however, the data are insufficient to quantify the energy savings when comparing the energy impact of a white roof to that of a concrete roof. would be misleading to attribute changes in energy use by air conditioning systems for either building solely to the changes in its roof reflectance (i.e., white roof with reflectance of 0.70 compared with concrete roof reflectance of 0.30). For this particular evaluation, it would have been very useful to have added an experimental period during which the west concrete roof would have remained untouched, while the east would have been whitened, or vice versa. Having this additional set of concurrent monitoring results from the two buildings under a range of weather conditions, for a period of time in the cooling season, would have enabled us to quantify the measured scale of cooling energy savings from a white roof compared with those of from a concrete roof. The energy savings potential attributed to application of a white coating compared with non-white concrete would then be more accurately quantifiable.

Based upon the measured results showing typical energy savings of air conditioning systems (associated with the change from black roof to white roof) in the range of approximately 46 – 50 kWh/day per 700 m^2 of roof area (i.e., 0.066 – 0.072 kWh/m^2/day, or annual savings of 20 – 22 kWh/m^2 of roof area), with surface reflectance changed from 0.10 (black roof) to 0.70 (white roof). We have estimated that the normalized energy savings per unit of reflectance reduction would be 77 – 84 kWh/day, or 0.11 – 0.12 kWh/m^2/day.

Given the available data and the normalized energy savings per unit of reflectance reduction, we can assume that approximately two-thirds of this savings could be achieved from the application of a white coating (reflectance 0.70) to the concrete roof (reflectance = 0.30) of the east building. Therefore, we estimated that cooling energy savings associated with the change from a concrete roof to a white-coated roof would be approximately 31 – 34kWh/day for 700 m^2 of roof area (i.e., 0.044 – 0.048 kWh/m^2/day). These would be equivalent to annual energy savings potential from roof-whitening (of concrete roofs) in the range of 13 – 14 kWh/m^2 of roof area, corresponding to a cooling energy use reduction in the range of 10 – 19% in the east building. Using GHG emissions factor of 820 kg CO_2 per MWh for India (CEA 2009), we estimated that annual direct CO_2 reduction associated with reduced energy use would be 11 – 12 kg CO_2 /m^2 of flat roof area by changing a concrete roof to white-coated roof.

In general, on a typical warmer day in summer, while similar cooling energy savings in the commercial building resulting from the cool roof was noted, total cooling energy tended to be higher than it would be on a cooler day. Therefore, the fraction of saved energy attributed to a cooler roof compared to the total cooling energy tended to be slightly lower than the fraction of saved energy on a cooler day.

With the assumption of an annual increase of 100,000 square meters of new roof construction for the next 10 years in the Metropolitan Hyderabad region, the annual cooling energy savings due to whitening concrete roof would be 13 -14 GWh of electricity in year ten alone, with cumulative 10-year cooling energy savings of 73 – 79 GWh for the region. The estimated savings for the entire country would be at least 10 times the savings in Hyderabad, i.e., more than 730 – 790 GWh. We estimated that annual direct CO_2 reduction associated with reduced energy use would be 11 – 12 kg CO_2/m^2 of flat concrete roof area whitened, and the cumulative 10-year CO_2 reduction would be approximately 0.60 – 0.65 million tons in India.

By cooling the outside air temperatures on a larger scale, cooler roofs would also save energy used for cooling systems by improving their operating efficiency, which would indirectly further reduce the CO_2 emissions.

With the price of electricity estimated at seven Rupees per kWh, the annual electricity savings on air-conditioning would be approximately 93 – 101 Rupees per m^2 of roof. This would translate into annual national savings of approximately one billion Rupees in year ten, and cumulative 10-year savings of over five billion Rupees for cooling energy in India.

6 Meteorological Simulations

One of the tasks in this study was to perform meteorological simulations to quantify the effect of heat island mitigation measures on urban climates in one selected region. Hyderabad, India, was selected as the region for model simulations. The effects of heat-island mitigation measures (cool roofs, cool pavements, and urban vegetation) on environmental temperatures were evaluated. The hypothesis is that cool surfaces and urban vegetation would reduce air temperatures in the region during hot summer seasons, thus mitigating urban heat-island impacts. A cooler urban environment can reduce cooling energy use in buildings, reduce air pollution, improve air quality, and improve pedestrian comfort. By reducing cooling electricity use, greenhouse gas emissions can be reduced from power plants. Details of the meteorological simulations are provided in Attachment 3.

Outcomes from the simulations suggest that there is a good potential for an air-temperature reduction of about 2°C in the Hyderabad area by using a combination of increased surface albedo and vegetative cover as urban heat-island control strategies. In addition, based on the preliminary simulations and assumptions, we found that air-temperature reduction on the order of 2.5 – 3.5°C can be achieved if moderate and aggressive heat island mitigation measures are adopted, respectively. Our study suggests that a more rigorous simulation using urbanized (meso-urban) meteorological models be conducted in the future, which may produce a more rigorous estimate of the air-temperature reductions for the entire urban area.

A large scale deployment of mitigation measures can bring additional indirect benefit to the urban area, such as cooling outside air and thereby improving the efficiency of cooling systems,

reducing GHG emissions, reducing smog, indirectly reducing pollution from power plants — all improving environmental quality and health impacts.

7 Outreach and Training

LBNL conducted several types of outreach activities to disseminate information about urban heat islands, cool roofs, and the findings of the monitoring experiment and meteorological analysis for Hyderabad. These included the establishment of a Web site; publication of a brochure; organization of a cool-roofs session at the annual Green Buildings Conference (GBC) of the Confederation of Indian Industry (CII) in Chennai; organization of a training workshop in Delhi; creation of a kiosk to disseminate information at IIIT; and continued future monitoring at an IIIT building. Specifically, during the course of the project, LBNL and IIIT staff made six presentations at different cities in India. LBNL also participated in outreach activities by presenting at the Cool Roofs session at the GBC-CII conference in Chennai and organizing a Training Workshop on Cool Roofs. The purpose was to inform and train the event participants in understanding the urban heat-island benefits of cool roofs, to demonstrate their practical applications in India — including the choice of materials available in the US and India — and to illustrate the costs and benefits of installing cool roofs on new and existing buildings. The details of the presentations for events and brochure are included in the Attachment 4.

8 Conclusions

In an effort to find ways to reduce energy use in buildings in urban areas, lower local air pollutant concentrations, and reduce greenhouse gas emissions, three mitigation measures were evaluated. The project goals were achieved by the following approaches: (1) Simulating and analyzing the energy savings and GHG benefits of cool roofs and tree planting measures, (2) Evaluating and demonstrating the benefits of installing cool roofs on a commercial building, and (3) Simulating the effect of the three measures (i.e., cool roofs, tree planting, and cool pavements) on urban meteorology, building energy use, and GHG emissions in an urban area.

In this field study, we have designed and performed field measurements and evaluations on the effectiveness of applying cool coatings on roofs and quantified their impact on energy and demand savings in two commercial buildings in India. Using the analytical approach developed for evaluating the field test results, we quantified direct energy effects of cool roofs on individual commercial buildings. Energy savings potential from roof-whitening (of previously black roofs) ranged from approximately 46 – 50 kWh/day per 700 m^2 of roof area (i.e., 0.066 – 0.072 kWh/m^2/day, or annual savings of 20 – 22 kWh/m^2 of roof area), corresponding to air-conditioning energy use reduction of 14 – 26% in commercial buildings. With surface reflectance changed from 0.10 (black roof) to 0.70 (white roof), the normalized energy savings per unit of reflectance reduction would be 77 – 84 kWh/day, or 0.11 – 0.12 kWh/m^2/day.

Given the available data and the normalized energy savings per unit of reflectance reduction, we can assume that approximately two-third of this savings could be achieved from the application of a white coating (reflectance 0.70) to the concrete roof (reflectance 0.30) in the east building. Therefore, we estimated that energy savings of air conditioning systems (associated with the change from a concrete roof to white-coated roof) would be approximately 31 – 34 kWh/day for 700 m^2 of roof area (i.e., 0.044 – 0.048 kWh/m^2/day). These were equivalent to annual energy savings potential from roof-whitening (from concrete roofs) in the range of 13 – 14 kWh/m^2 of

roof area, corresponding to an air-conditioning energy-use reduction in the range of 10 – 19% in the east building. The annual direct CO_2 reductions associated with reduced energy use would be 11 – 12 kg CO_2/m^2 of flat roof area by changing from a concrete roof to white-coating roof.

While these results showed that the real and substantial energy savings in cool-roof buildings were similar in both warm and cool seasons, the percentage reduction in air-conditioning energy use was nearly twice as high on the coolest days compared with the warmest. This is because air conditioning use is much higher to begin with on warmer days. In other words, a cool roof can significantly reduce overall cooling energy use in commercial buildings, but the relative impact of roof-whitening on air conditioning is more pronounced on cooler, rather than warmer, days.

We found from meteorological simulations that there is a good opportunity for air temperature reduction of about 2°C in the Hyderabad area by using a combination of increased surface albedo and vegetative cover as urban heat-island control strategies. In addition, air-temperature reduction on the order of 2.5 – 3.5°C can be achieved if moderate and aggressive heat island mitigation measures are adopted, respectively.

Large-scale deployment of mitigation measures can bring additional indirect benefit to the urban area, such as cooling outside air; thereby improving the efficiency of cooling systems, reducing GHG emissions, reducing smog, and indirectly reducing pollution from power plant —all improving environmental quality and health impacts.

In sum, this study demonstrates the effectiveness of cool-roof technology to the Indian industrial and scientific communities and provides an estimate of the national energy savings potential of cool roofs in India. The outcomes can be used to support recommendations for developing cool roof building standards in India. The study also suggests that additional field studies maybe helpful to further confirm the scale of potential energy savings through the installation of cooler roofs in India. Future field studies should build upon the successes and lessons learned from this field study. In the future, a more rigorous meteorological simulation using urbanized (meso-urban) meteorological models should be conducted, which may produce a more rigorous estimate of the air-temperature reductions for the entire urban area.

9 References

Akbari, H., M. Pomerantz, and H. Taha. 2001. "Cool surfaces and shade trees to reduce energy use and improve air quality in urban areas," Solar Energy, 70(3):295-310.

Akbari, H., Rosenfeld, A., and Taha, H. 1990. "Summer Heat Islands, Urban Trees, and White Surfaces," ASHRAE Transactions, 96(1), American Society for Heating, Refrigeration, and Air Conditioning Engineers, Atlanta, Georgia.

Taha, H. 1996. "Modeling the Impacts of Increased Urban Vegetation on the Ozone Air Quality in the South Coast Air Basin," Atmospheric Environment, 30(20):3423-3430.

United States Geological Survey (USGS), 1990. Cartographic Projection Procedures for the UNIX Environment. USGS Report 90-284.

Central Electricity Authority (CEA). 2009. CO2 Baseline Database for the Indian Power Sector, User Guide Version 5.0. Government of India, Ministry of Power, November 2009 http://www.cea.nic.in/planning/c%20and%20e/user_guide_ver5.pdf

Attachment 1. Demonstration Site Selection

We worked with the USAID Mission and counterpart organizations and selected interested building owners to participate in the project. Based upon the key criteria for assessing the suitability of urban areas in the three countries for heat-island mitigation, we carried out a series of technical analyses and contacted various leads in order to select the focus country.

Geographic site to represent a hot summer climate, where there are existing data on temperatures, air pollutant concentrations, and emissions sources; land use distribution maps; and available, ongoing modeling work (e.g., on pollutant transport, climate change, urban air sheds, ozone, particulates) by local researchers.

Buildings with operational air-conditioning systems to allow before- and after- roof retrofits that have potential for significant GHG-emissions reduction, and to serve as a viable demonstration site.

Preference to be given to the place where cooperation is appreciated among local governments, academic/research institutions, and industry and building associations.

We used the following criteria for selection of candidate buildings for monitoring:

- Office building with regular schedules
- Air conditioned
- Single or double story
- Small or mid-size
- Existing building with dark roof that is planning to install cool (white) roof
- Low-roof insulation
- Simplified air conditioning system
- Easy access to power panels (that is the case for most buildings)

The parameters used in this analysis included (1) local climate, (2) potentials for electricity and GHG savings, (3) available data and resource capacity for climate simulations and local air pollution modeling, (4) manufacturers as potential collaborators, and (5) government agencies and other institutions as partners.

Table 3 summarizes our analysis with respect to the criteria we used to evaluate the suitability of a country and city for this project. The evaluation with respect to the criteria listed in the table suggested that the local air-pollution modeling component of the project would be best implemented either in São Paulo or Mexico City because both cities have a strong database and previous history of air pollution modeling activities, particularly relating to changes in temperature, gridded data sets, and ozone formation. Of the two cities, São Paulo was preferable because it had a summertime ozone problem that is amenable via cool roofs mitigation; while the Mexico City's relatively cool climate meant that cool roofs solution would not be as significant as São Paulo.

Table 3. Summary: Candidate study countries and criteria for evaluation

	Brazil	India	Mexico
2002 GDP (1995 US$ per capita, market exchange rate)	4,641	493	3,737
Cooling degree days (Median value, ~ 50 cities in each country)	3128	5986	2384
Electricity savings for a commercial building (kg CO2 per kWh)	1239	1694	1120
Average CO2 Emissions (2000) (kg CO2/MWh)	57 Marginal rate: 250	953	575
Greenhouse Gas Emissions Reduction for a commercial building (kg CO2/1000ft2/year)	309	1621	640
Key Air Pollutants Studied	Particulates, ozone, NOx, HC	Particulates, NOC, HC	Particulates, ozone, NOx, HC
Urban air pollution modeling	Extensive for São Paulo Strong Local capacity exists	Limited efforts focused on particulates Some local capacity	Extensive for Mexico City Limited local capacity exists
USAID Mission Interest	Received letter with expression of interest; Mission active in rural sector, but many contacts in urban sector and energy efficiency programs	Received letter with expression of interest; Mission very active in urban sector with significant energy efficiency programs	Received letter with expression of interest; Mission has active air pollution program in Mexico City, and contacts in energy efficiency and air pollution control
Government activities (incl. utility companies, local and state government)	Agencies have many ongoing programs on energy efficiency and air pollution control	Agencies have many ongoing programs on energy efficiency and air pollution control	Agencies have some ongoing programs on energy efficiency, and strong program on air pollution control in Mexico City
US Industry interest	At least 15 and perhaps more manufacturers interested in working with LBNL in any country	At least 15 and perhaps more manufacturers interested in working with LBNL in any country	At least 15 and perhaps more manufacturers interested in working with LBNL in any country
Potential local counterparts	University of São Paulo, ICLEI	Green Business Center; Hyderabad, IIEC, Delhi, ICLEI, and ITC Inc.	Former head of CONAE, National Institute of Ecology, ICLEI, and DF Environment Secretariat

On the other hand, while the data in India on air quality were limited, it was adequate to develop and implement simpler models that would illustrate the benefits of cool roofs technology. One way to conduct analysis is to combine meteorological simulations and statistical analysis of available air-quality data. In this process the meteorological modeling can be performed and the

air-quality impacts can be assessed indirectly based on semi-empirical and/or statistical approaches, depending on the type of available aerometric data. In this approach, predicted meteorological fields and their perturbations can be used to develop scenarios of local changes in meteorology.

At the start of the project, we conducted an analysis to estimate the potential energy savings and GHG reduction benefits of installing cool roofs on a typical office building in three countries – Brazil, India and Mexico. This was one of the criteria that was used in the selection of a country and city for the demonstrating the benefits of cool roofs. As shown in Table 4, the GHG benefits were several times higher in India than in the other two countries.

Table 4 shows the same results for particular cities in the three countries. As can be observed in the table, building simulation analysis shows that Hyderabad, India would have yielded about the median level of electricity and GHG savings from the installation of a cool roof on a typical building.

Table 4. Estimated energy savings due to cool roofs for the median climate in Brazil, India, and Mexico

Country	Median CDD (18 degrees C base)	Electricity Savings (kWh/m2/year)	GHG Emissions Factor* (kg CO2 per MWh)	Greenhouse Gas Emissions Reduction (kg CO2/m2/year)
Brazil	1738	13.3	250	3.3
São Paulo	1353	5.4	250	3.1
India	3326	18.2	953	17.4
Hyderabad	3221	17.9	953	17.1
Pune	2484	7.9	953	7.8
Mexico	1324	12.1	575	6.9
Monterrey	2024	6.5	575	3.7

Note: * GHG emissions factor was based on International Energy Agency (IEA) data for each country. Marginal values should be used for each country, but these are not very different from average values that are readily available for India and Mexico, where the fuel mix for electricity generation is not changing very much. For Brazil, we use marginal values as reported in the literature. Because of its large hydroelectric generation, the average value for Brazil is lower, about 0.575 kg CO2 per kWh. The cooling degree-days, CO2 and GHG emissions, and potential energy savings for Indian cities were estimated to have significantly higher values because of the country's hotter climate and higher coal use for electricity generation. India, like Brazil, has strong programs on energy efficiency, and strong potential local counterparts. In fact, the USAID Mission in India actively promotes energy efficiency in buildings through its ECO II and other programs. Since most of the Indian cities listed in have a relatively hotter summer climate, replication of a demonstration in India would have a higher energy-saving impact and GHG reduction benefits than a demonstration in Brazil or Mexico. In addition, the U.S. cool roofing industry had indicated that they were actively working in India, which presented a favorable opportunity for performing testing and demonstration in India.

Based on the analysis, LBNL recommended that the project be situated in India. Because of its high median temperature, cool roofs in India are estimated to yield the highest electricity savings per unit of roof area. In addition, because of the high percentage of coal use for electricity generation, cool roofs are estimated to yield the largest GHG reductions per kWh of electricity savings in India. The building simulation analysis was carried out for several cities in India. Table 5 shows simulated cooling energy savings and GHG emission reductions in several other Indian climates. For the buildings demonstration work, we selected two buildings in Hyderabad in consultation with local partners.

Table 5. Estimates of Annual Cooling Energy Savings for Office Buildings in India.

City	Elevation (m)	HDD18	CDD18	Savings cooling (kWh/m2)		Greenhouse Gas Emissions Reduction (kg CO2/m2)	
				pre-80	post 80	pre-80	post 80
Agartala	16	38	2,755	16.5	6.2	15.7	5.9
Ahmedabad	55	14	3,514	18.8	7.2	17.9	6.8
Amritsar	234	540	2,322	15.1	5.7	14.4	5.4
Anantapur	349	1	3,797	19.7	7.5	18.8	7.2
Aurangabad	582	9	2,765	16.5	6.2	15.7	5.9
Balasore	20	9	3,273	18.1	6.9	17.2	6.5
Bangalore	920	1	2,280	15.0	5.6	14.3	5.4
Begampet	545	2	3,221	17.9	6.8	17.1	6.5
Belgaum/Sambre	747	2	2,395	15.4	5.8	14.6	5.5
Bhopal	523	58	2,750	16.5	6.2	15.7	5.9
Bhubaneshwar	45	4	3,487	18.7	7.1	17.8	6.8
Bhuj	78	62	3,357	18.3	7.0	17.5	6.6
Bikaner	223	215	3,375	18.4	7.0	17.5	6.7
Bombay	8	1	3,386	18.4	7.0	17.6	6.7
Calcutta	5	10	3,211	17.9	6.8	17.0	6.5
Calicut	4	1	3,560	19.0	7.2	18.1	6.9
Chitradurga	733	0	2,764	16.5	6.2	15.7	5.9
Cochin	1	3	3,680	19.3	7.4	18.4	7.0
Coimbatore	402	0	3,326	18.2	6.9	17.4	6.6
Cuddalore	12	0	3,782	19.6	7.5	18.7	7.1
East Akola	305	7	3,479	18.7	7.1	17.8	6.8
Gadag	649	0	2,897	16.9	6.4	16.1	6.1
Gauhati	54	65	2,420	15.4	5.8	14.7	5.5
Goa	58	0	3,478	18.7	7.1	17.8	6.8
Gwalior	205	224	3,009	17.3	6.5	16.4	6.2
Hissar	216	253	3,038	17.4	6.6	16.5	6.3
Hyderabad*	530	6	3,221	17.9	6.7	17.1	6.4
Indore	562	56	2,653	16.2	6.1	15.4	5.8
Jabalpur	391	81	2,834	16.7	6.3	15.9	6.0
Jagdalpur	552	18	2,690	16.3	6.1	15.5	5.8

Jaipur	390	177	2,899	16.9	6.4	16.1	6.1
Kakinada	8	0	3,859	19.9	7.6	18.9	7.2
Kota Airport	273	65	3,469	18.7	7.1	17.8	6.8
Kurnool	280	1	3,918	20.1	7.7	19.1	7.3
Lucknow/Amausi	128	174	2,851	16.8	6.3	16.0	6.0
Madras	16	0	3,954	20.2	7.7	19.2	7.3
Mangalore/Bajpe	90	0	3,443	18.6	7.1	17.7	6.7
Masulipatnam	2	0	3,736	19.5	7.4	18.6	7.1
Minicoy	1	4	3,793	19.7	7.5	18.8	7.2
Nagpur Sonegaon	309	8	3,325	18.2	6.9	17.4	6.6
Nellore	19	1	4,203	20.9	8.0	20.0	7.6
New Delhi/Safdarjung	214	238	2,881	16.9	6.4	16.1	6.1
Patiala	249	375	2,467	15.6	5.9	14.9	5.6
Patna	60	110	2,847	16.8	6.3	16.0	6.0
Poona	559	6	2,484	15.6	5.9	14.9	5.6
Raipur	296	11	3,348	18.3	7.0	17.4	6.6
Rajkot	134	13	3,405	18.5	7.0	17.6	6.7
Ratnagiri	34	0	3,345	18.3	7.0	17.4	6.6
Sholapur	477	0	3,479	18.7	7.1	17.8	6.8
Surat	10	4	3,570	19.0	7.2	18.1	6.9
Tiruchirapalli	85	1	4,140	20.8	7.9	19.8	7.6
Trivandrum	64	0	3,490	18.7	7.1	17.9	6.8
Veraval	6	14	3,059	17.4	6.6	16.6	6.3

Note: Assumptions: Pre-80 roof R-value = 5 and air conditioning = COP of 2.3, Post-80 roof R-value = 11 and air conditioning = COP of 2.9. Measured electricity saving for the new office buildings monitored in Hyderabad with R11 roof insulation was 25-34 kWh/m2. The measured savings can be twice as high as the simulated savings for a new office.

Attachment 2. Field Measurement Details

A2.1Buildings and Systems Characteristics

The Satyam Learning Centre, Hyderabad has two buildings: the East wing and the West wing. Both the buildings are nearly identical, have same atmospheric conditions, design and almost same kind of usage pattern.

Both buildings (i.e., east building, west building) are G+1 structure. They are made from concrete and bricks and the structure is a typical beam and column construction. Both the East and the West wings face each other and are oriented on the East-West axis. There are two staircases in each of the West and the East wings. It has a conventional concrete slab with gypsum board false ceiling. The floor height is 12' with a clear space of 8'3", 3' for the air conditioning ducts and false ceiling. The thickness of the slab is 6" and it has 3" thick flooring.

SLC is a learning center with labs, cabins, cubicles, discussion rooms, library, toilets, pantry, electrical rooms, UPS rooms etc. with a high usage level of air conditioning. The first floor of both the blocks is occupied by labs which are primarily used for training and lie in the central core with other areas arranged around it. The East wing has 4 labs, each of 22'3"x34'10" for 30 people, 120 computers for all the four labs whereas the West wing has 2 computer labs of about 44'x34'housing 60 computers each. The labs are well insulated from three sides by corridors thus there is less ingress of external heat load to the main air conditioned space.

The air conditioning is done through ductile split units of different capacities with AHU's on both the floors to facilitate the distribution of conditioned air to all the required spaces. Each wing has two air handling units consisting of about 27TR capacity in each. Unlike the corridors of the East wing, the corridors of the West wing were air-conditioned initially but the diffusers were closed later (before the start of the experiment). However, it was observed that there was some leakage in these diffusers, which might be the reason for slightly more AC consumption in the West wing.

The East and the West wings have separate AHU's. There are two AHU's on the first floor of each building. The study required monitoring of top floor (1st floor) air-conditioning load, which was possible due to availability of separate systems on the top floor of each building.

The building has single glazed sealed windows on the periphery. The panel rooms are located on the same floor, where the Data Logger was installed.

A2.2 Measurement Equipment

Table 6 summarizes the measurement locations and sensor types. Various research-grade sensors were used to measure indoor and outdoor air temperatures, outdoor air relative humidity, roof surface temperatures, roof heat fluxes, solar radiation, and electric power consumed by the HVAC, UPS, and lighting systems serving the test spaces.

Table 6. Measurement point summary

Measurement Points	Sensor Type	Locations
8 indoor air temperatures	Campbell Scientific 108-L temperature probe	1 in each of 4 ceiling return plenums and 4 conditioned spaces (west building Labs 1 and 2; east building Labs 1 and 3)
1 outdoor air temperature	Campbell Scientific 108-L temperature probe inside fan-aspirated radiation shield	1 on weather tower near center south side of west building roof
1 outdoor air relative humidity	Vaisala HMP45C-L relative humidity and air temperature probe inside naturally-aspirated radiation shield	1 on weather tower near center south side of west building roof
8 roof surface temperatures	Minco S667 surface temperature sensor with Minco TT246 temperature transmitter	1 on top surface of roof and 1 between bottom surface of roof and insulation above each of 4 ceiling plenums (west building Labs 1 and 2; east building Labs 1 and 3)
4 heat fluxes	Campbell Scientific HFT3 heat flux sensor	1 between bottom surface of roof and insulation above each of 4 ceiling plenums (west building Labs 1 and 2; east building Labs 1 and 3)
1 total horizontal solar radiation	Kipp and Zonen CM3 pyranometer	1 on weather tower near center south side of west building roof
14 HVAC, UPS, and lighting electric power consumptions	Continental Control Systems Wattnode WNA-3Y-400P pulse output watt-hour transducer with split-core current transformers	1 for each of 8 HVAC systems, 1 for each of 4 UPS systems, and 1 for each of 2 lighting systems serving conditioned spaces (west building Labs 1 and 2; east building Labs 1 through 4)

2.2.1. Data Logger and Communication

A Campbell Scientific XP-CR1000 13-bit data logger with a rechargeable battery backup power supply was used in each of the two buildings to collect data from the various sensors. The instrumentation and data loggers were installed and commissioned on January 14, 2006 (west building) and January 15, 2006 (east building). Power meters for the two UPS systems in the east building were not installed until January 21, 2006

Each sensor was scanned approximately every 1 second and averaged values were recorded every 30 seconds. Data were downloaded remotely about once a week using Campbell Scientific PC 400 software and a modem connected to the RS232 port of the data logger. Out-of-range data were investigated to determine whether a sensor or monitoring error existed, and appropriate corrective actions were taken if needed.

2.2.2. Air Temperatures

Indoor Air Temperatures

Air temperature in each of the four ceiling return plenums and four conditioned spaces was measured using a Campbell Scientific 108-L probe. The probe is a 6.5 mm diameter; 76 mm long white powder-coated aluminum tube filled with epoxy that contains a small thermistor element located about 3 mm from the probe tip. Its rated time constant in air at 5 m/s is 200±10 seconds. In each plenum, the probe was suspended near the center of the plenum; in each conditioned space, the probe was suspended underneath the plenum probe at about 10 cm below the bottom of the plenum.

Prior to installing the air temperature sensors, all of these sensors (and the other temperature sensors described below) were "calibrated" relative to each other by placing them inside a single aspirated tube in our laboratory. The laboratory air was heated for several hours and then allowed to cool. During this time, the air in the laboratory was constantly mixed with several fans. The average temperature, based on two of the sensors, was calculated for each 30 second period and the offset, or bias, for each sensor relative to this average, was calculated. The associated bias was removed from each sensor reading when it was recorded during our field experiment. Based on our calibration data, we estimate that the RMS error for an individual temperature measurement is 0.04ºC or better.

Outdoor Air Temperature

Three devices were mounted on a weather tower that we located near the center south side of the west building, about 4 m above the roof: an outdoor air temperature probe, a combined relative humidity and air temperature probe, and a pyranometer.

Outdoor air temperature was measured using a Campbell Scientific 108-L probe. To shield this probe from solar radiation and hot surfaces that cause radiation-induced temperature measurement errors, we constructed a fan-aspirated housing made of white poly-vinyl chloride (PVC) plastic pipes and fittings. The probe was located centrally inside the horizontal section of the aspirator, with the probe tip about 160 mm downstream of the air inlet.

The horizontal section of the housing is a nominal 3/4 inch diameter Schedule 40 pipe that has inside and outside diameters of about 21 and 27 mm, respectively. At the upstream end of this pipe, a nominal 3/4 inch diameter Schedule 40 vertical pipe is attached by a downward facing 90º "Ell" fitting to prevent rain entry. A coarse screen is located inside a "reducer bushing" at the bottom of the vertical pipe to prevent the entry of large insects. At the downstream end of the horizontal pipe, a nominal 2 inch diameter Schedule 40 vertical pipe is attached by a "reducer bushing" and a downward facing 90º "Ell" fitting. This vertical pipe contains a small 12 VDC axial fan with a rated flow of 7 cfm (0.03 m3/s). The corresponding average velocity in the annular space between the pipe wall and probe is about 12 m/s.

The estimated thermal conductivity of the pipe and fitting walls is about 0.15 W/(m K), based on values reported by Harvel Plastics (2007). The aspirator exterior from the inlet to the downstream end of the horizontal section is covered by a 14.5 mm thick closed-cell elastomeric insulation with a rated thermal conductivity of 0.039 W/(m K). The outer surface of the insulation is covered by thin aluminum tape that we coated with a white solar-reflective paint.

We estimate that the aged solar reflectivity and thermal emissivity of the coating are 0.70 and 0.85, respectively. For the weather conditions and roof surface temperatures that occurred during our experiment, we estimate that the maximum radiation-induced bias error for the aspirated air probe was about 0.12ºC.

2.2.3. Surface Temperature

Two roof surface temperatures above each of the four ceiling return plenums were each measured using a Minco S667PDZ60B thin-film platinum resistance temperature sensor connected to a Minco Temptran TT246PD1AC temperature transmitter. The transmitter converts the attached sensor's resistance into a 1 to 5 VDC signal that is proportional to the sensor's temperature. Each transmitter was located inside a small waterproof box.

Each probe is encased in silicone rubber with an adhesive foil backing and is approximately 15 mm long, 5 mm wide, and 3 mm thick. Its rated time constant is 1.3 seconds in water at 1 m/s. Over each plenum air temperature sensor, one surface temperature sensor was attached to the top of the concrete roof using epoxy and then covered with a thin layer of cement. After removing a small section of the roof insulation on the underside of the roof, a second sensor was attached to the bottom of the roof using epoxy, immediately below the top sensor. The roof insulation was then replaced. Roof surface temperature sensors were both covered with the same coating applied to the rest of the roof.

2.2.4. Outdoor Air Relative Humidity

Outdoor air relative humidity (RH) was measured using a Vaisala HMP45C-L probe located inside a Campbell Scientific 41003-5 10-plate naturally aspirated Gill radiation shield, which was attached to the weather tower. The probe includes a HUMICAP thin-film polymer capacitive sensor and a platinum resistance temperature sensor. This "RH" air temperature measurement is in addition to the fan-aspirated outdoor air temperature measurement described above. Measuring the outdoor air temperature immediately adjacent to the RH sensor allows one to determine the humidity ratio of the air, if needed for subsequent analyses.

The manufacturer's calibration lists the probe accuracy as ±1% RH from 0 to 15% RH, and ±1.5% RH from 15 to 78% RH. Calibrations were not provided beyond 78% RH, but the rated accuracy is ±2% RH from 78 to 90% RH and ±3% RH from 90 to 100% RH.

2.2.5. Horizontal Insolation

Total horizontal solar radiation was measured using a Kipp and Zonen CM3 pyranometer, which consists of a thermopile covered by a black coating and located inside a glass hemisphere. The device was attached to a Campbell Scientific 14282 leveling mount, which was in turn attached to the weather tower. The pyranometer was calibrated by the manufacturer to correlate its voltage output to the incident solar radiation flux. Its rated accuracy is ±10% for daily sums.

2.2.6. Roof Heat Fluxes

The heat flux at the top surface of the roof insulation was measured using a Campbell Scientific HFT3-L heat flux sensor. Each sensor contains a thermopile encased in epoxy and is approximately 39 mm in diameter and 4 mm thick. The sensors were attached to the bottom of the roof near the surface temperature sensor using epoxy, and oriented for positive heat flow down through roof.

Each sensor was calibrated by the manufacturer to correlate the voltage output of the sensor to heat flux. The sensor has a measurement range of ±100 W/m2 and a rated accuracy of ±5% of the reading.

2.2.7. Electric Power Consumption

Power consumed by the 14 HVAC, uninterruptible power supply (UPS), and lighting systems listed in Table 7 was measured using Continental Control Systems WattNode WNA-3Y-400-P three-phase four-wire power meters, each connected to three Continental Control Systems CTS-0750 split-core current transformers (CTs).

Each power meter outputs square-wave pulses with a frequency that is proportional to the instantaneous electric power. The maximum pulse frequency corresponding to full scale output is 4 Hz. The rated accuracy of the power meter is 0.45% of reading plus 0.05% of full scale. The accuracy of the current transformers is rated as 1% of reading for 10% to 130% of rated current.

For safety reasons, the pulse output of the power meter is optically isolated from its high-voltage side. A 1 kΩ resistor connected to the data logger 5 VDC output is used to supply the collector-emitter bias current for the optoisolator switching transistor.

Table 7. Power meter assignments and scale factors.

Channel Name	Electrical Service	Locations Served	CT Full Scale Rating (A)	Wh per pulse[1]
wac1	16.5 ton HVAC	West building, Lab 2	50	2.5
wac2	16.5 ton HVAC	West building, Lab 1	50	2.5
wac3	11 ton HVAC	West building, Lab 1	30	1.5
wac4	11 ton HVAC	West building, Lab 2	30	1.5
wups1	UPS	West building, 1st floor	30	1.5
wups2	UPS	West building, 1st floor	30	1.5
Wlights	Lighting	West building, 1st floor	30	1.5
eac1	16.5 ton HVAC	East building, Labs 3&4	50	2.5
eac2	16.5 ton HVAC	East building, Lab 1	50	2.5
eac3	11 ton HVAC	East building, Labs 3&4	30	1.5
eac4	11 ton HVAC	East building, Lab 2	30	1.5
eups1	UPS	East building, 1st floor	30	1.5
eups2	UPS	East building, 1st floor	30	1.5
Elights	Lighting	East building, 1st floor	30	1.5

A2.3 Data Collection and Analysis

All sensors were continuously scanned and averaged values were recorded every 30 seconds. Data were downloaded remotely via a modem about once a day. Out-of-range data were investigated to determine whether a sensor or monitoring error existed.

[1] We configured the data logger to record the number of pulses output by each power meter every 30 seconds. Therefore, the 30-second average power in Watts is the number of pulses recorded in 30 seconds multiplied by the Table 2 scaling factor times 120 (3600 s/h divided by 30 s). For example, the 30-second average power when 50 A CTs are used is the number of pulses multiplied by 300 (2.5 x 120).

The temperature sensors were all "calibrated" relative to each other by placing them in a single aspirated tube in our laboratory. We estimate the remaining uncertainty of an individual temperature measurement to be xxx K. We estimate the uncertainty of the temperature rise in the duct to be at least 0.06 K Table 8 summarizes the installation, pre-retrofit monitoring (Pre), and post-retrofit monitoring (Post) periods. From January 15, 2006 to March 22, 2006, we monitored the buildings with the roof exteriors as found (bare concrete with no coatings). During the period of March 23 to 26, 2006, we installed a cool roof (initial reflectivity of 0.80 and aged reflectivity of about 0.7) on the west building and a hot roof (initial and aged reflectivity of 0.12) on the east building. Monitoring continued with this cool versus hot configuration to July 23, 2006. By August 3, 2006, we installed a cool roof on the east building and continued monitoring until mid-November 2006.

Table 8. Monitoring periods and roof conditions.

Period	Dates	West Building Roof	East Building Roof
	13-15 January 2006	Monitoring equipment installed	Monitoring equipment installed
Phase I	16 January 16 to 22 March, 2006	Concrete roof	Concrete Roof
	23-26 March 2006	White coating of roof	Black coating of roof
Phase II	27 March to 22 July 2006	Cool roof	Hot roof
	23 July to 3 August 2006		White coating of roof
Phase III	4 August to 16 December 2006	Cool roof	Cool roof

A2.4 Field Measurement Results

2.4.1. Temperature data

For the three monitoring phases, Figure 5- Figure 10 present the hourly time series temperature (at two location on each roof) for outdoor air temperature, roof surface, under roof surface, plenum air, and the inside air for a two weeks period before and after changing the roof reflectance. The surface temperature-rise (surface minus outdoor air) is also shown. The maximum roof surface temperature for the East and West building during Phase I (both buildings having concrete roofs) is about 50°C. The maximum surface temperature-rise during Phase I is about 20°C. After installing the white roof on the West building and the black roof on the East building, the maximum surface temperatures changes to 38°C and 65°C, respectively. For the West building with the white roof, the surface temperature through-out the day is lower than the air temperature! For the East building with the black roof, the maximum surface temperature-rise increased to about 28°C. After installing the white roof on the East building, the temperature characteristics become similar to the West building.

The under-the-roof temperatures also show the same characteristics as the roof surface temperature, although the temperature difference between the concrete period and the white period is less pronounced. The plenum air temperature is highly influenced by the inside air temperature.

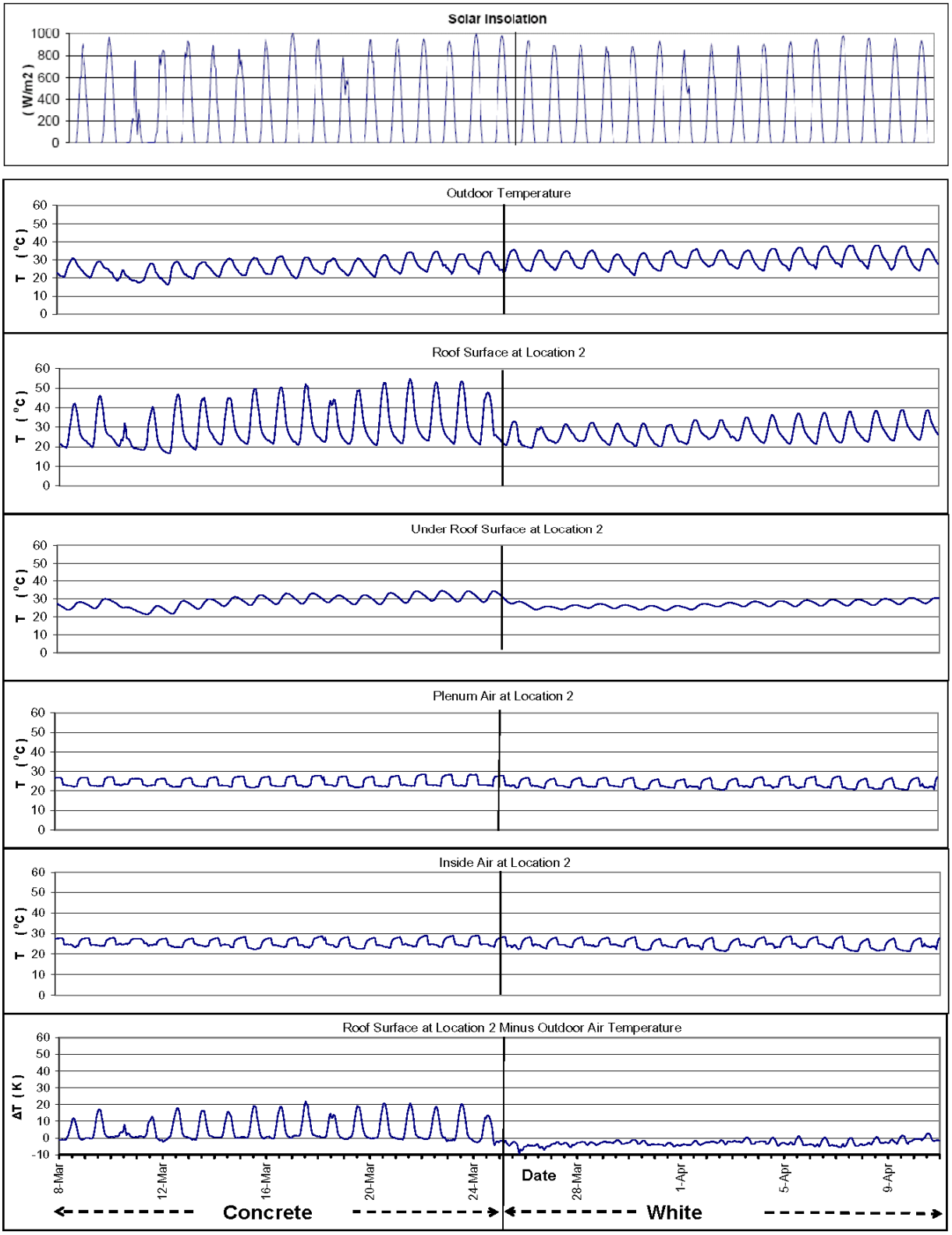

Figure 5. West building, Location 1, hourly temperature. Concrete to White.

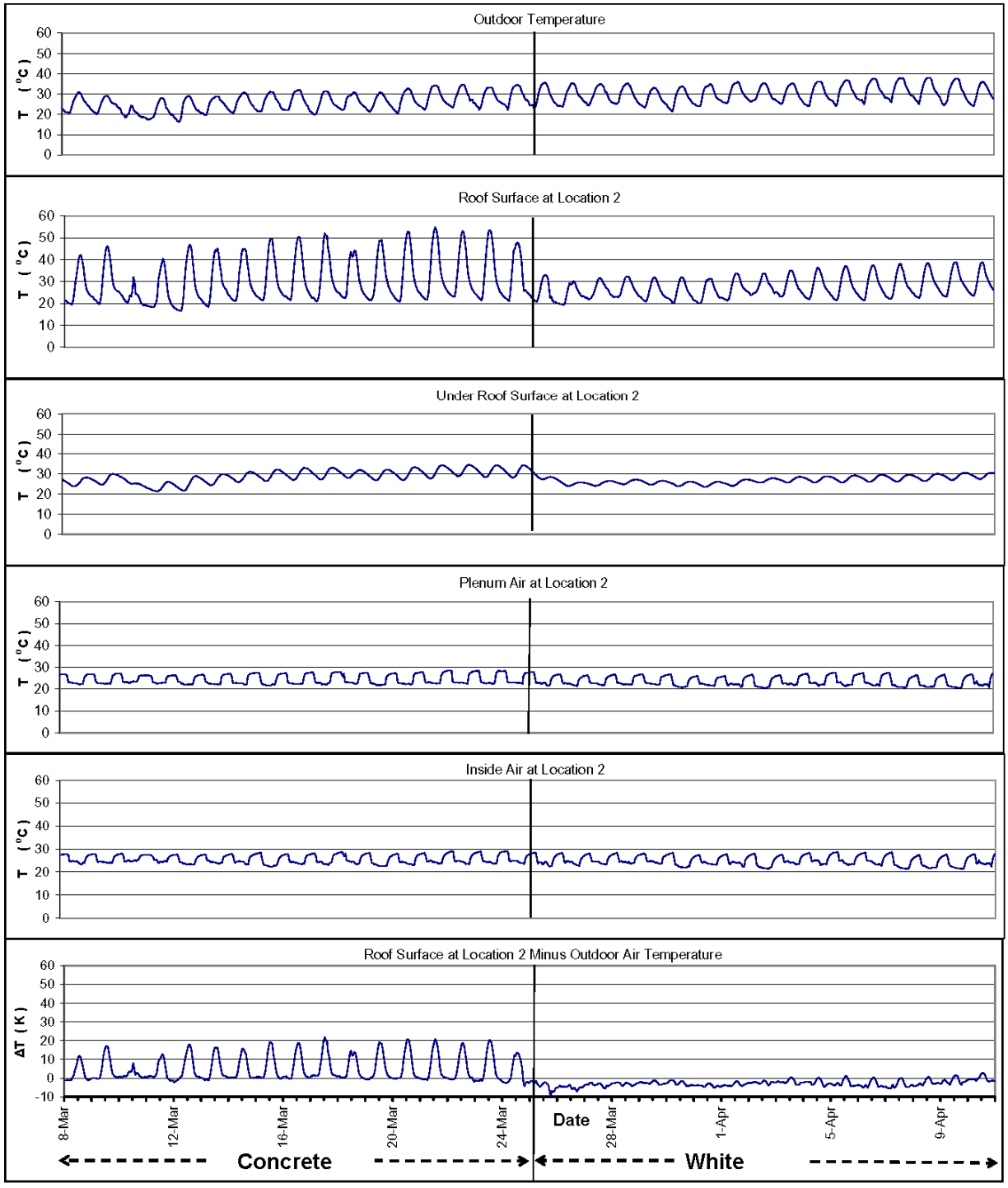

Figure 6. West building, Location 2, hourly temperature. Concrete to White.

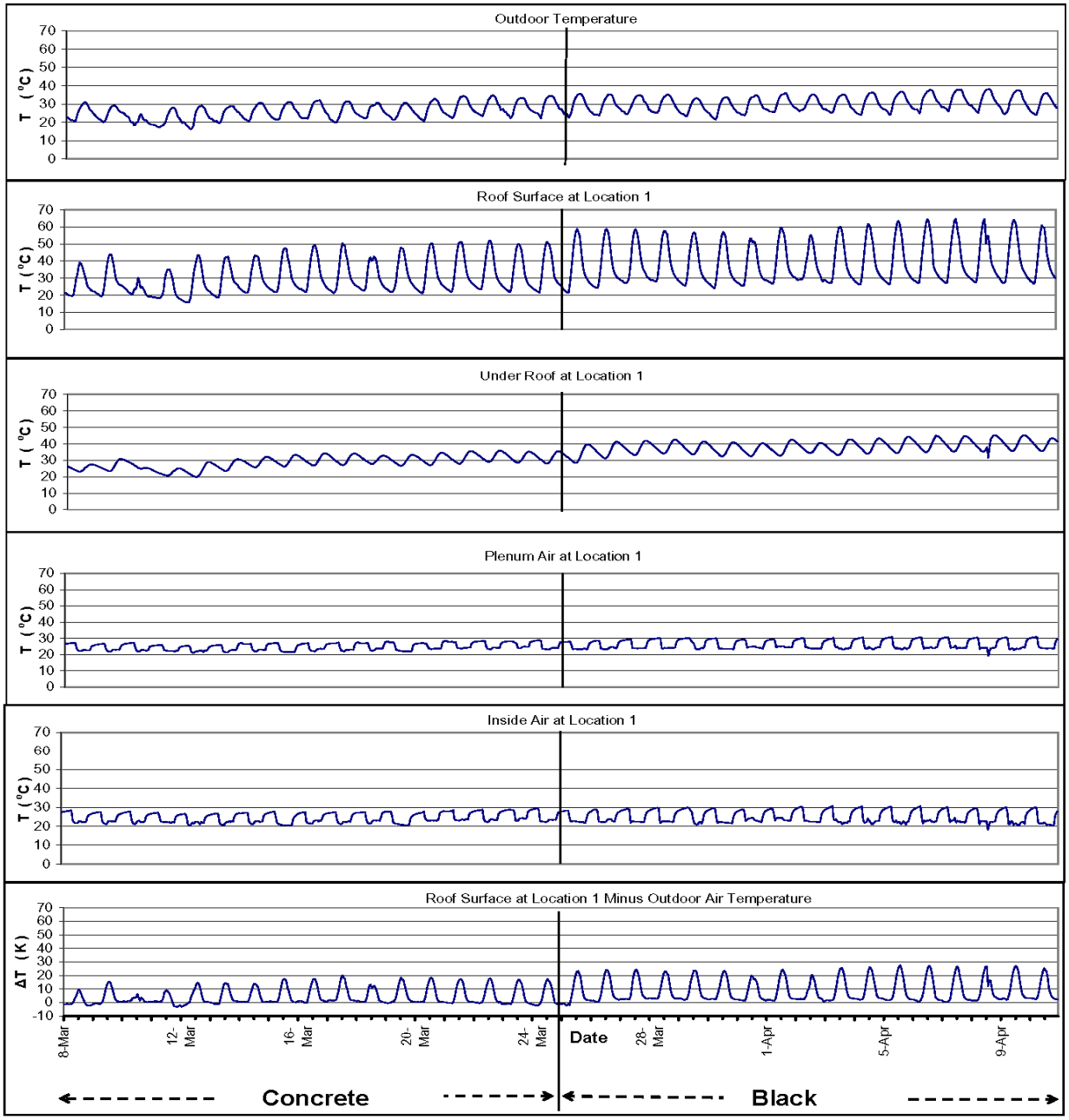

Figure 7. East building, Location 1, hourly temperature. Concrete to Black.

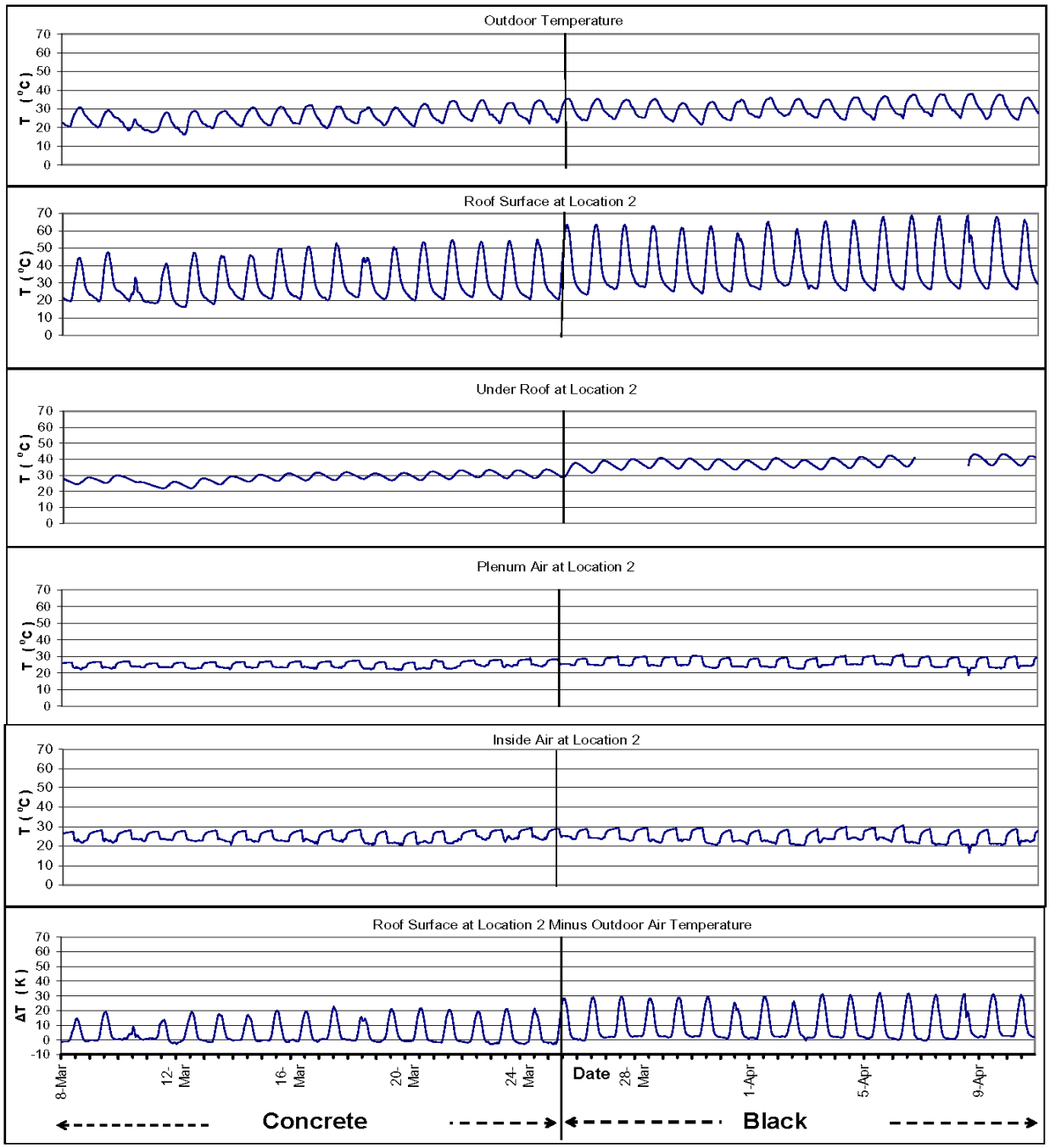

Figure 8. East building, Location 2, hourly temperature. Concrete to Black.

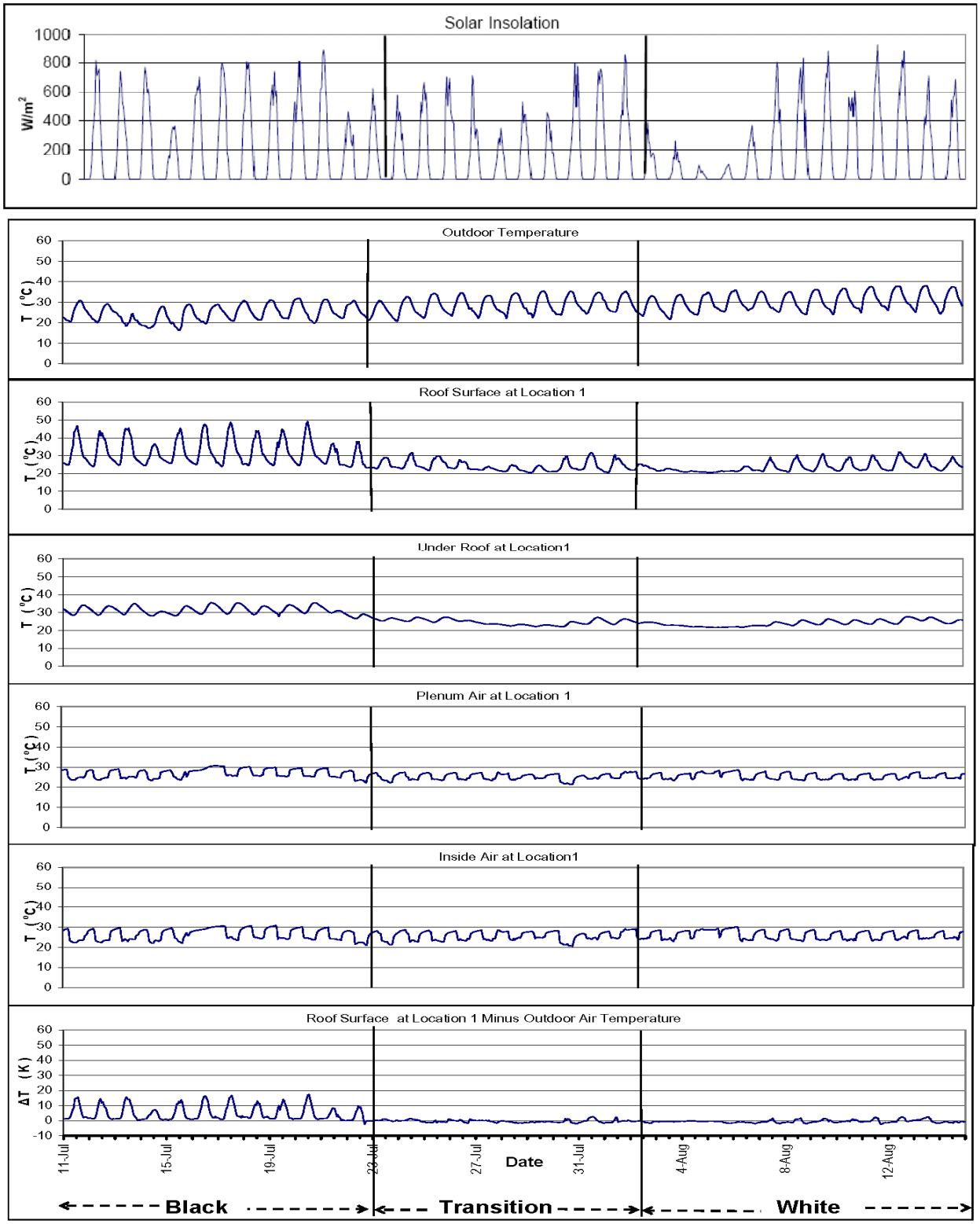

Figure 9. East building, Location 1, hourly temperature. Black to White.

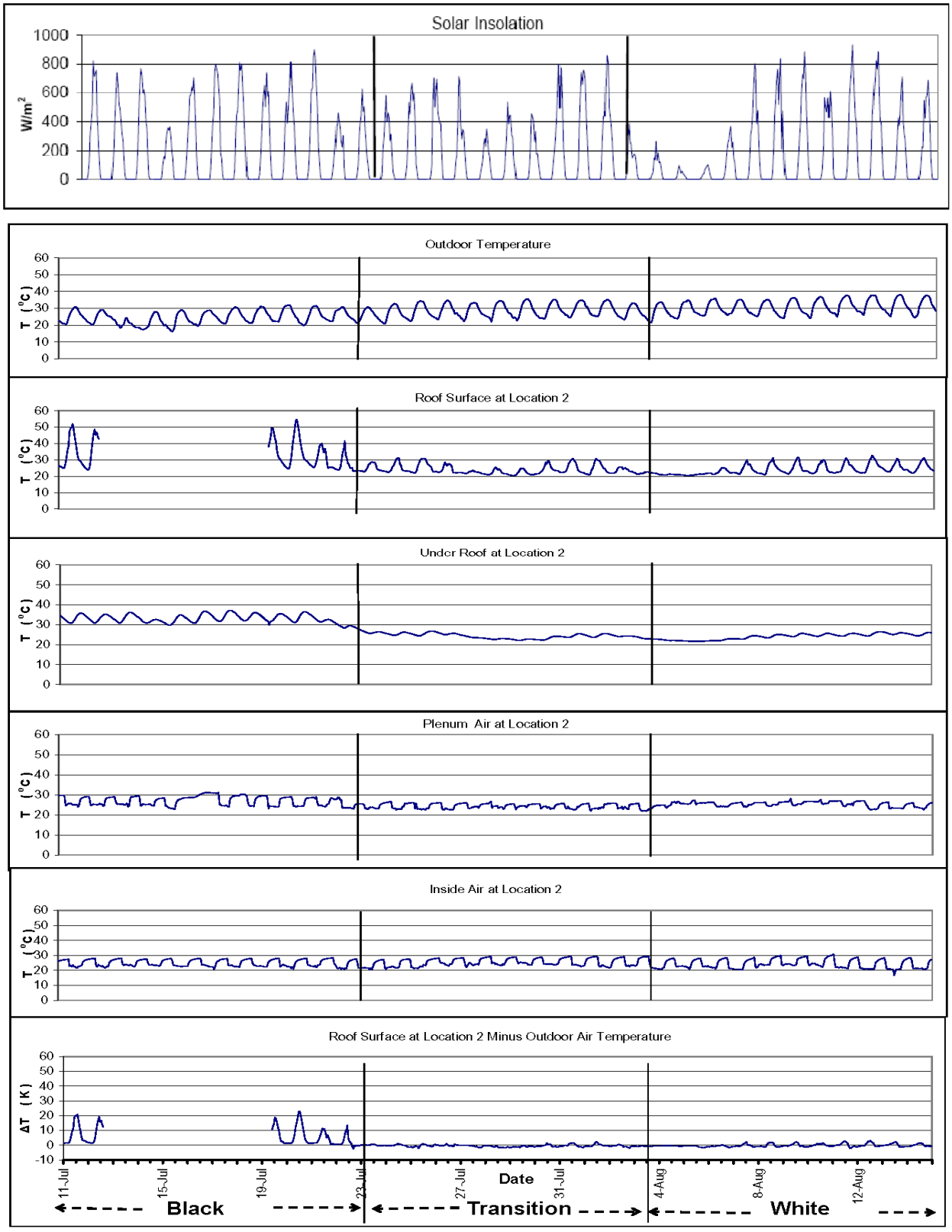

Figure 10. East building, Location 2, hourly temperature. Black to White.

Figure 11 - Figure 16 show the corresponding daily-averaged time series data. For the West building, after installing the white roof, the average daily temperature is typically below the ambient air temperature. While, the average surface temperature on the East building with a black roof is about 10°C warmer than the ambient air.

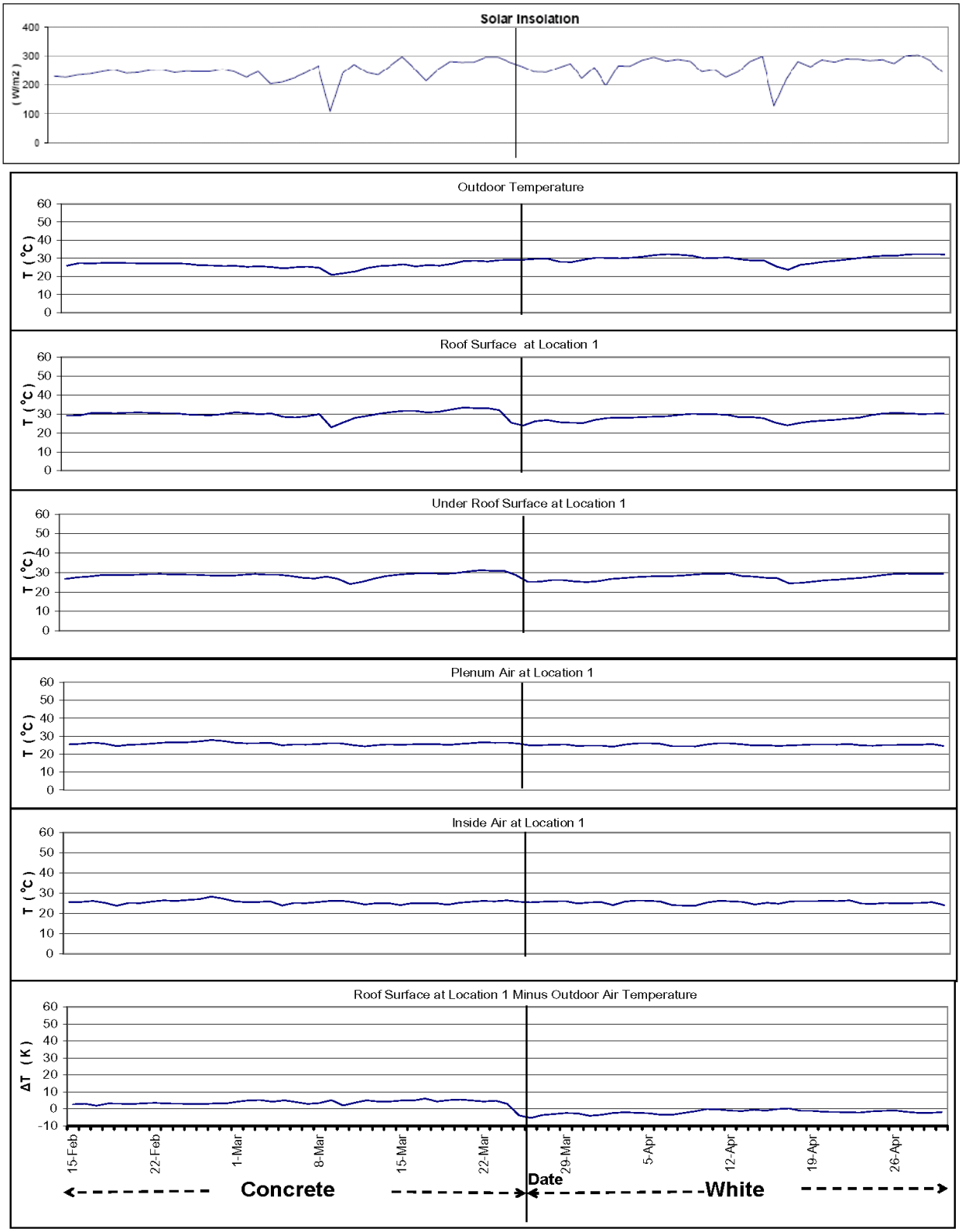

Figure 11. West building, Location 1, Daily temperature. Concrete to White.

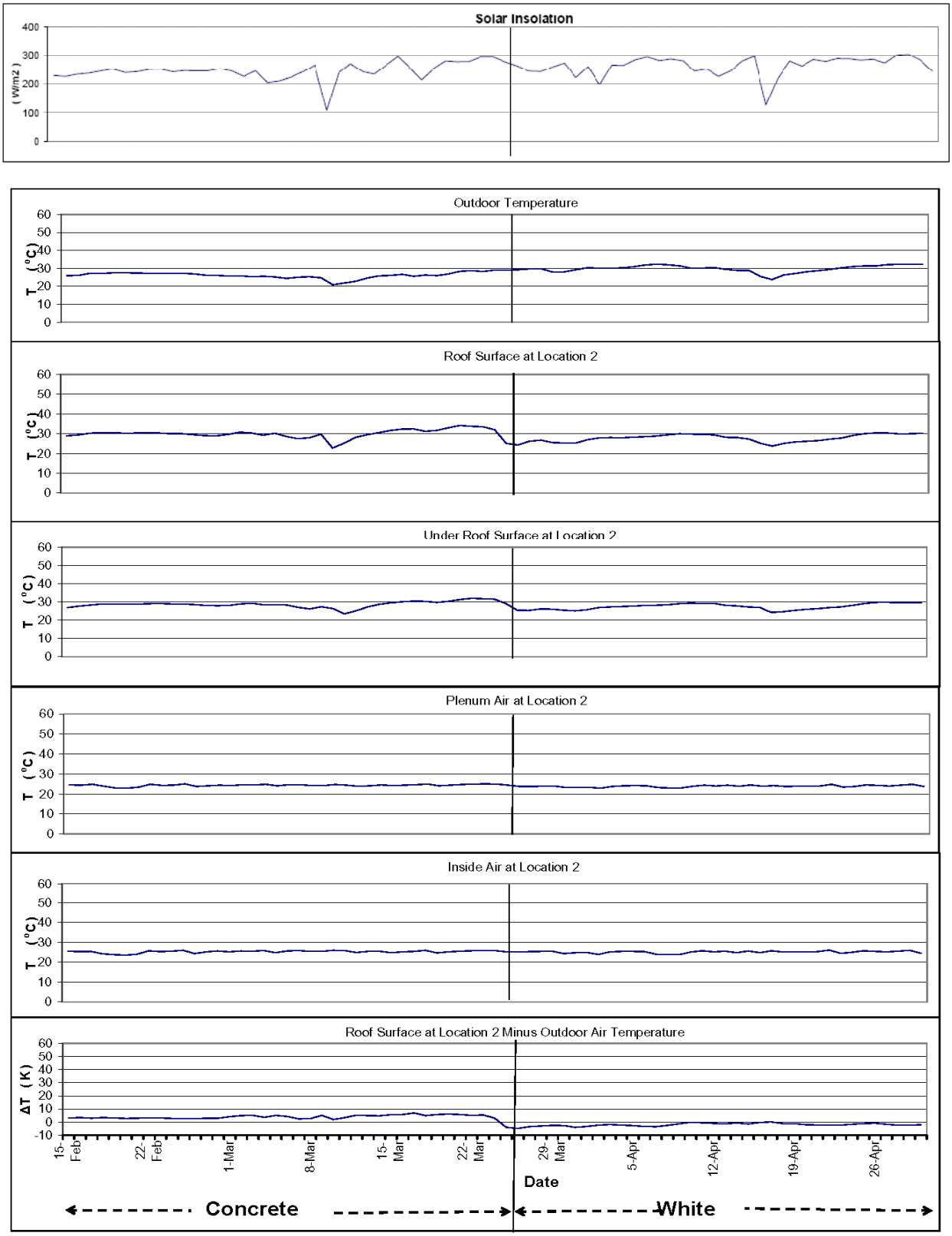

Figure 12. West building, Location 2, Daily temperature. Concrete to White.

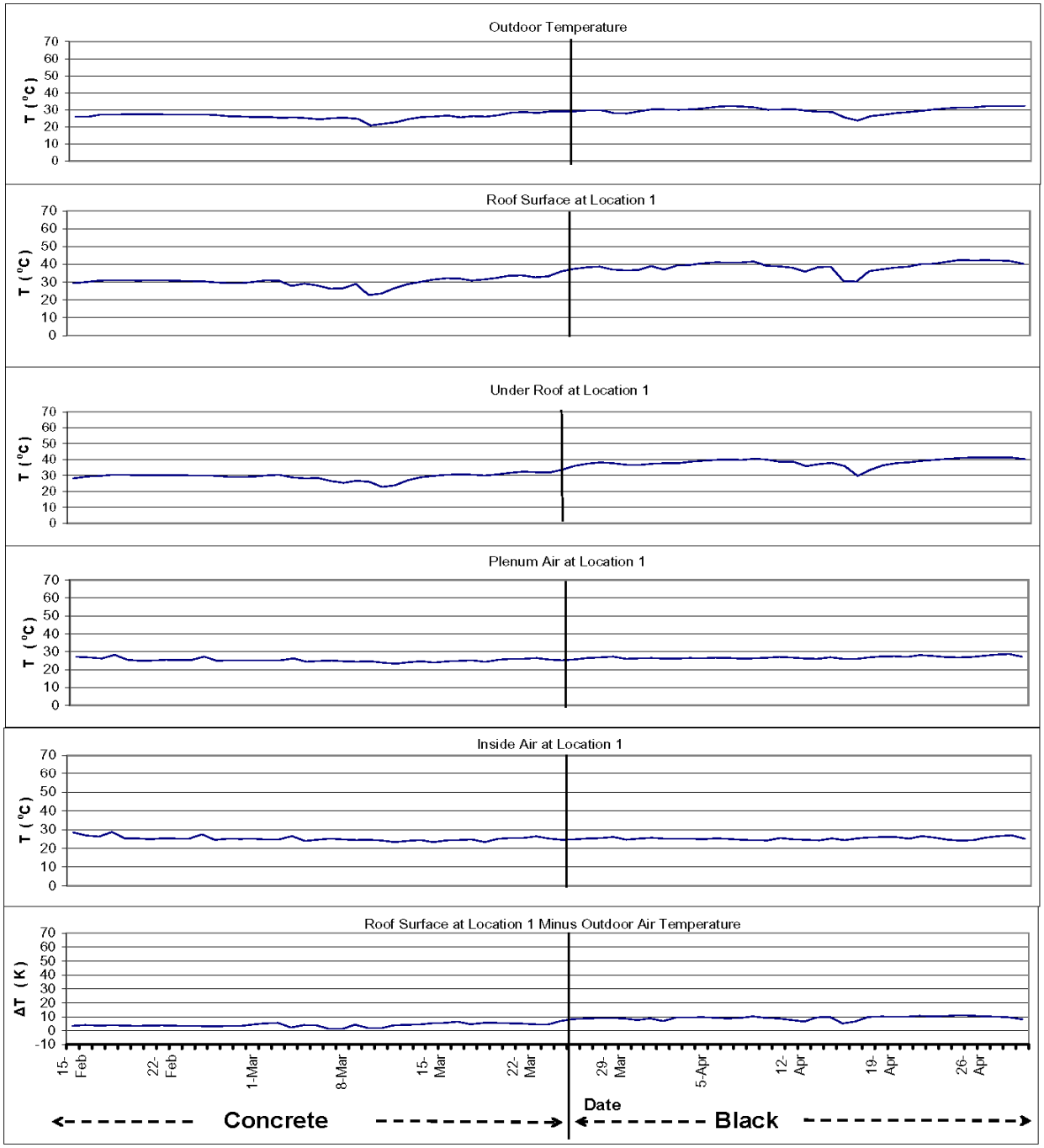

Figure 13. East building, Location 1, daily temperature. Concrete to Black.

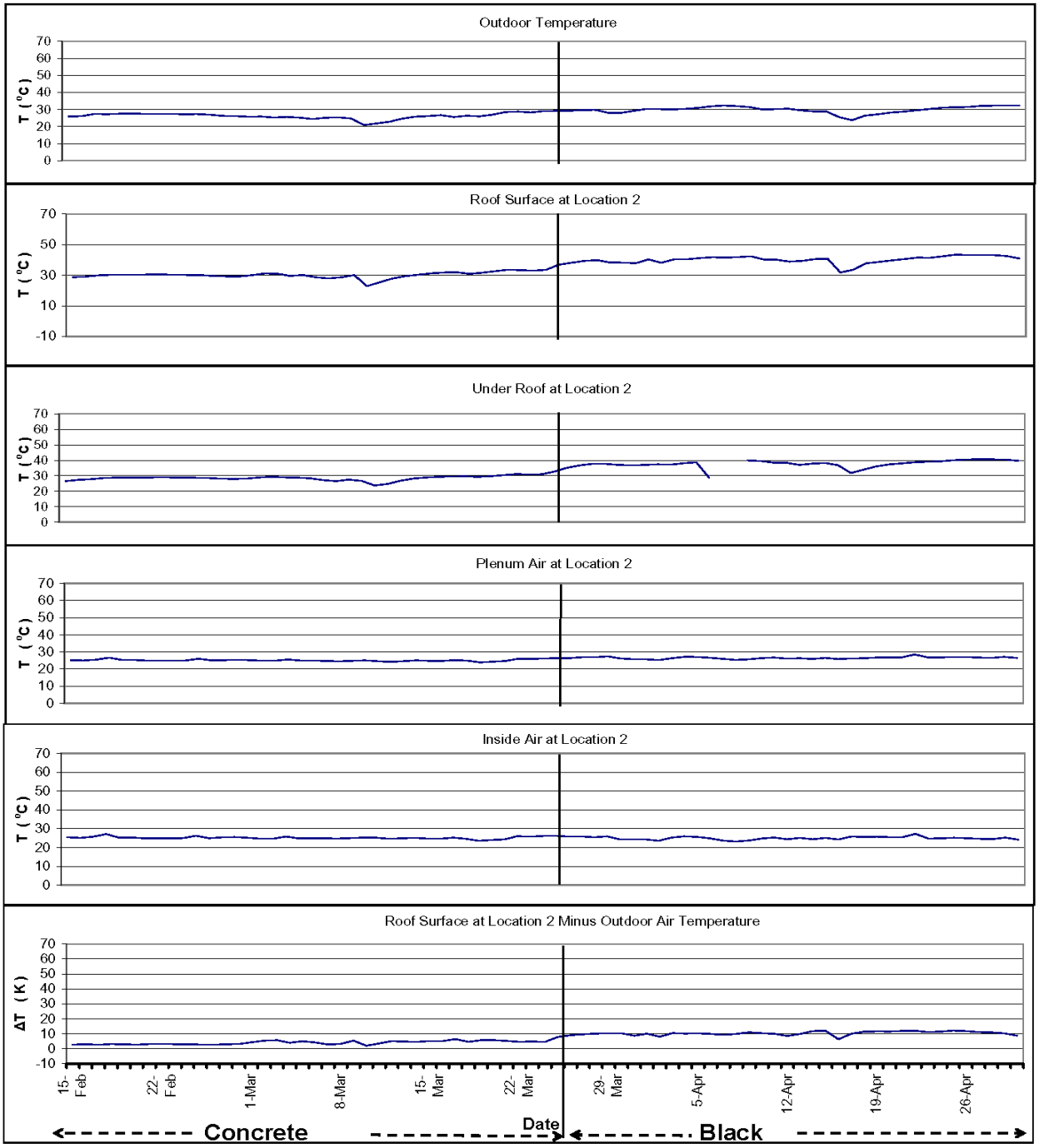

Figure 14. East building, Location 2, daily temperature. Concrete to Black.

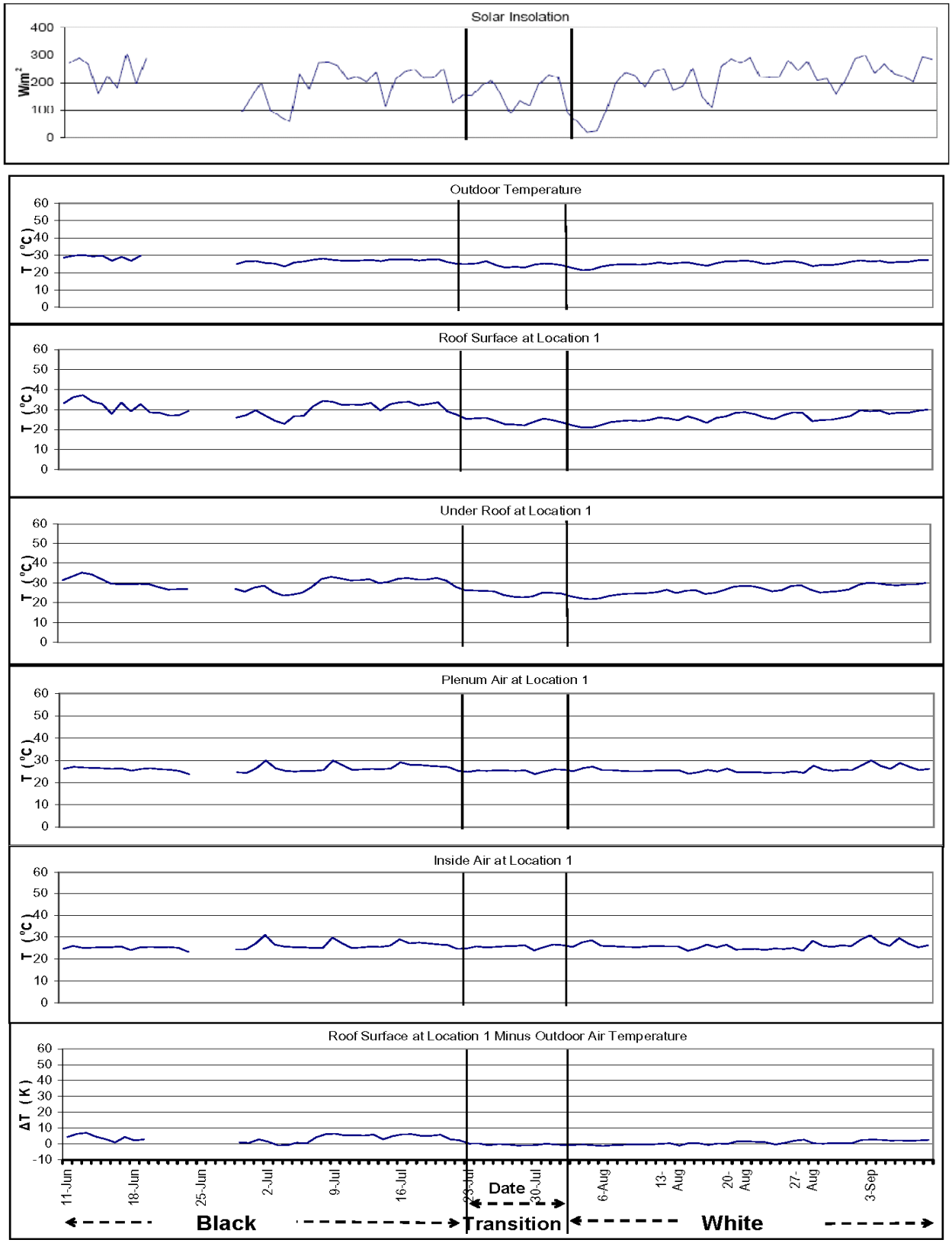

Figure 15. East building, Location 1, daily temperature. Black to White.

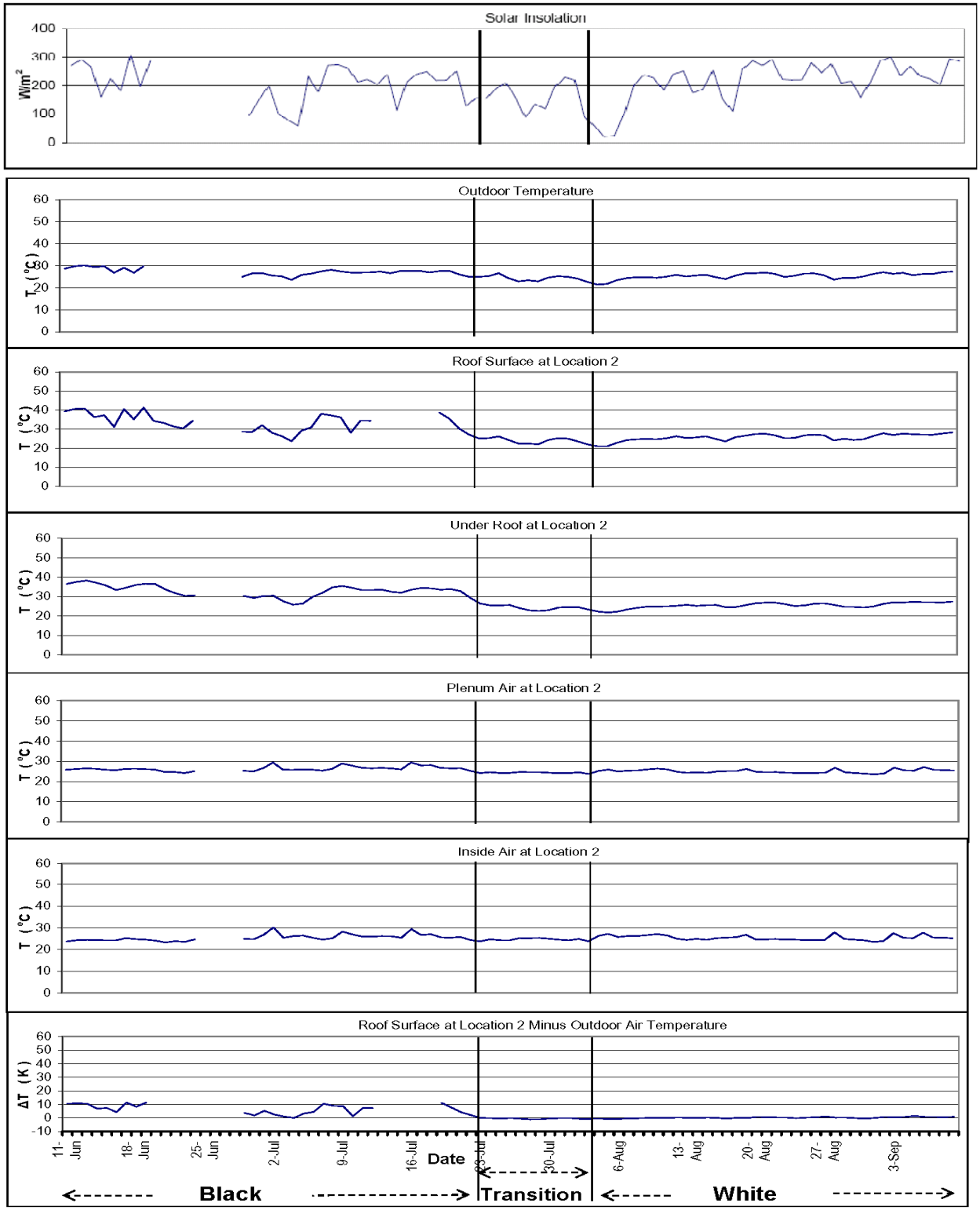

Figure 16. East building, Location 2, daily temperature. Black to White.

Figure 17 - Figure 19 compare the hourly and daily temperatures for the East and West buildings. During the Phase I and Phase III of monitoring, the temperatures for both buildings are identical. During the Phase II, the maximum surface temperature on the East building is about 30K warmer than the West building. The plenum temperatures show a range of 10K (20°C to 30°C), depending on the outside surface temperature.

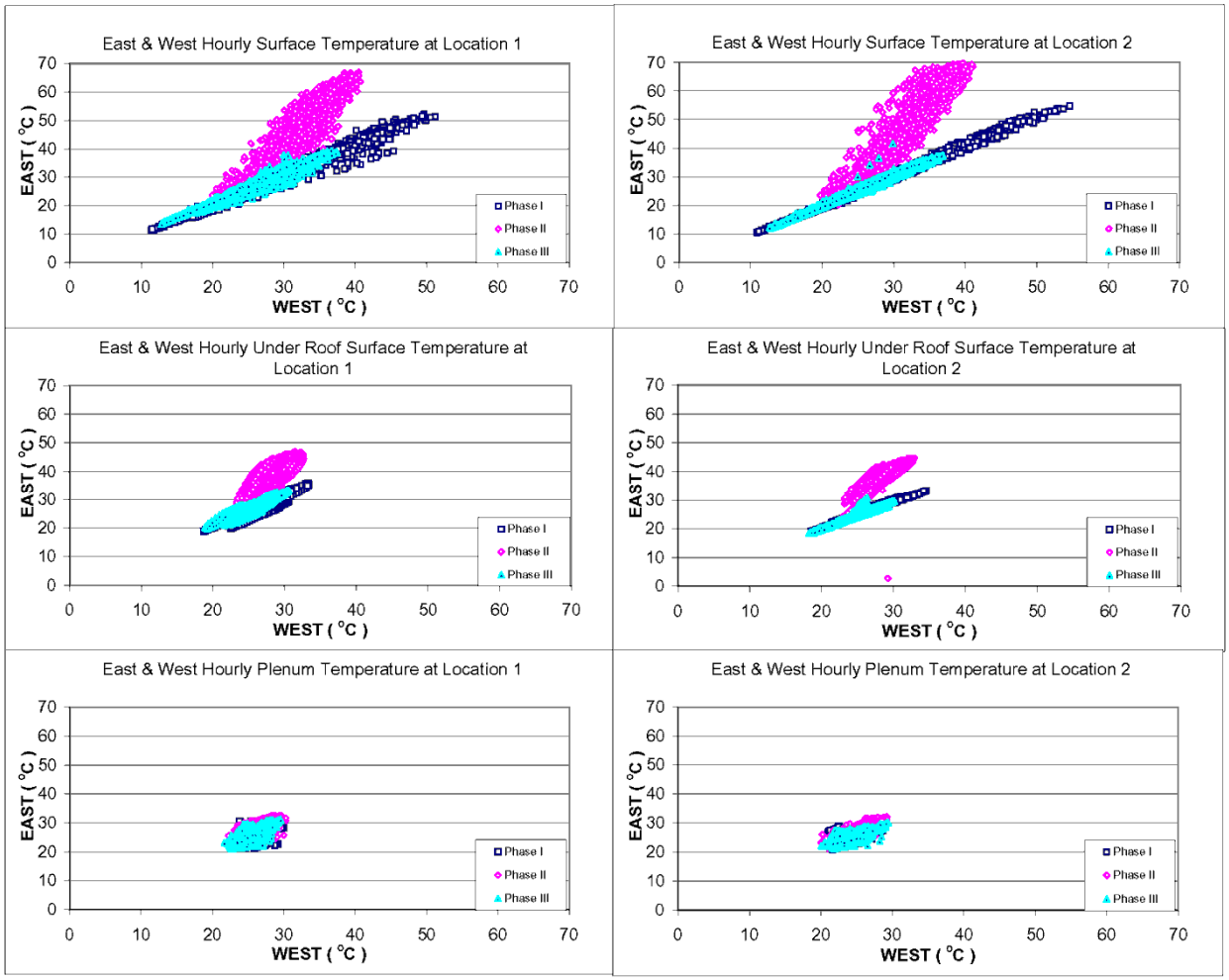

Figure 17. Comparison of hourly temperatures for East and West buildings.

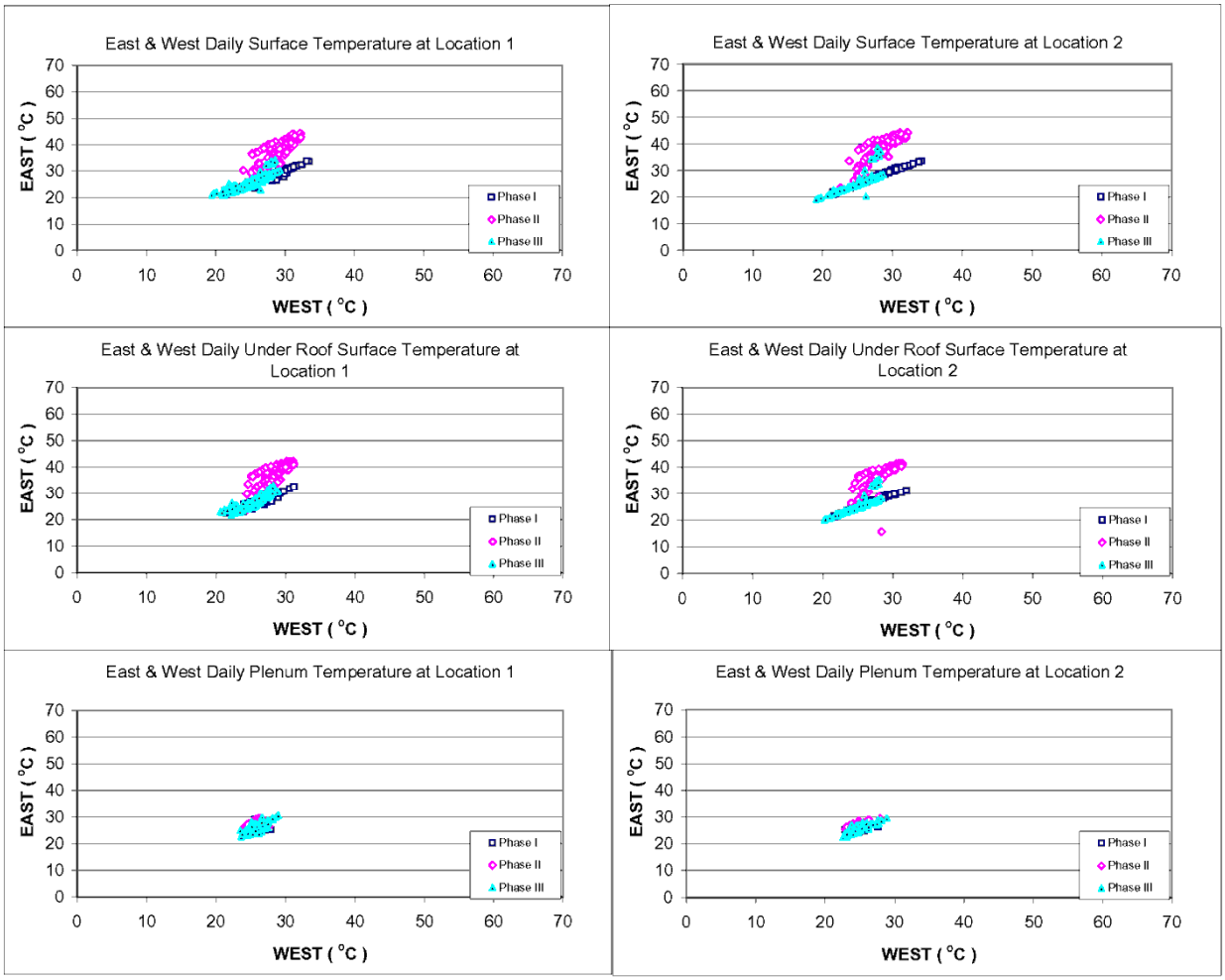

Figure 18. Comparison of daily temperatures for East and West buildings.

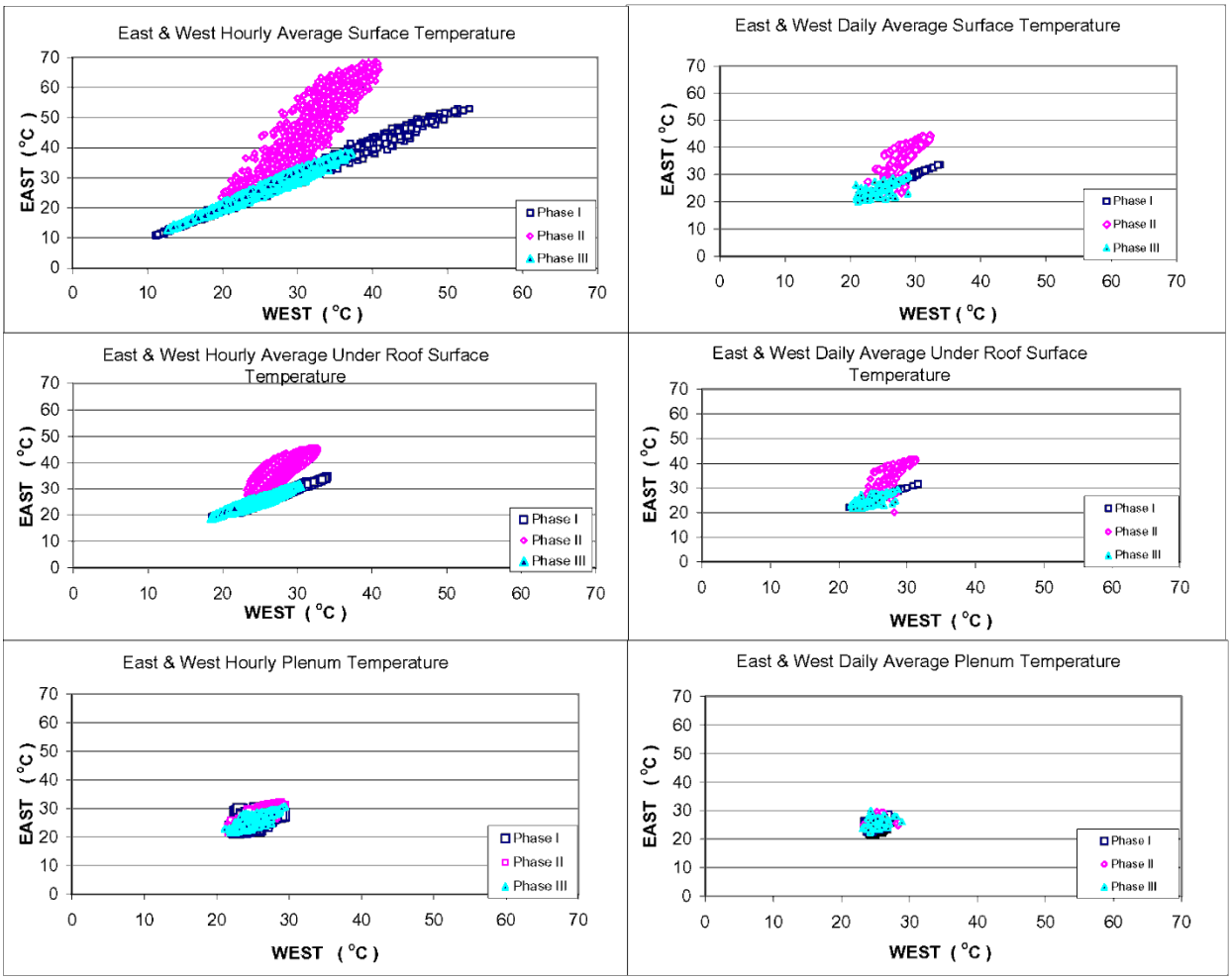

Figure 19. Comparison of average hourly and daily temperatures for East and West buildings.

2.4.2. Heat flux data

For the three monitoring phases, Figure 20 - Figure 22 present the hourly time series (at two locations on each roof) for roof heat flux for the West and East buildings. The maximum roof heat flux for the East and West building during Phase I (both buildings having concrete roofs) is about 10 – 12 W/m2. After installing the white roof on the West building and the black roof on the East building, the maximum roof heat flux ranges from 4 – 8 W/m2 and 14 – 20 W/m2, respectively. The difference between the maximum roof heat flux in the East and West building is about 10 -12 W/m2. In Phase III, the difference between the maximum roof heat fluxes in the East building after installing a white roof is about 10 W/m2. Assuming an overall air conditioning COP of 1.5, a quick estimate of spot peak power demand savings is about 7 W/m2.

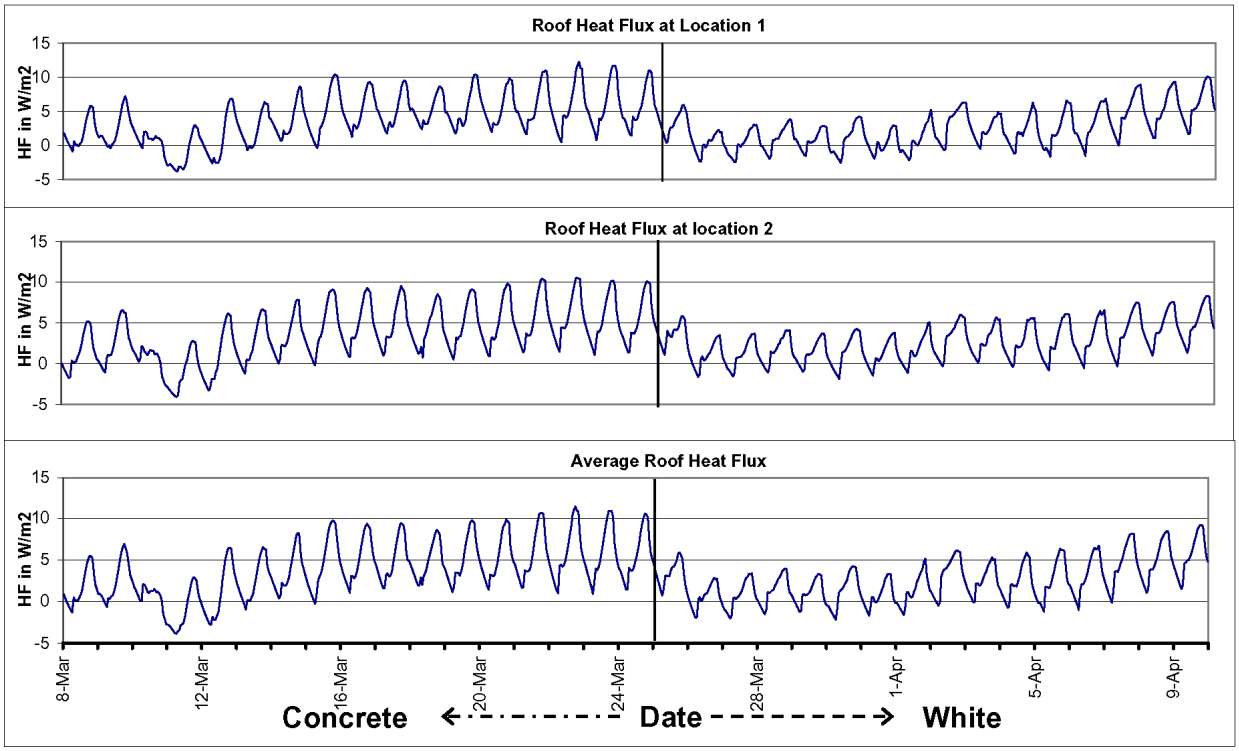

Figure 20. West building, Hourly heat flux. Concrete to White.

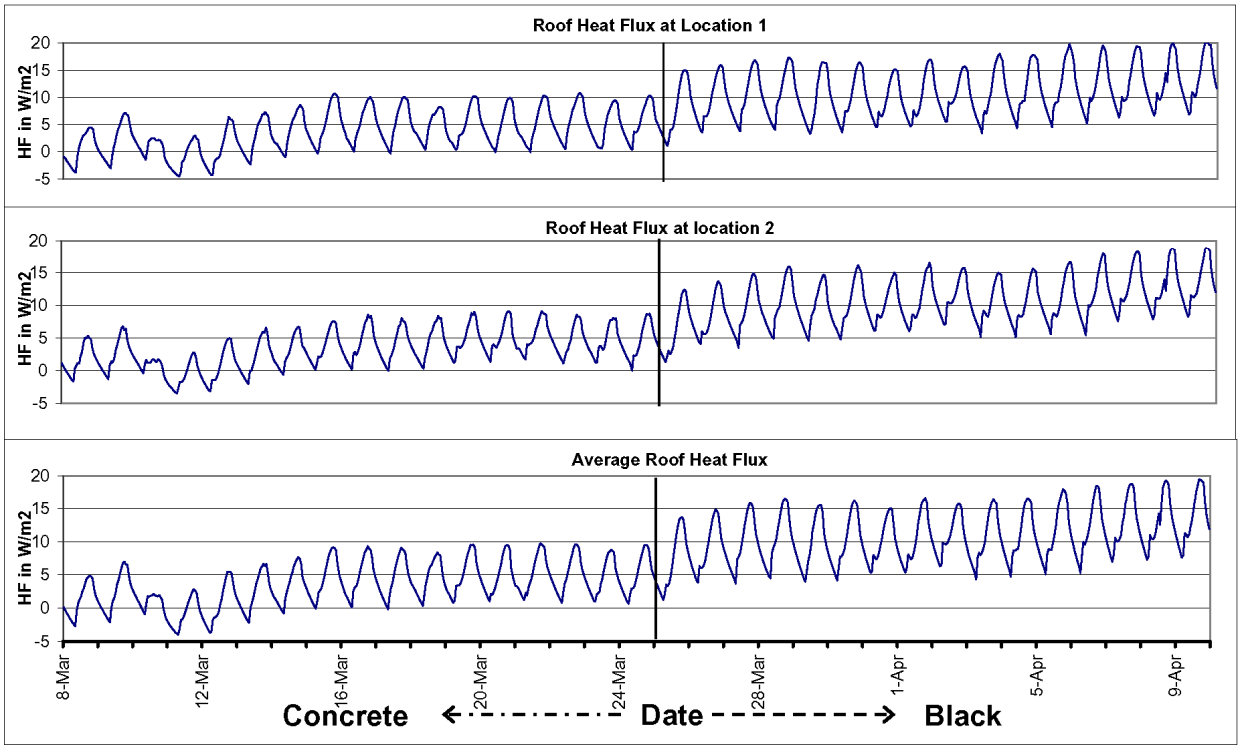

Figure 21. East building, Hourly heat flux. Concrete to Black.

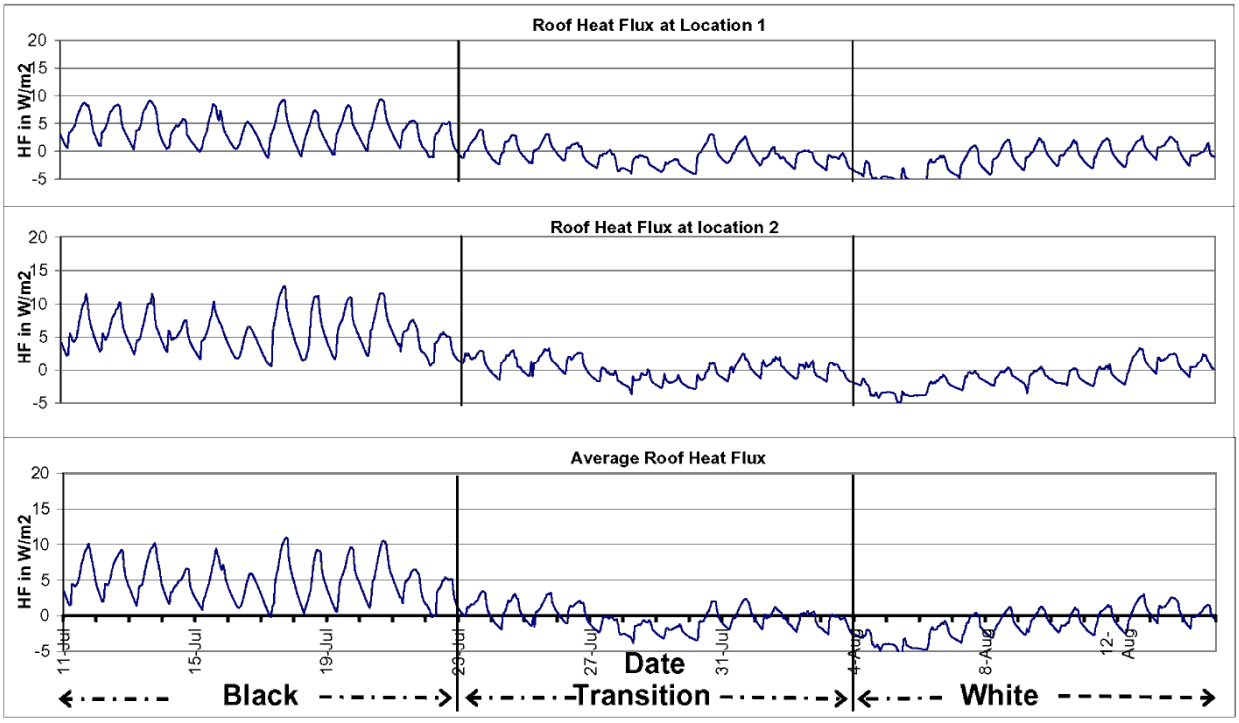

Figure 22. East building, Hourly heat flux. Black to White.

Figure 23 - Figure 25 show the corresponding daily-averaged time series data. Figure 26 compares the hourly and daily roof heat flux for the East and West buildings. During the Phase I and Phase III of monitoring, the roof heat fluxes for both buildings are almost identical. During the Phase II, the maximum roof heat flux on the East building is about 10-12 W/m2 higher than the West building. The maximum daily roof heat flux on the East building is about 8 W/m2 higher than the West building.

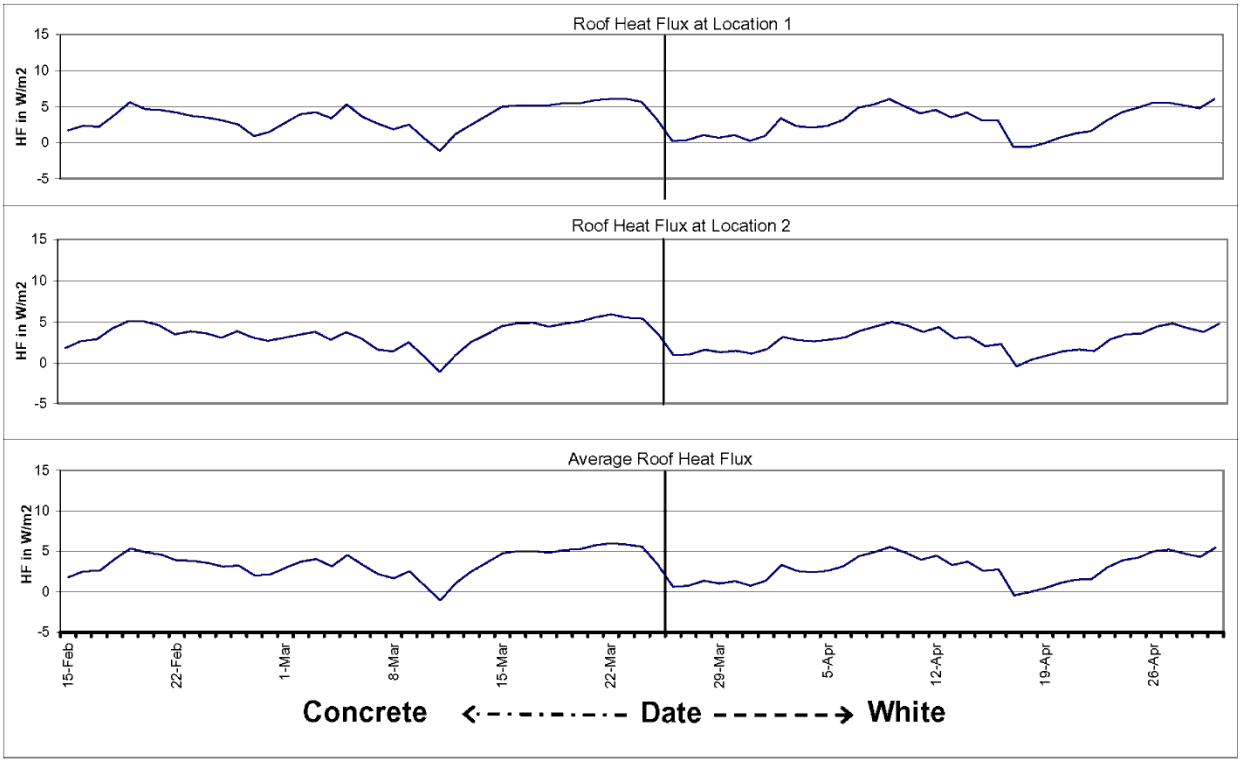

Figure 23. West building, Daily heat flux. Concrete to White.

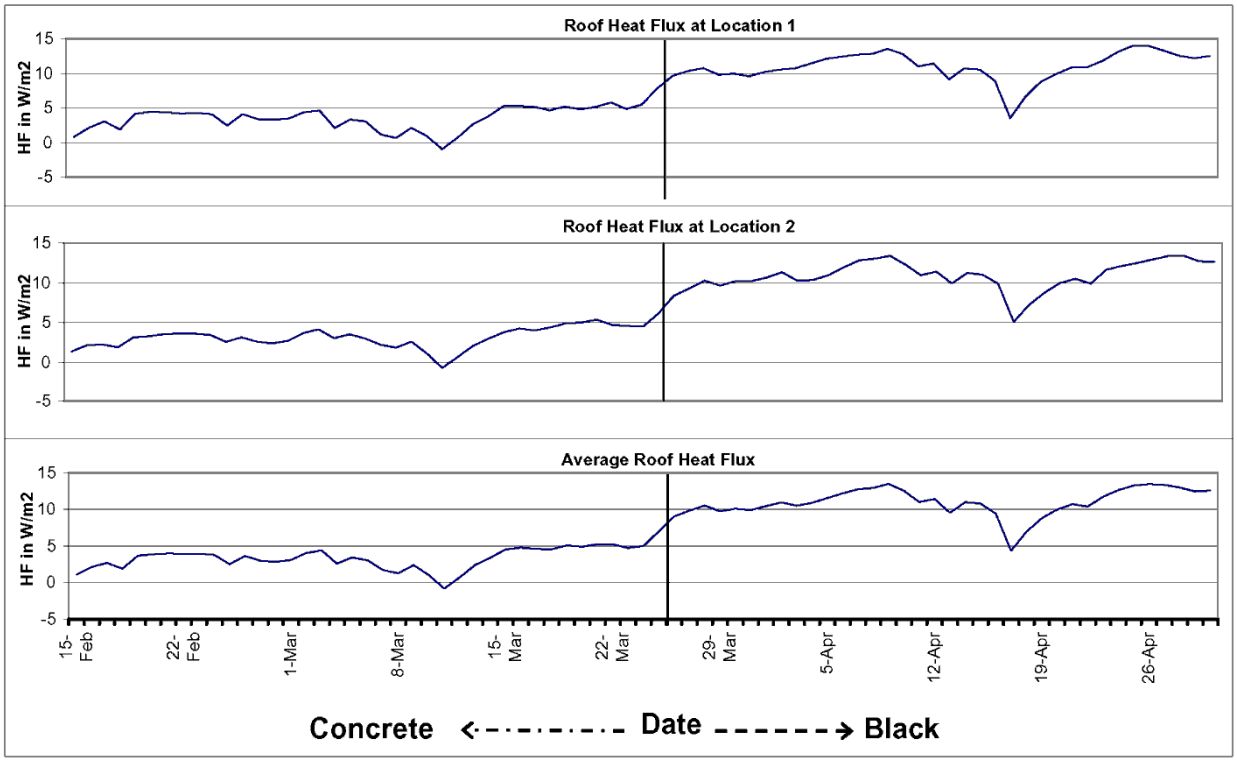

Figure 24. East building, Daily heat flux. Concrete to Black.

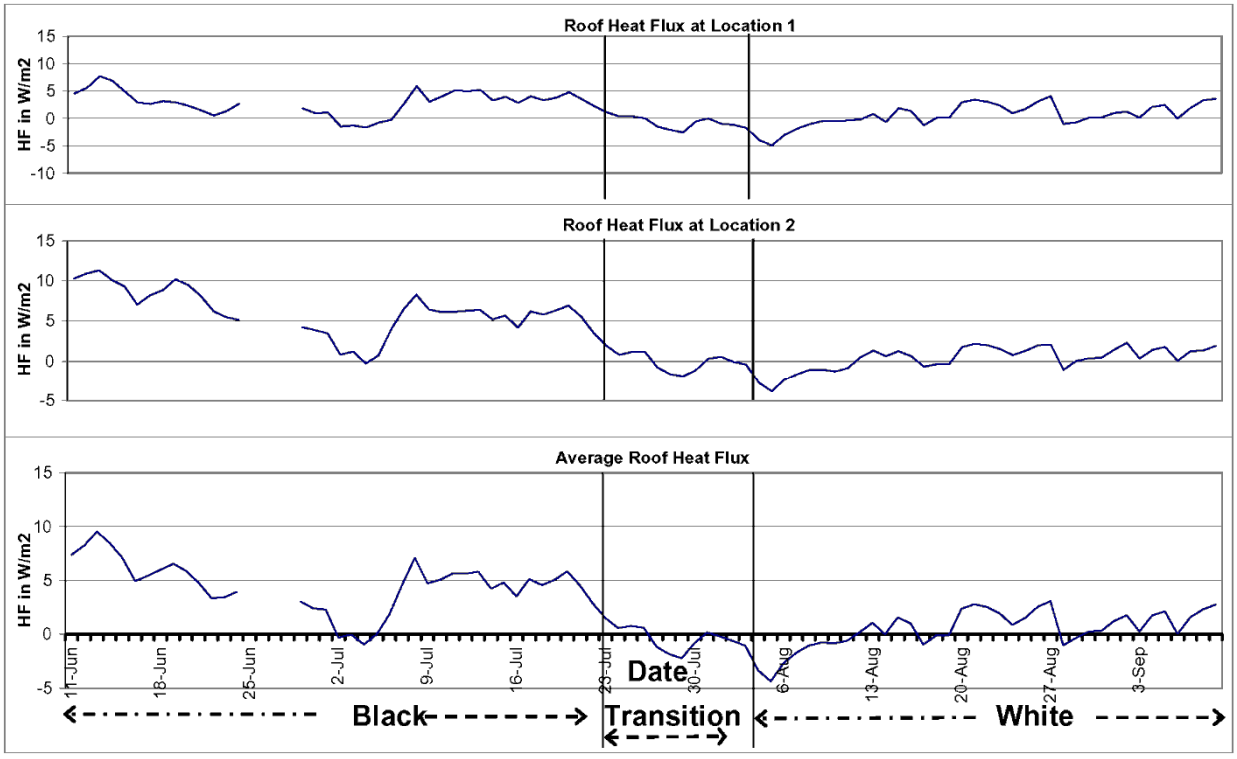

Figure 25. East building, Daily heat flux. Black to White.

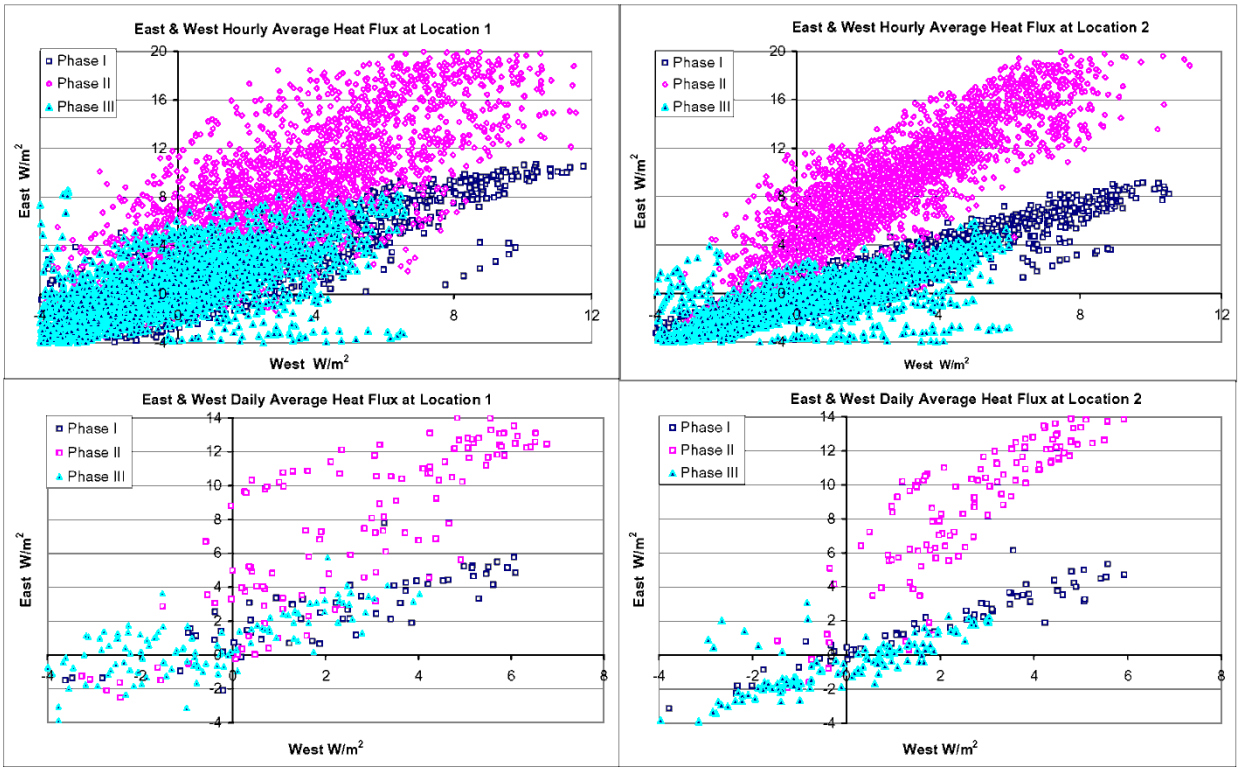

Figure 26. Comparison of roof heat flux for East and West buildings.

Figure 27 and Figure 29 show the hourly heat flux for the East building as a function of outside air and as a function of (Tout –Tin).

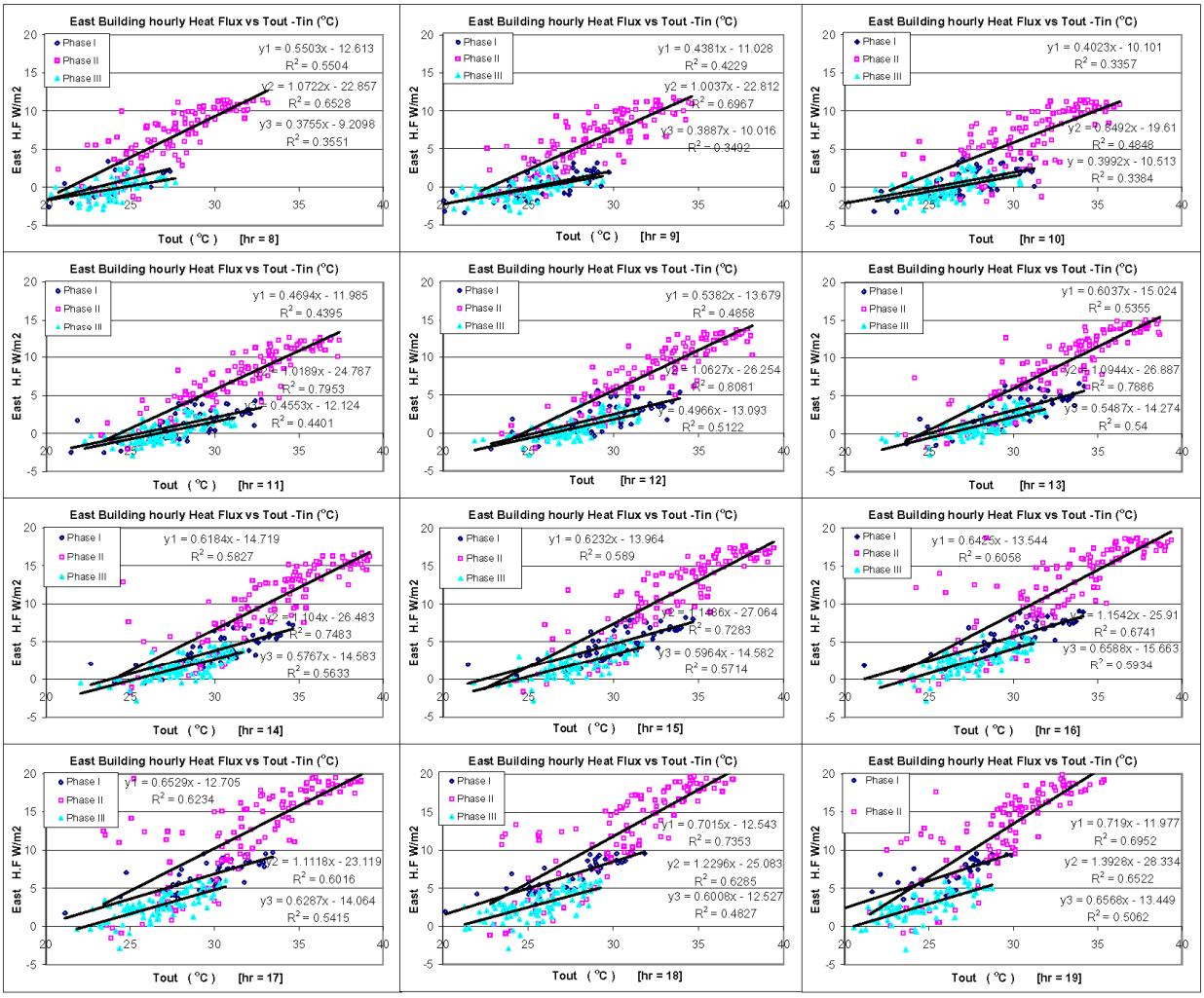

Figure 27. Roof heat flux vs. outside air temperature for the East building. (a) Hours 8-19.

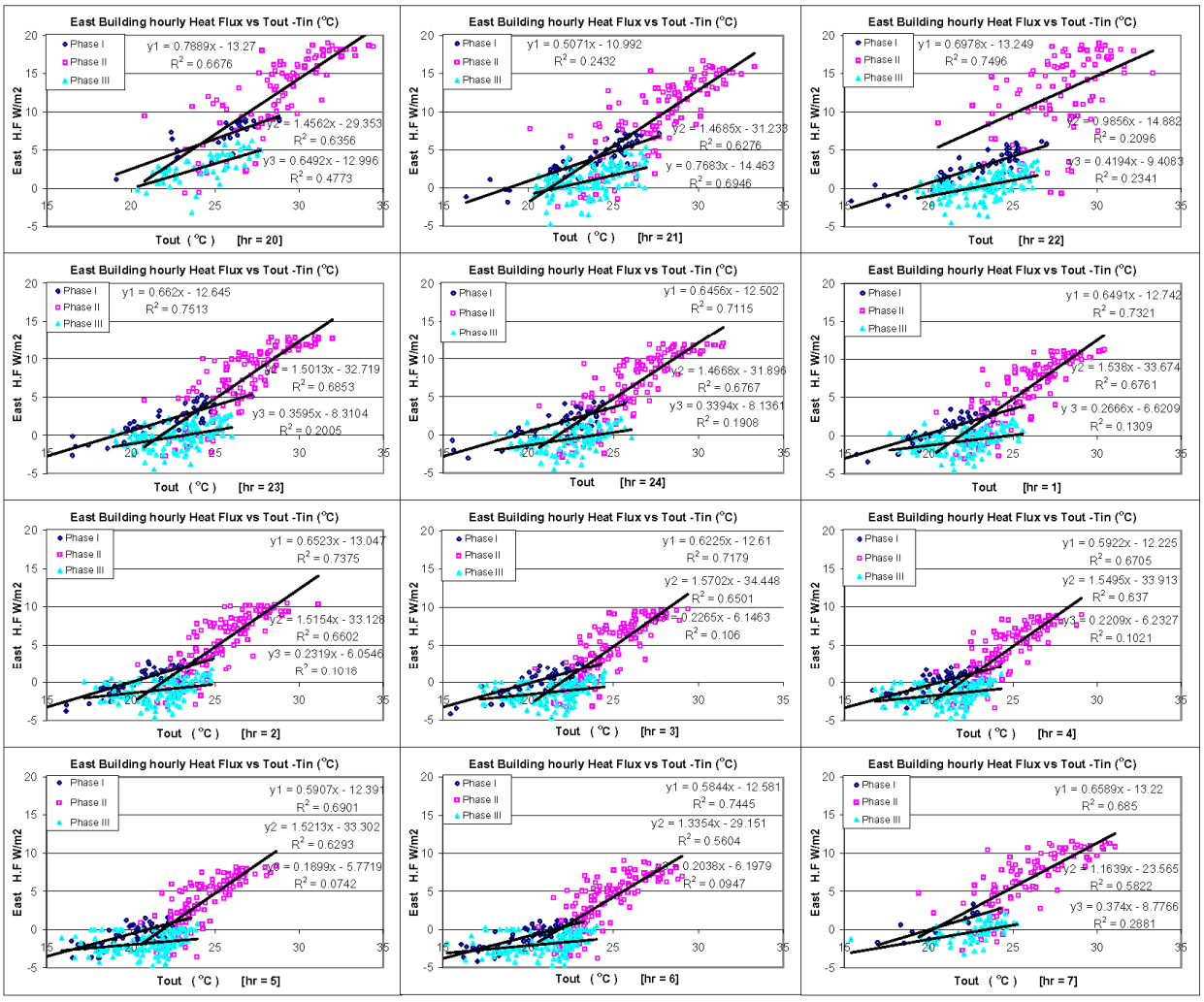

Figure 28. Roof heat flux vs. outside air temperature for the East building. (b) Hours 1-7 and 20-24.

Figure 31 and Figure 33 show the hourly heat flux for the West building as a function of outside air and as a function of (Tout –Tin).

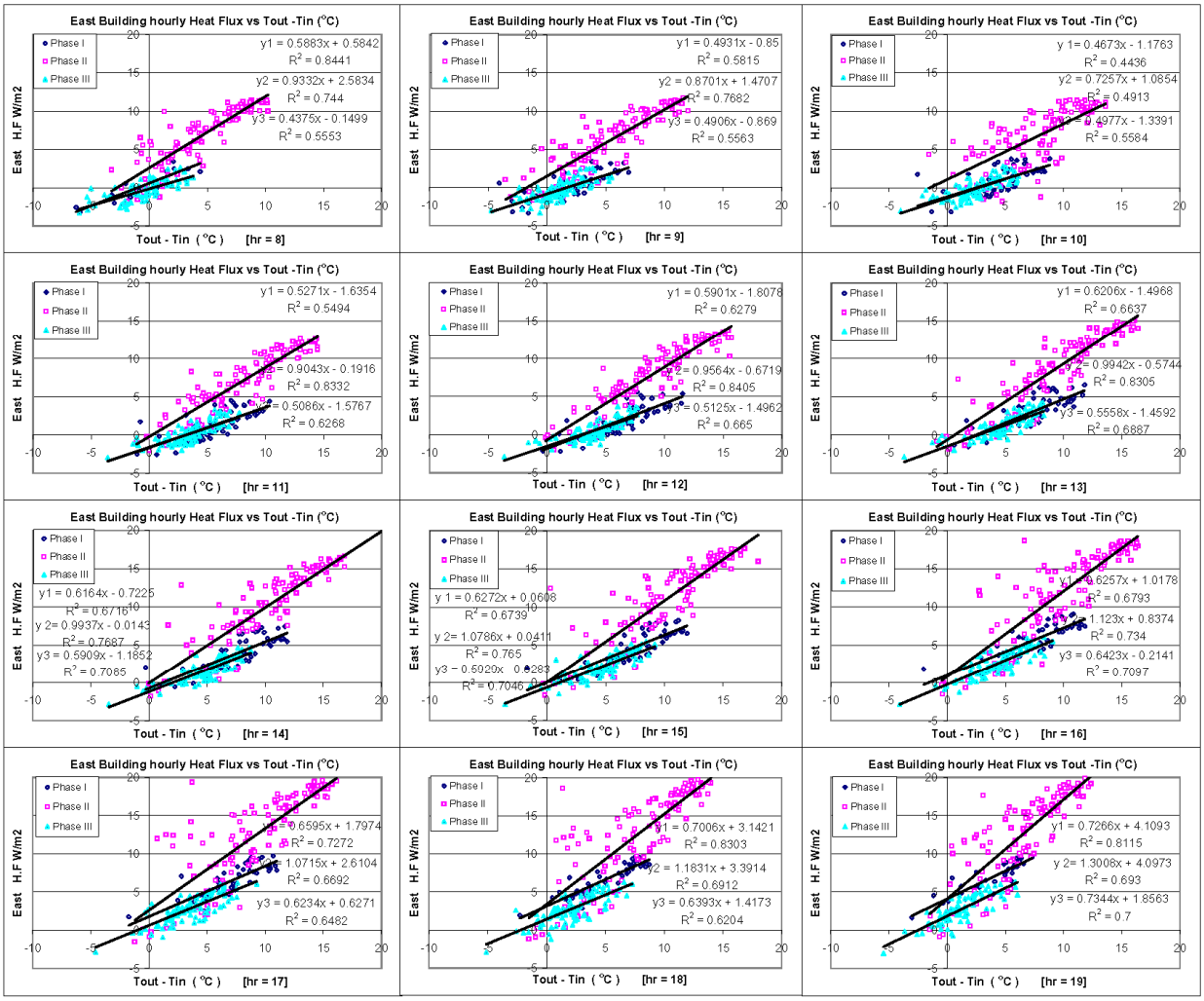

Figure 29. Roof heat flux vs. (Outside air - inside air) temperature for the East building. (a) Hours 8-19.

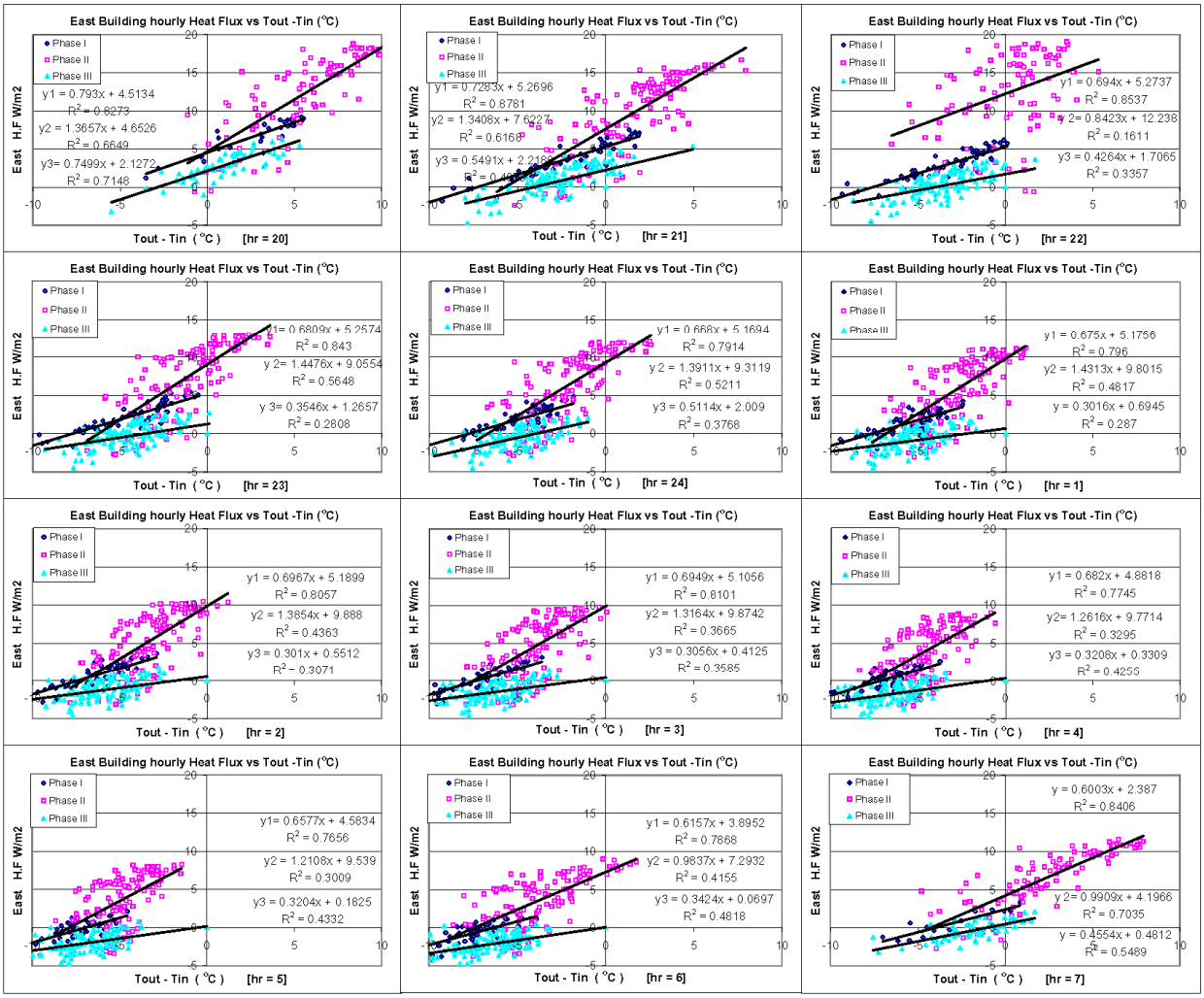

Figure 30. Roof heat flux vs. (Outside air - inside air) temperature for the East building. (b) Hours 1-7 and 20-24.

Figure 35 - Figure 38 show the daily heat flux through the roof as a function of average outside temperature and average (outside – inside) temperature, for both buildings during all monitoring phases. These figures clearly show the reduction in conduction heat flux for cool roofs vs. the hot roof. These reduced heat fluxes would directly lead to significant air conditioning savings.

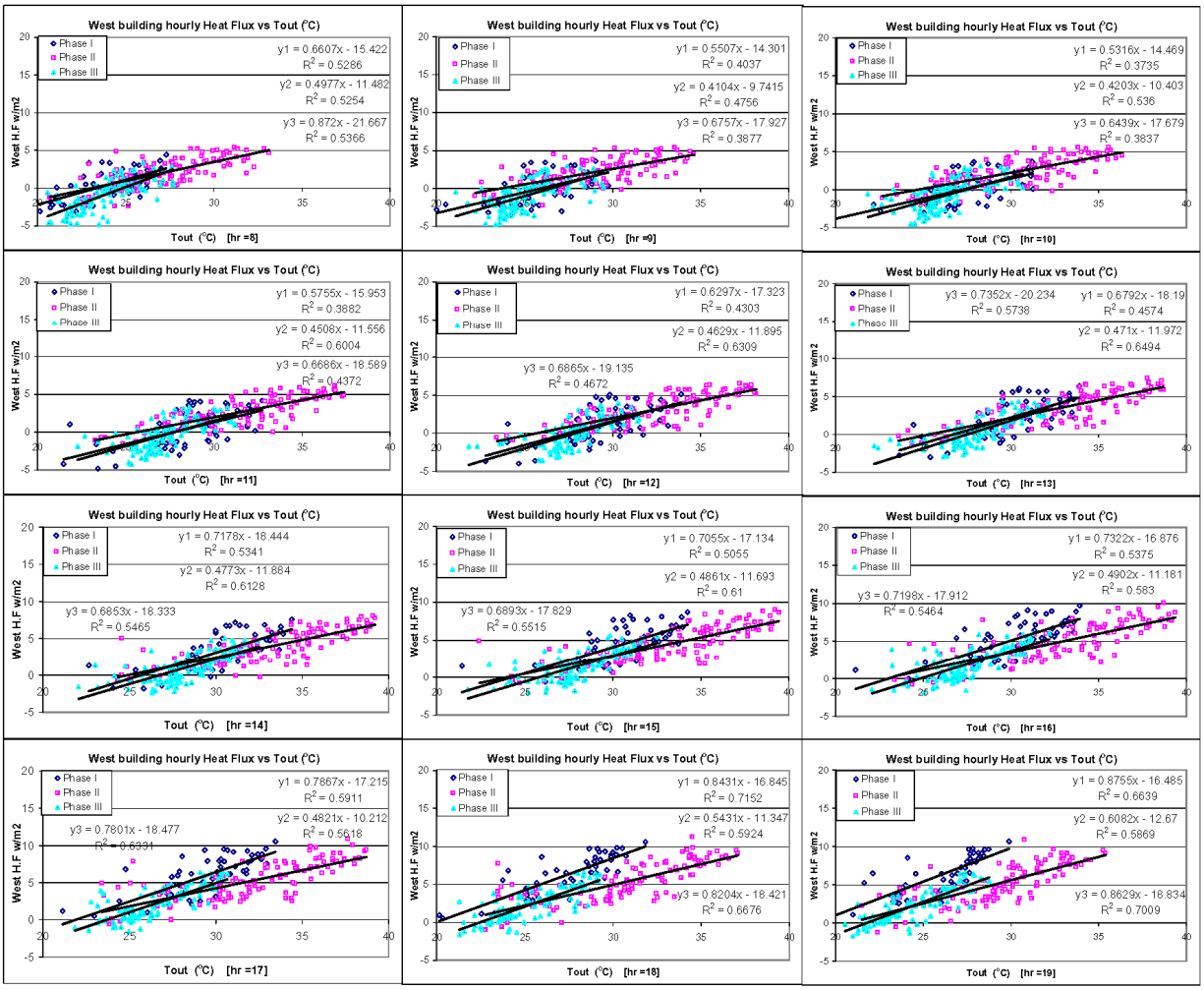

Figure 31. Roof heat flux vs. outside air temperature for the West building. (a) Hours 8-19.

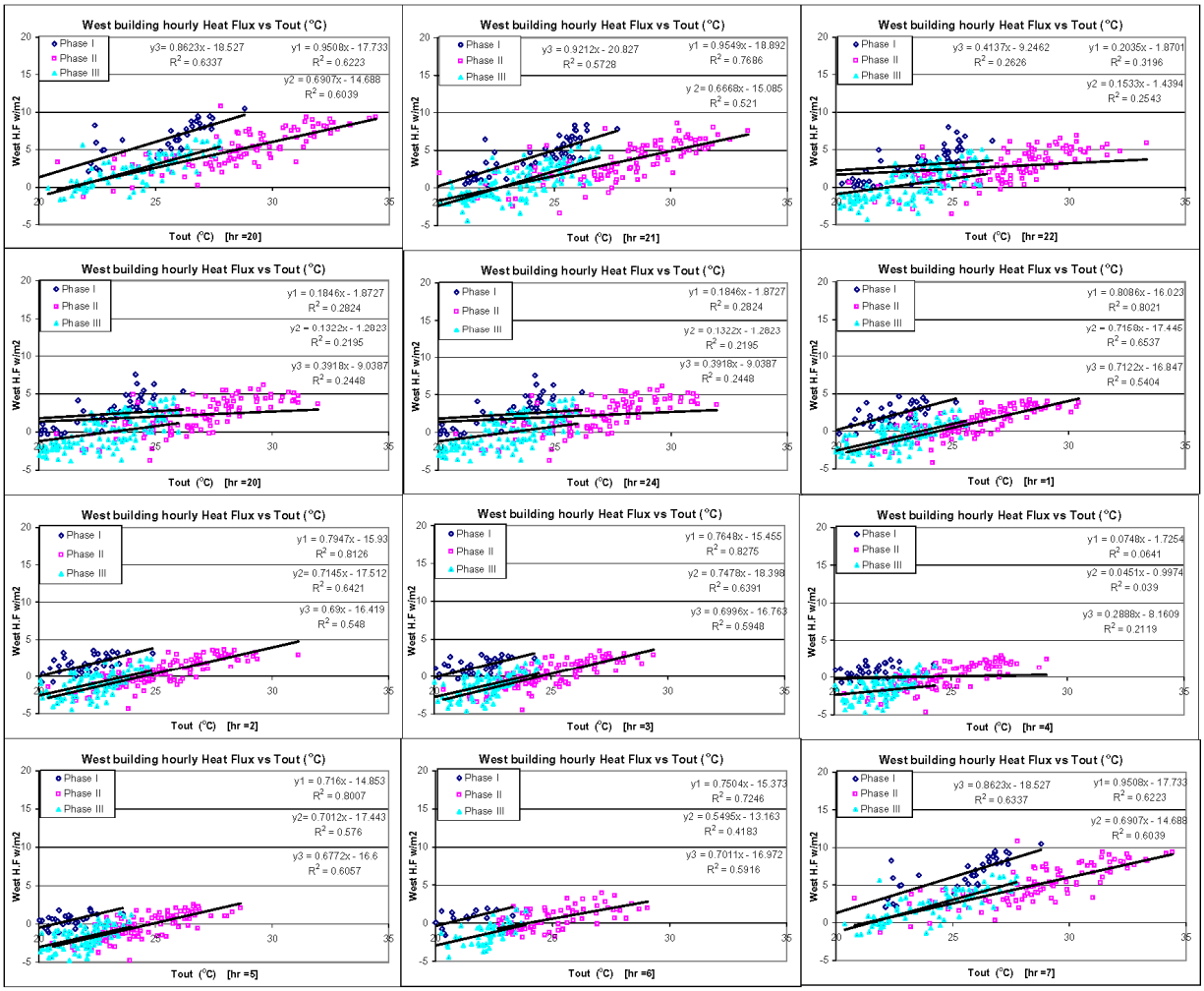

Figure 32. Roof heat flux vs. outside air temperature for the West building. (b) Hours 1-7 and 20-24.

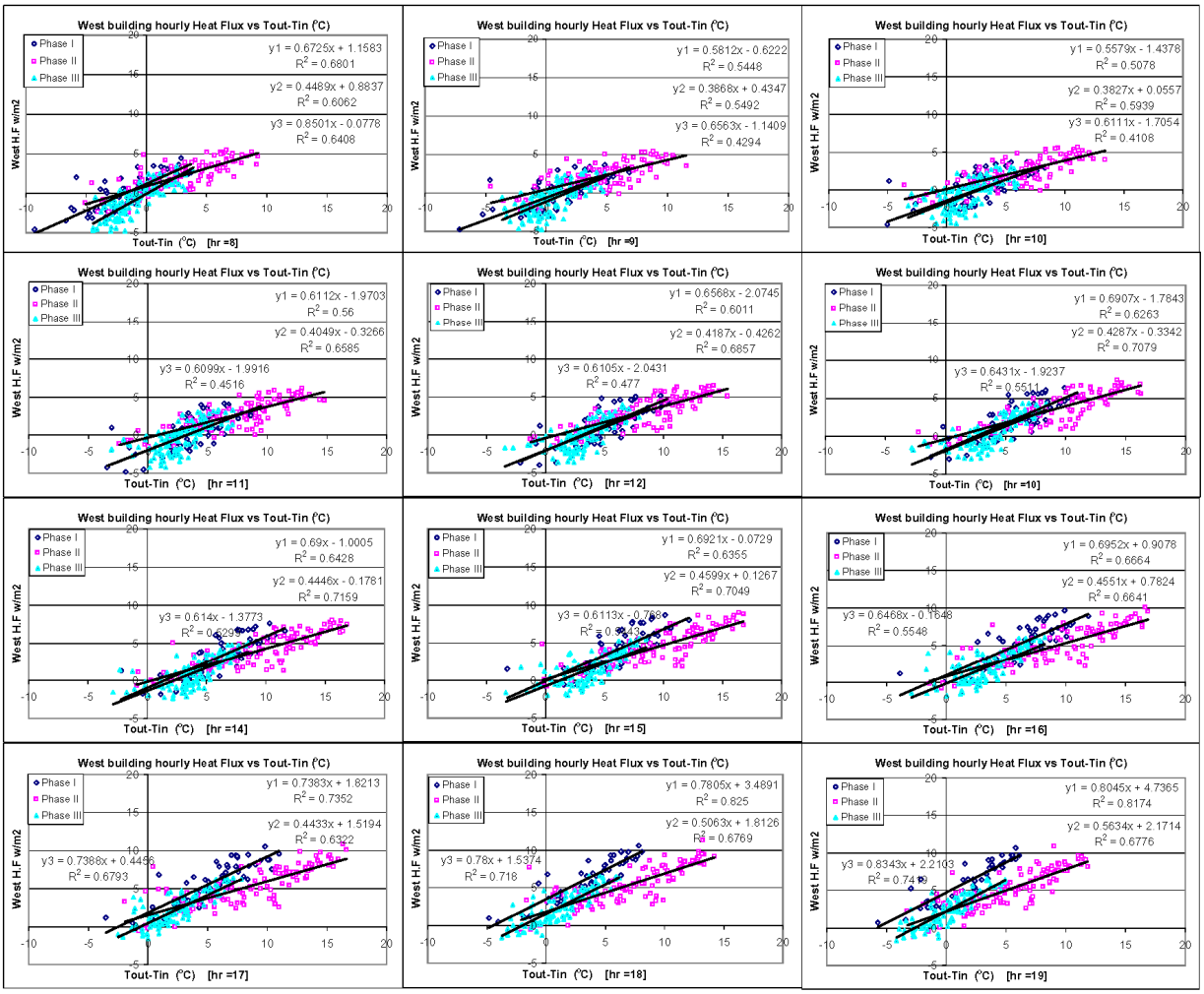

Figure 33. Roof heat flux vs. (Outside air - inside air) temperature for the West building. (a) Hours 8-19.

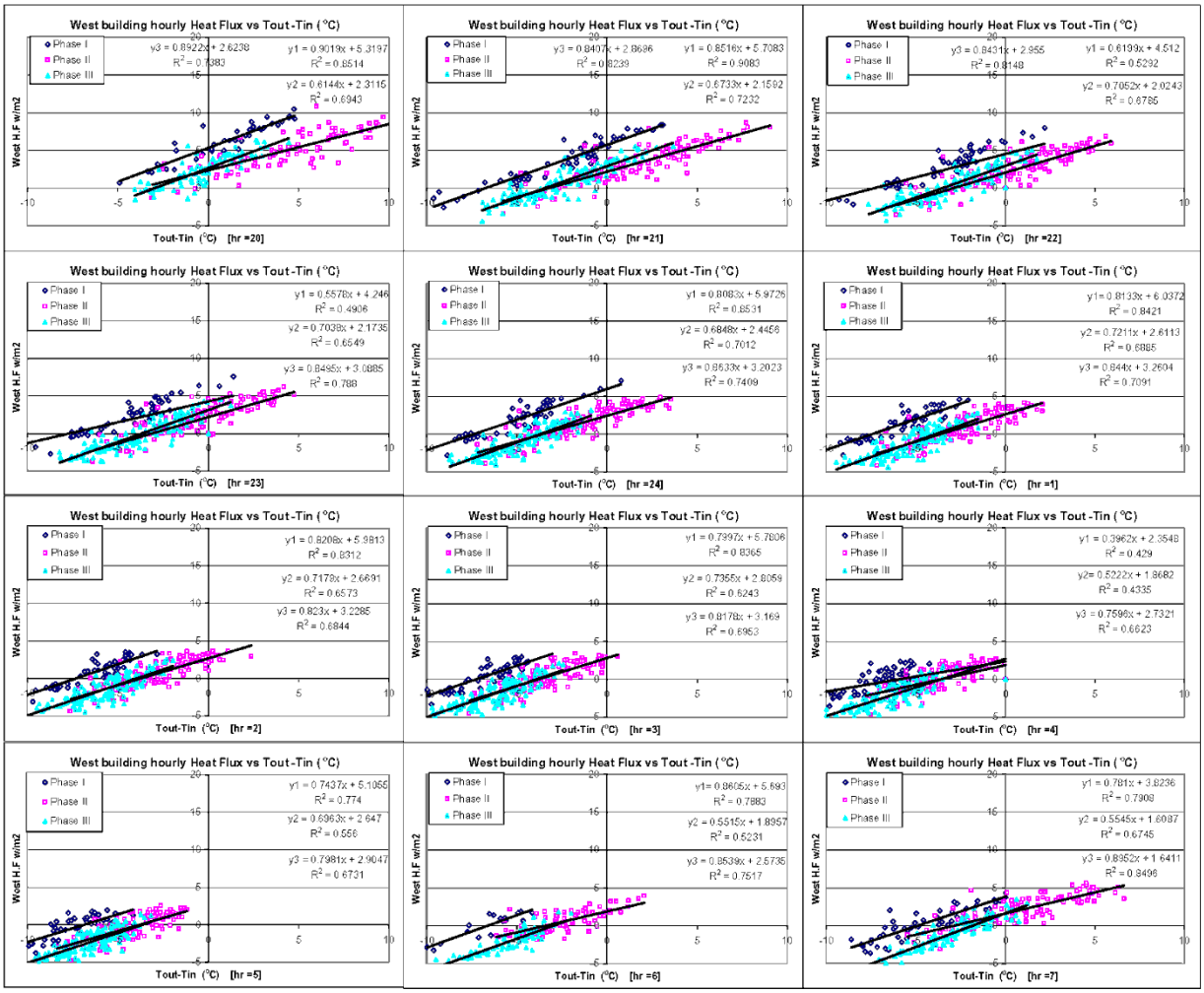

Figure 34. Roof heat flux vs. (Outside air - inside air) temperature for the West building. (b) Hours 1-7 and 20-24.

Figure 39 shows the hourly and daily heat fluxes for the East and West building vs. the outside temperature and the difference between the outside and inside temperatures. For the West building, both the hourly and daily heat fluxes are reduced when a white roof was installed (Phase II and III) compared to the concrete roof conditions. For the East building, the heat flux increased when the black roof was installed (Phase II) and decreased when the white roof was installed (Phase III). Overall, the figures presented contain interesting findings from the measured data and are included to illustrate the variation of heat flux related to the days selected.

2.4.3 Energy Use

Figure 40 - Figure 43 show the hourly and daily air conditioning and non-air conditioning energy use for a very short period before and after changing the roof color. The figures contain interesting findings from the measured data and are included to illustrate the spot savings on the days selected. The average hourly air conditioning demand is about 30-50 kW. The effect of cool coating on the air conditioning energy use is only visible for the East building when a white roof is replacing the black roof. The difference in the peak hourly demand is about 10-15 kW. The difference in the daily consumption appears to be about 50-100 kWh per day.

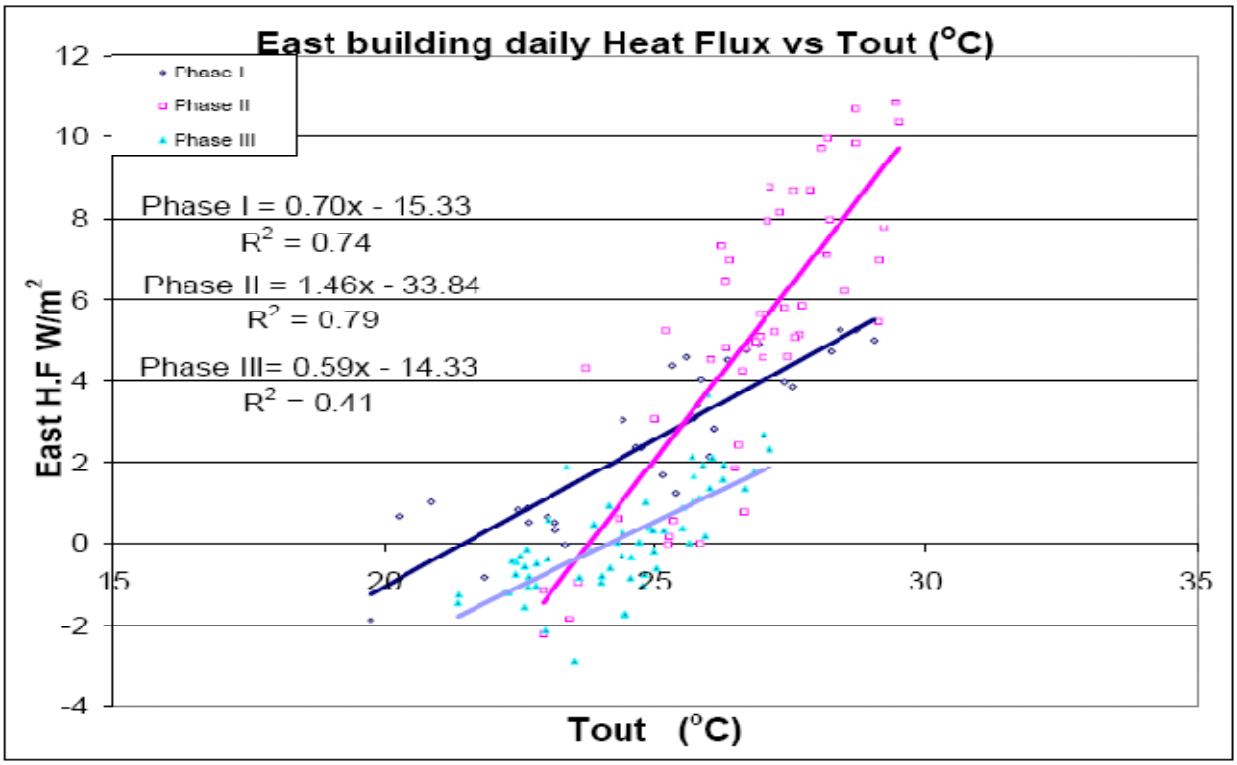

Figure 35. Daily roof heat flux vs. outside air temperature for the East building.

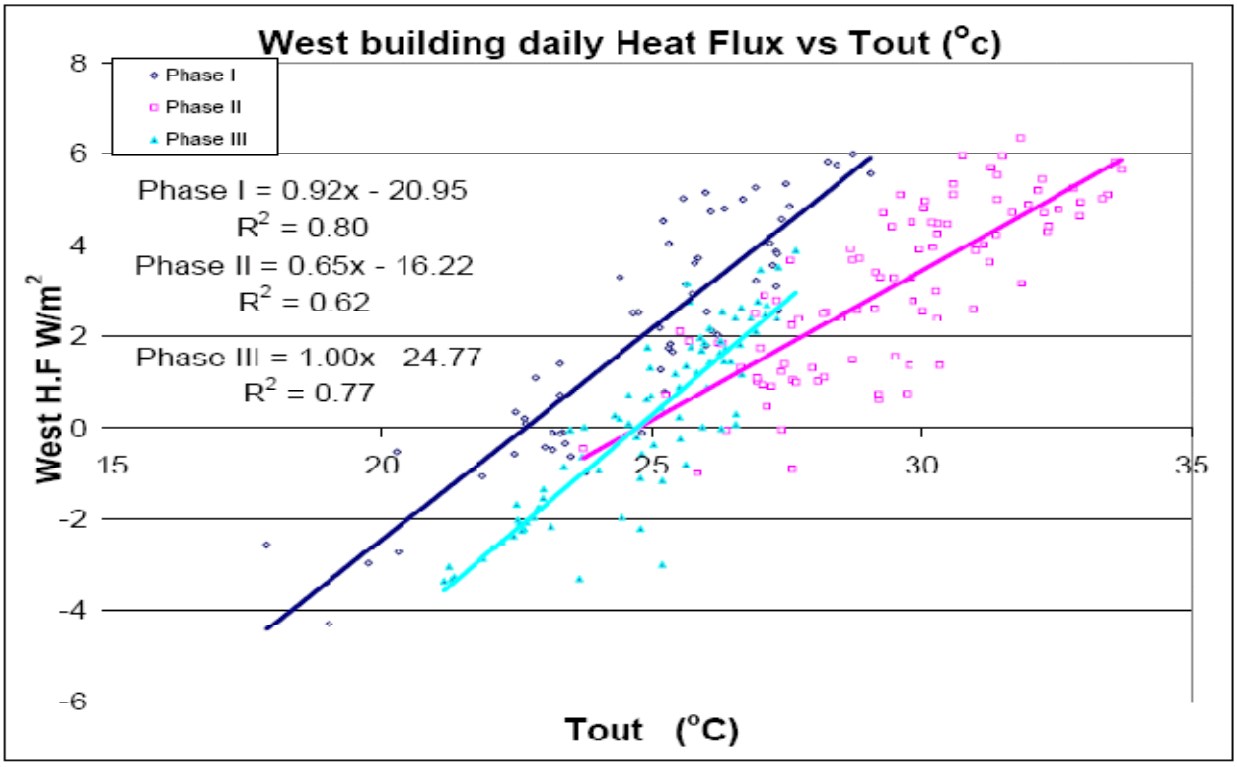

Figure 36. Daily roof heat flux vs. outside air temperature for the West building.

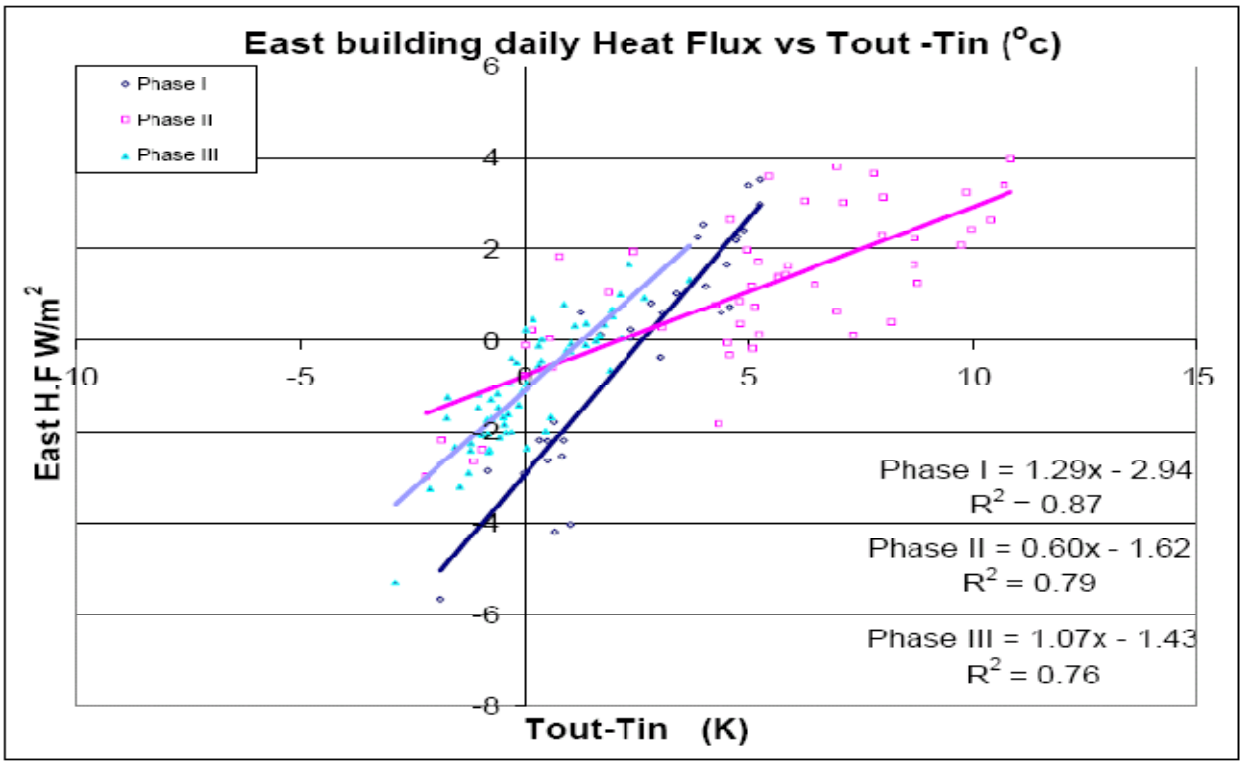

Figure 37. Daily roof heat flux vs. (outside air – inside air) temperature for the East building.

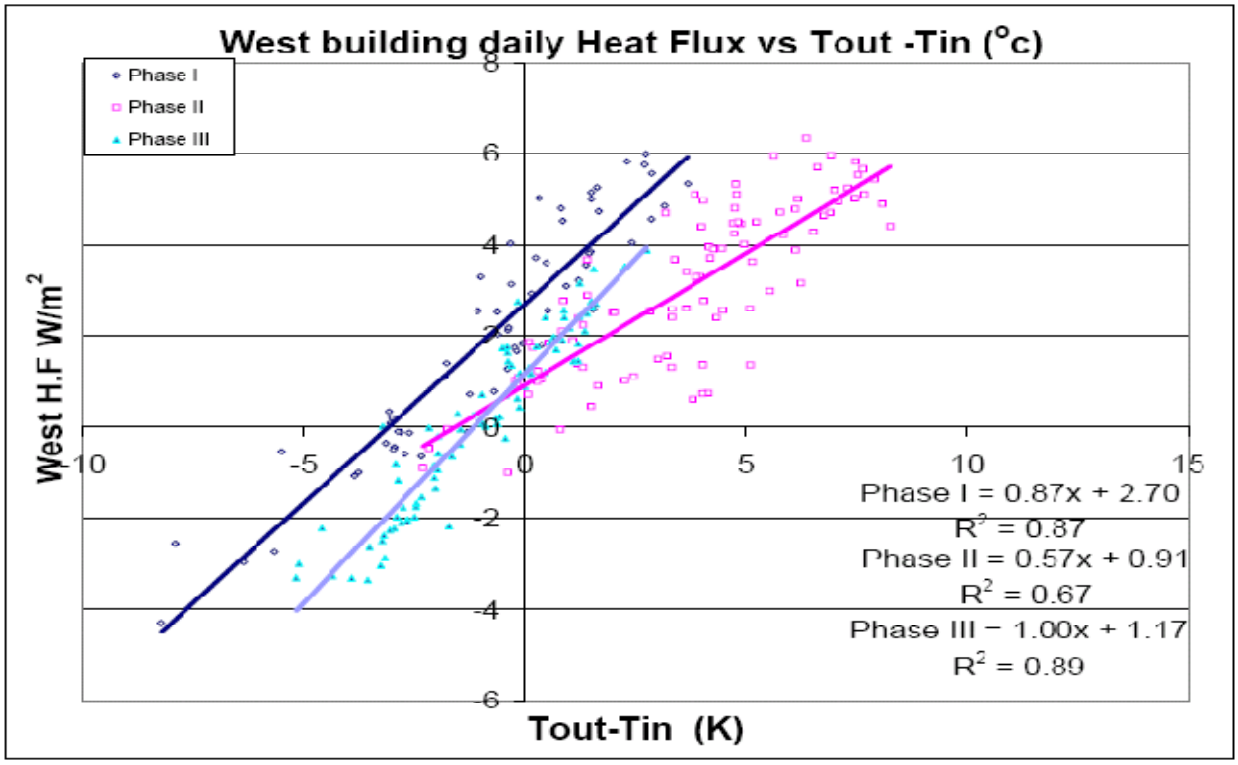

Figure 38. Daily roof heat flux vs. (outside air – inside air) temperature for the West building.

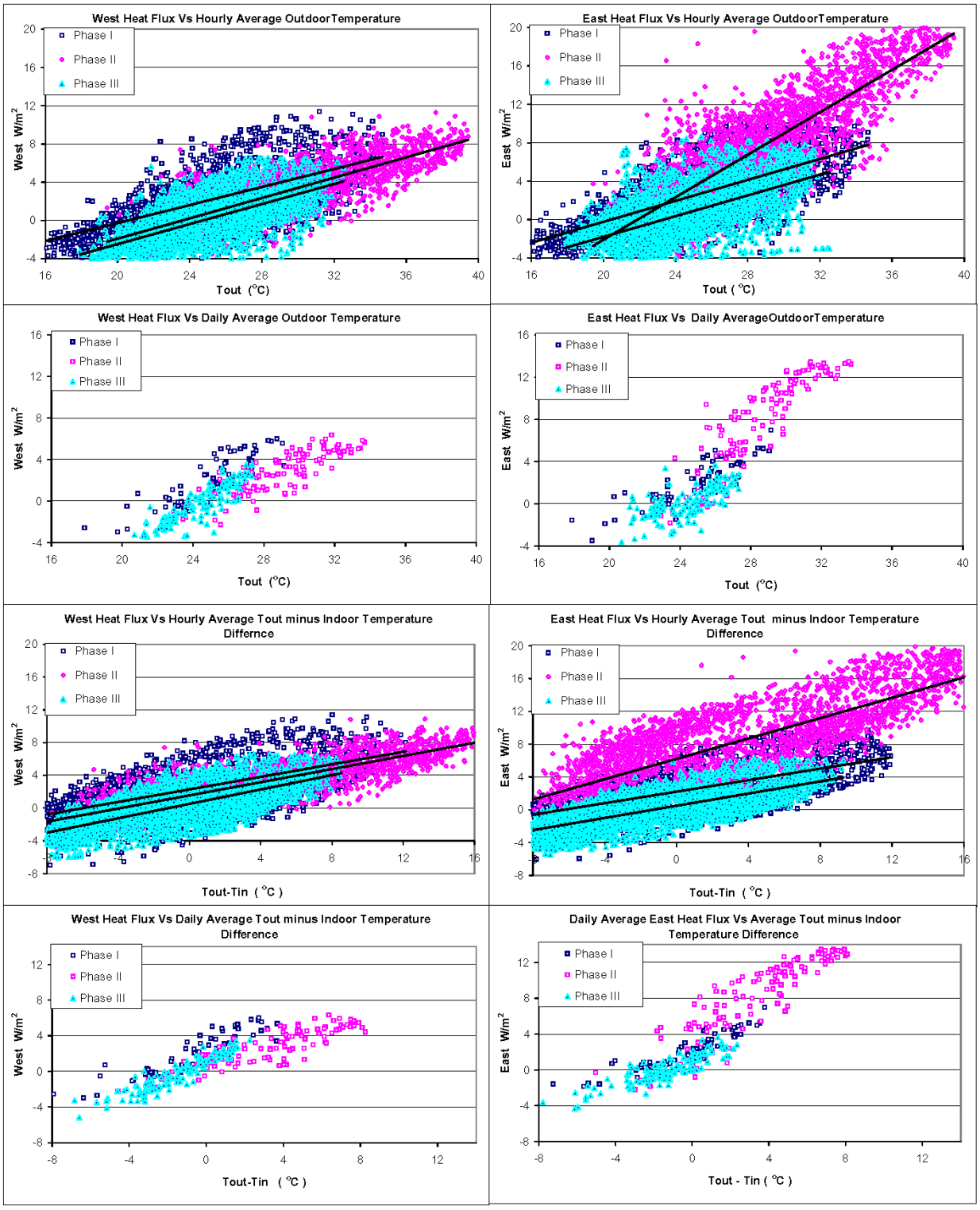

Figure 39. Hourly and daily heat flux for the East and West building vs. the outside temperature and the difference between the outside and inside temperatures.

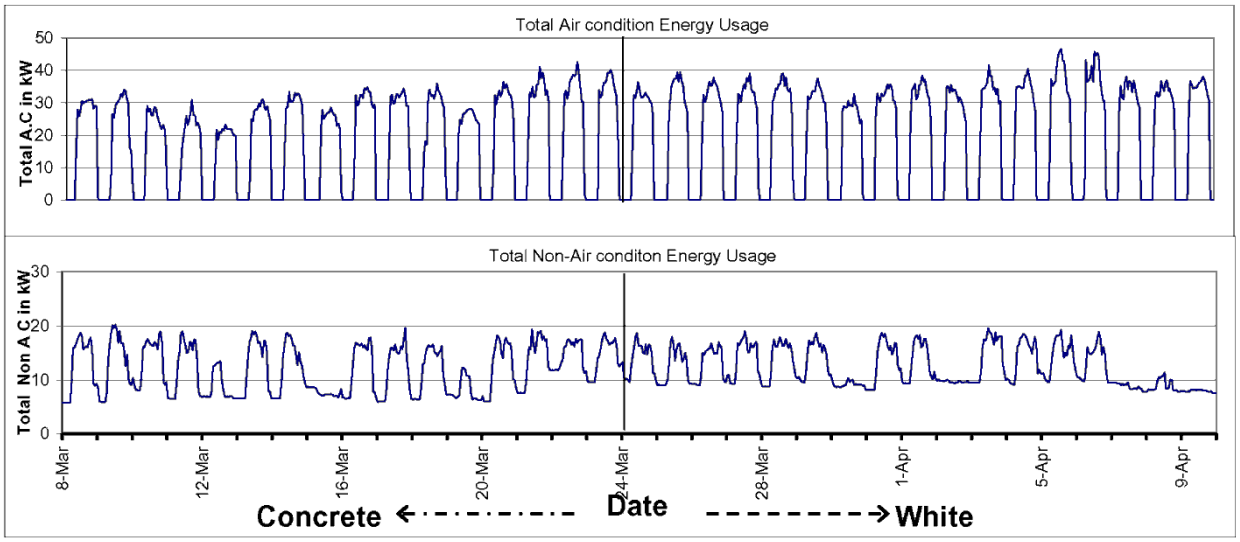

Figure 40. Hourly time series of air conditioning and non-conditioning electricity use for the West building going from concrete roof to white roof.

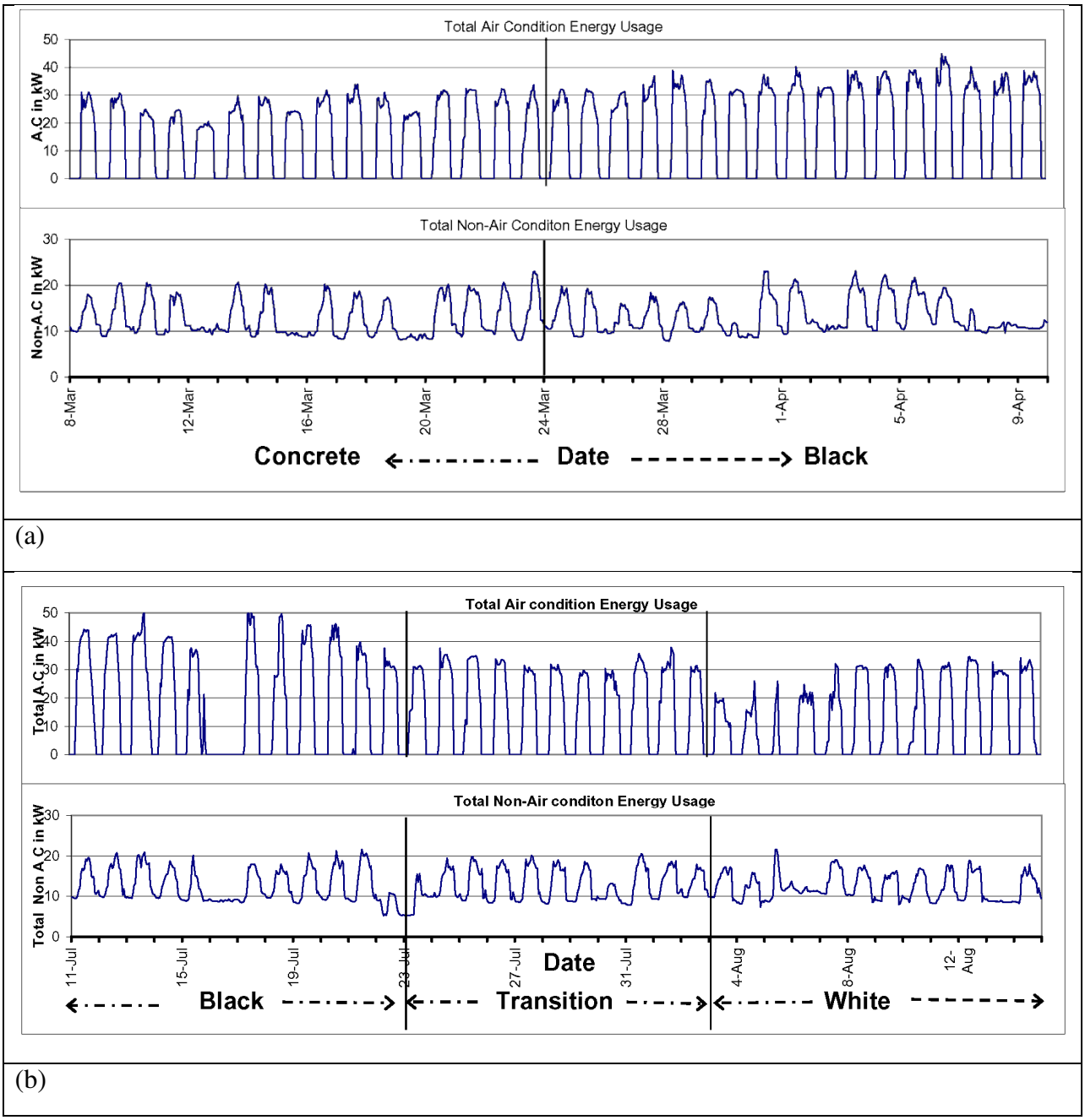

Figure 41. Hourly time series of air conditioning and non-conditioning electricity use for the East building (a) going from concrete roof to black roof, (b) going from black roof to white roof.

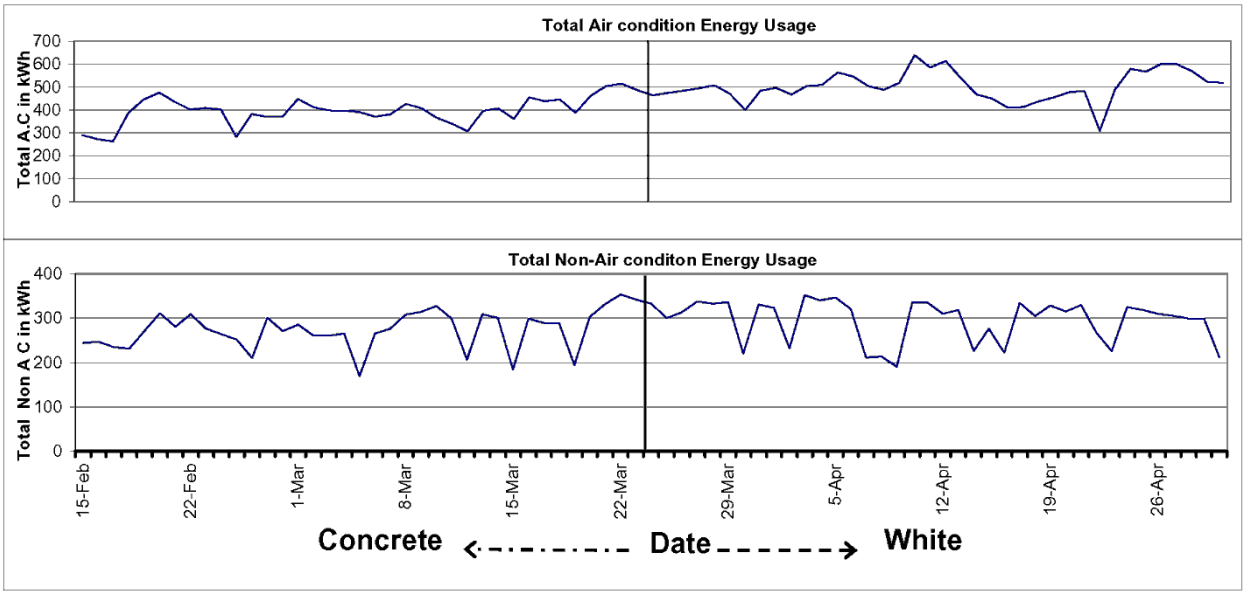

Figure 42. Daily time series of air conditioning and non-conditioning electricity use for the West building going from concrete roof to white roof.

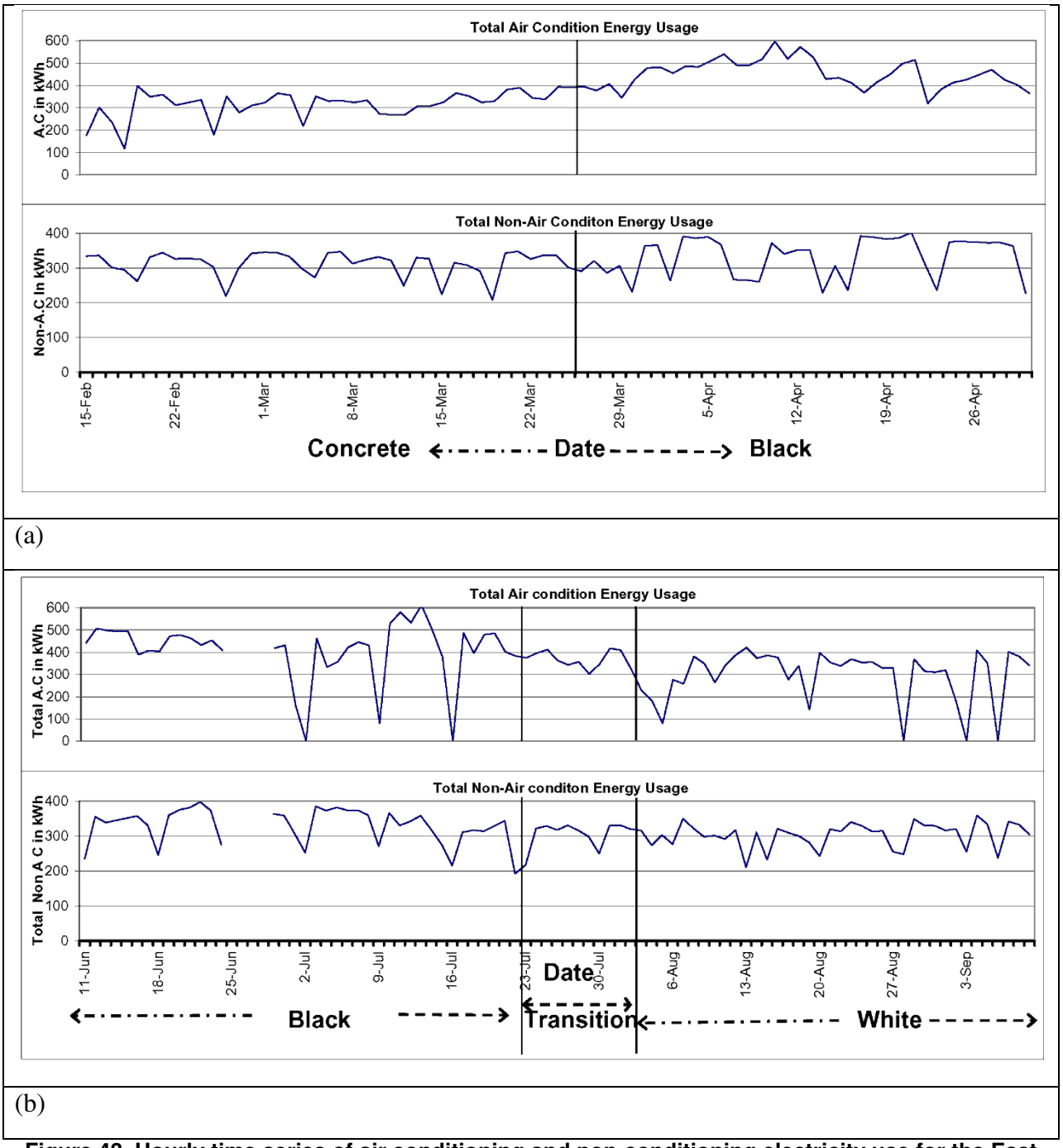

Figure 43. Hourly time series of air conditioning and non-conditioning electricity use for the East building (a) going from concrete roof to black roof, (b) going from black roof to white roof.

Figure 44 and Figure 45 show the hourly air conditioning energy use for East and West buildings plotted against the hourly temperature. The air conditioning energy use for the East building during the Phase II (black roof) for hours 9-18 is about 6-7 kW higher than AC energy use for both Phase I (concrete roof) and Phase III (white roof). The difference in hourly air conditioning energy use between Phase I and Phase III is about 1-2 kW. The estimated daily electricity savings between the Phase I to Phase III is about 10-20 kWh/day on the selected days.

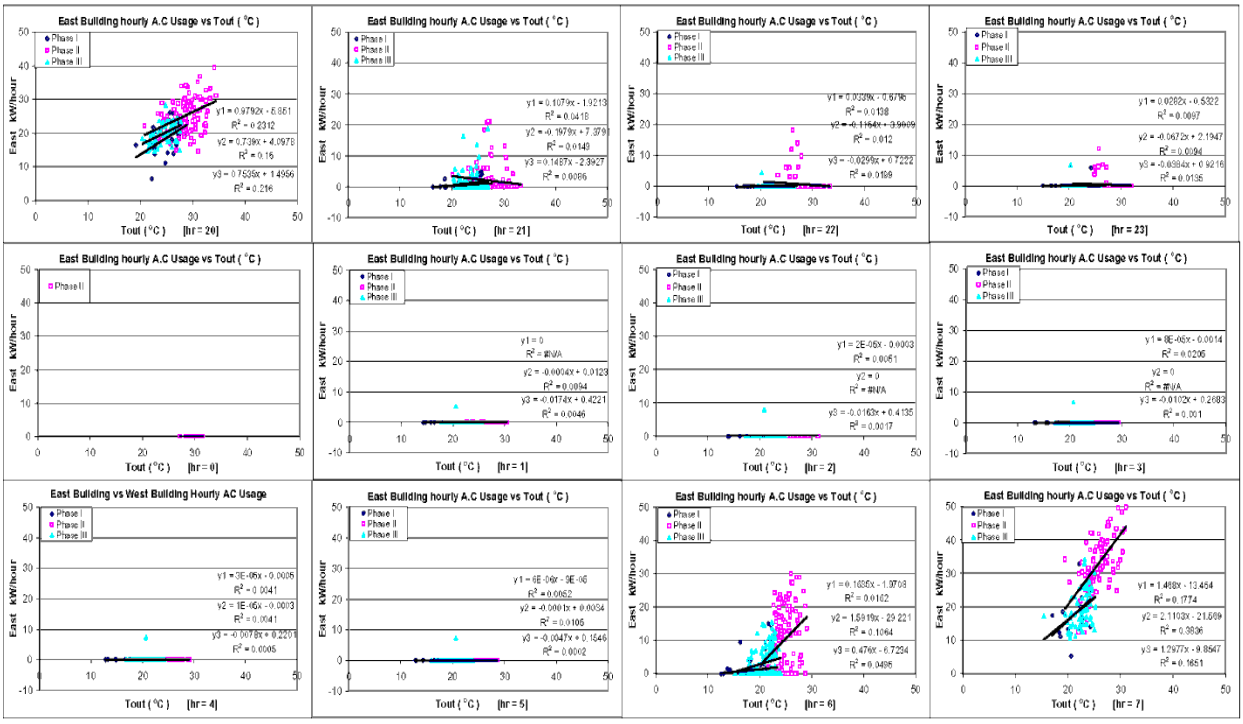

Figure 44. East hourly AC use vs. Tout

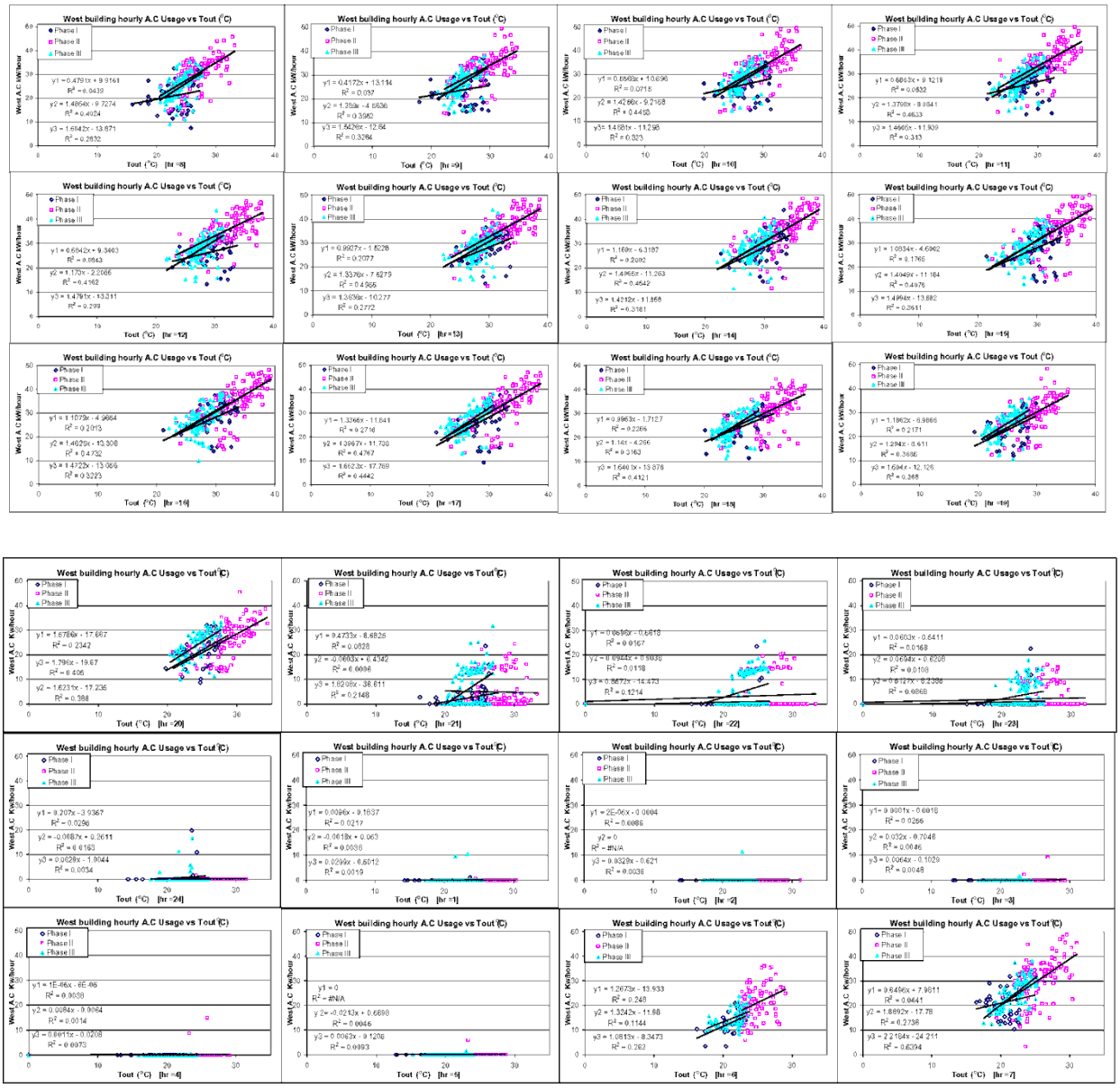

Figure 45. West hourly AC use vs. Tout

The same observations can be made by looking at the plots of hourly air-conditioning energy use vs. the difference between outside and inside temperatures in Figure 46 and Figure 47

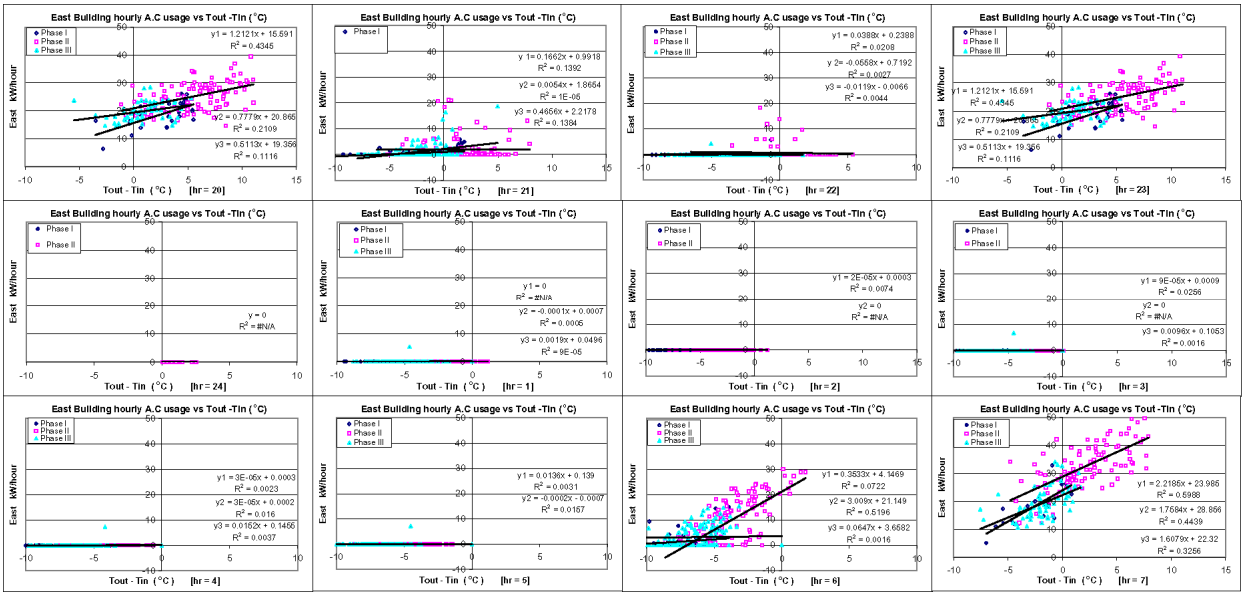

Figure 46. East hourly AC use vs. Tout – Tin

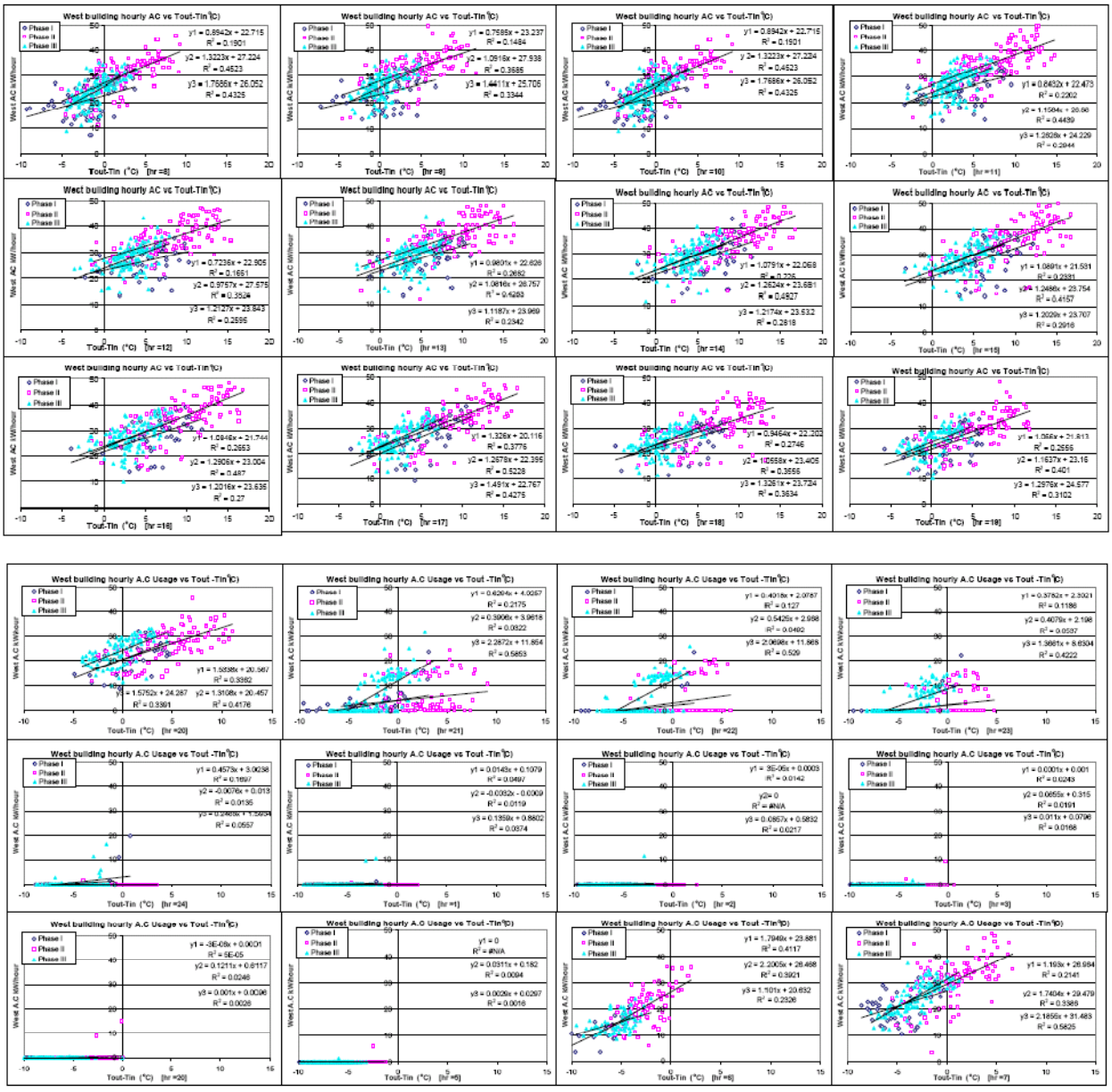

Figure 47. West hourly AC use vs. Tout – Tin

Attachment 3. Meteorological Simulations for Hyderabad, India[2]

We performed meteorological simulations to quantify the effect of heat island mitigation measures on urban climates. Hyderabad, India was selected as the region for model simulations. The effects of heat-island mitigation measures (cool roofs, cool pavements, and urban vegetation) on environmental temperatures were evaluated. The hypothesis is that cool surfaces and urban vegetation would reduce air temperatures in the region during hot summer seasons, thus mitigating urban heat-island impacts. A cooler urban environment can reduce cooling energy use in buildings, reduce air pollution and improve air quality, improve pedestrian comfort, and by reducing cooling electricity use, reduce greenhouse gas (GHG) emissions from power plants.

We carried out preliminary meteorological simulations in the Hyderabad region and characterize the effects of the heat island mitigations measures. The simulation approach was developed to perform the following meteorological-modeling tasks:

- Characterizing the modeling domains and grids in terms of land use and land cover (LULC) as well as surface physical properties,
- Developing surface-based heat-island mitigation scenarios for urban albedo and vegetative cover increase, and
- Performing multi-episodic mesoscale meteorological simulations for each base and modification scenario using the PSU/NCAR MM5.

Characterizations: The purpose of the surface characterization process is to provide three-dimensional (3-D) or two-dimensional (2-D) geometrical and physical parameter values (depending on the model parameterizations selected and used in an application) as needed in solving and scaling the conservation relations, e.g., in boundary-layer dynamics and thermodynamics. The physical characterization of the surface, in this effort, is based on the LULC makeup at each grid cell of the modeling domains. To identify LULC, we used the 24-category U.S. Geological Survey (USGS 1990) LULC classification scheme that is built into the meteorological model and available aerial photography analysis for a region encompassing Hyderabad and surrounding areas.

For this purpose, the earthPRO data were used over a sub-domain of 35×30 km around the urbanized regions of Hyderabad (blue rectangle in Figure 48). Fields of interest that were derived include 1) albedo, 2) emissivity, 3) roughness length, 4) soil moisture content, and 5) thermal inertia. For this purpose, a portion of the 1-km domain shown in Figure 48 is analyzed in further detail based on earthPRO data. The analysis sub-domain is shown again in Figure 49 and delineated with a large white rectangle.

[2] The quality and quantity of available data and resources in India for urban climate and air quality simulations were low. We invited several organizations including EPTRI, IIT, Indian Meteorological Department (IMD) for collaborating in this project. In spite of significant initial interest, however, we discovered that because of the lack of prior modeling experience in this area it would be best to conduct most of the analysis at LBNL, and then share the results in an outreach workshop and conference.

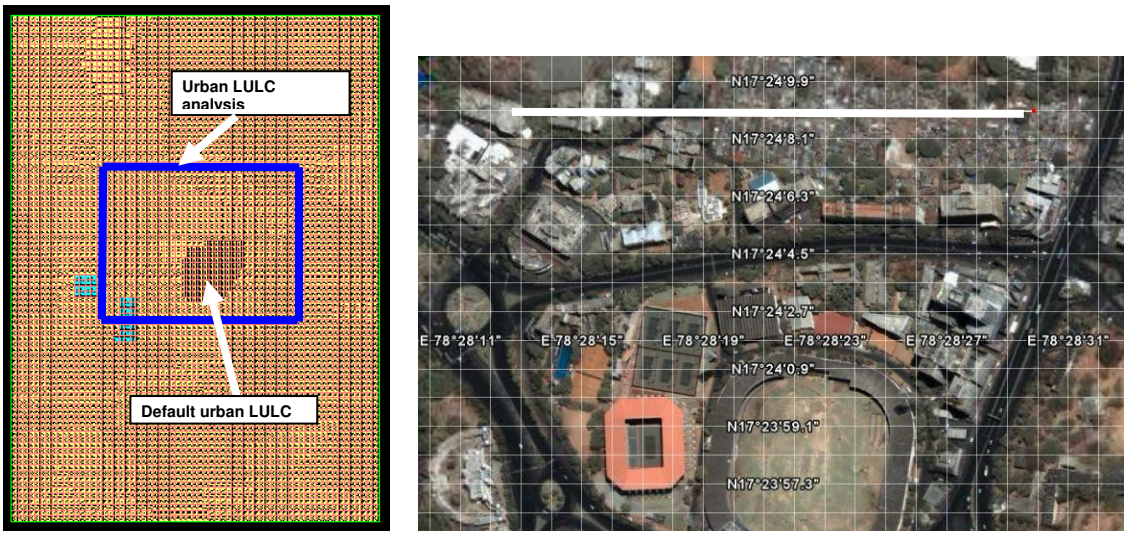

Figure 48. Left: 1-km (fourth) MM5 domain with the earthPRO analysis sub-domain shown with a blue rectangle. Right: an example detail from earthPRO data for Hyderabad (the thick white line is 1 km).

Figure 49. Sub-domain (dimensions: EW = 35 km, NS = 30 km) for 1-km LULC and surface characterization.

This sub-domain (light-white rectangle) corresponds to blue rectangle shown in Figure 1. W-E, S-N coordinates are 78.3°E – 78.6°E, 17.23°N – 17.56°N. The small bold white rectangle is for time-series analysis (denser urbanized areas).

Figure 50 shows the resulting albedo and soil moisture fields on the 1-km MM5 grid in this application (other fields such as those of roughness length and thermal inertia are not shown here). As can be seen, the average albedo of the urban area in Hyderabad (at 1 km resolution) is about 0.13 and the average soil moisture is at 0.01, which is similar to other urban areas in Europe or the U.S. Many urban regions have area-wide average albedos in the range of 0.1 to 0.18 which depends on several factors including urban geometry. Soil moisture content is similar to that used in mesoscale modeling (e.g., MM5).

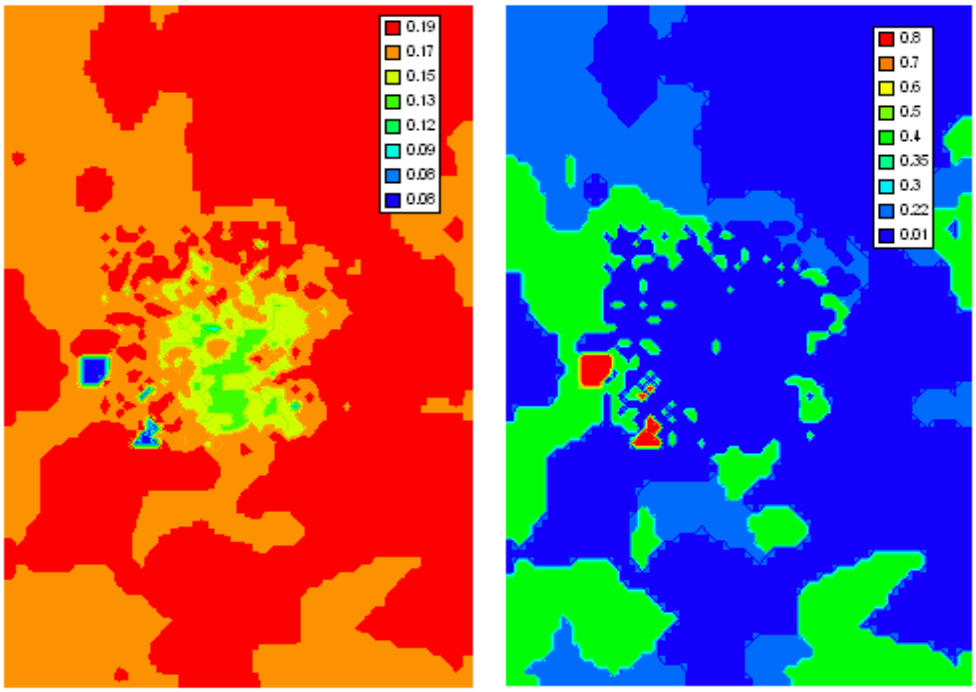

Figure 50. Base-case albedo (left) and soil moisture (right) on the 1-km MM5 grid. These fields were developed by meshing results from the earthPRO analysis with the background default MM5 LULC and properties input.

Scenarios: Three cases (one base case and two mitigation scenarios) per episode were simulated. The base case is identified as case00. The base values for albedo (per surface type, not land use) were estimated by evaluating aerial photography of the region. These are listed in Table 9 for each surface type as an average over the modeled region. In a similar manner (aerial photography) the base vegetative cover was also estimated. It is listed as an average per LULC in Table 10. These values are then weighted by the surface aerial makeup in each model grid cell and the gridded values of albedo and soil moisture computed accordingly.

The heat-island mitigation scenarios evaluated here are

1) A combined moderate increase in albedo and vegetation cover (case11), and
2) Higher combined increases in albedo and vegetation cover (case22).

The basis for developing these surface modification scenarios is summarized in the last two columns of Table 9 and Table 10. Table 9 lists the increases in albedo for each surface type of interest, whereas Table 10 shows the percentage increase in vegetative cover for each of the main urban land uses. Table 11 shows the resulting values for albedo and vegetation cover increases per LULC. As mentioned above, the values in this table are for dominant LULC in each analysis sub-cell and are scaled down by the fraction of corresponding LULC in each cell.

Table 9. Assumed levels of albedo increase per surface type.

Surface type	Typical base albedo	Increase in albedo	
		Moderate increase (cases 10 and 11)	Large increase (case 20 and 22)
Residential roof	0.18	0.10	0.30
Commercial roof	0.20	0.20	0.40
Road	0.10	0.15	0.25
Sidewalk/Driveway	0.12	0.10	0.20
Parking lot	0.10	0.15	0.25

Table 10. Scenarios for vegetation cover increase

Urban categories		Typical base cover	Change for scenarios 10 and 11	Change for scenarios 20 and 22
10,11	Residential	10%	9%	18%
12,19	Commercial/Services	12%	9%	18%
13	Industrial	5%	4%	8%
7,14	Transportation/Communication	3%	2%	4%
15,18	Industrial and commercial	7%	6%	12%
16	Mixed urban or built up	10%	5.5%	11%
17	Other urban or built up	7%	5.5%	11%

Table 11. New values of surface albedo and soil moisture for perturbation scenarios

LULC		(case11)	(case11)	(case22)	(case22)
7	Sports arenas, track fields	0.250	0.05	0.3	0.07
10	Residential and unidentified built-up	0.240	0.10	0.29	0.12
11	Residential	0.217	0.13	0.27	0.15
12	Commercial/Services	0.252	0.09	0.31	0.12
13	Industrial	0.242	0.06	0.35	0.07
14	Transportation/Communication	0.245	0.03	0.27	0.03
15	Industrial and commercial	0.242	0.07	0.30	0.10
16	Mixed urban or built up	0.207	0.07	0.28	0.08
17	Other urban or built up	0.180	0.08	0.20	0.10
18	Residential and industrial	0.220	0.10	0.29	0.12
19	Residential and commercial/educational	0.220	0.10	0.29	0.12

Episodic Simulation: Three episodes were simulated in this application (two days of each episode are presented in this technical report). The episodes are:

- May 1-4, 1990 → characterized by dominant southerly flow (in the Hyderabad region)
- May 1-4, 1995 → characterized by dominant southerly flow (in the Hyderabad region)
- May 1-4, 2000 → characterized by dominant westerly and northerly flow (in Hyderabad)

Figure 51 shows a time series of simulated air temperature in an urban area of Hyderabad. The difference is relatively small between the 1990 and 1995 episodes. The 2000 episode, on the other hand, seems to have a slightly larger diurnal temperature swing, suggestive of relatively drier conditions associated with the different flow.

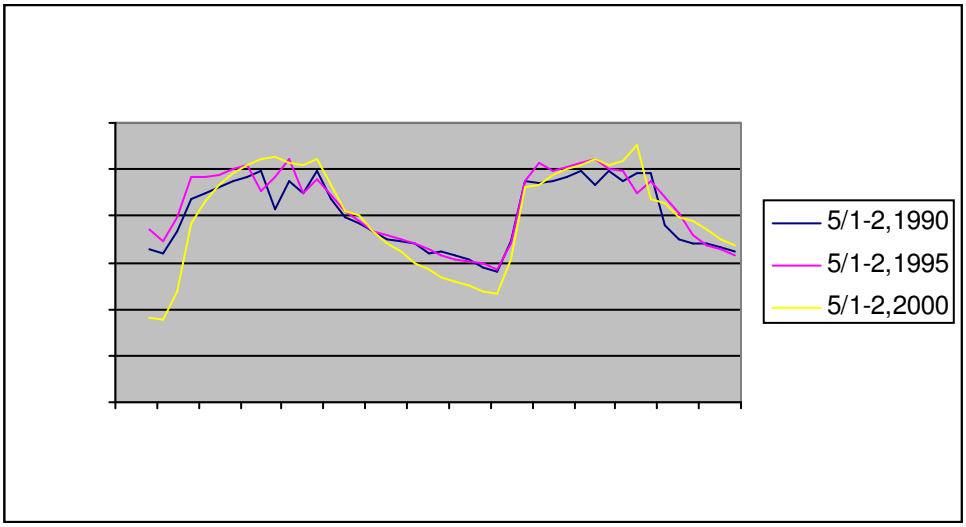

Figure 51. Urban air temperature in south Hyderabad on 2 days of three episodes. Results based on 1-km simulations.

Figure 52, Figure 53, and Figure 54 show time series of temperature differences (from the base case) for cases 11 and 22 for May 1st and 2nd of each respective year, 1990, 1995, and 2000 (episodes 1 through 3).

In these figures, temperature difference is shown in blue for case11 and in red for case22. It can be seen that that there is generally a small cooling at night but larger cooling during the day. In some cases, there is no cooling at certain hours during the day (e.g., hours 1200 through 1400 LST in episode 2 on the first day). This occurs when there are changes in the flow or mixing fields, which affect the surface heat transfer rates and thus temperature. Another feature seen in the figures is that cooling for case22 is generally larger than cooling in case11, as one would expect, but there are times when both cases 11 and 22 produce the same amount of cooling, or can even overlap when cooling in case11 exceeds cooling in case22.

Maximum cooling reaches up to 2.5°C in episodes 1 and 2 and up to 1.8°C in episode 3. Recall that this time-series analysis is only for a sample urban area south of Hyderabad and does not capture the larger cooling shown in figures above. The purpose here simply is to show the diurnal pattern of temperature change. To further evaluate the potential impacts of surface modifications, one can also calculate the number of degree hours, DH—for example, to quantify

the deviation of air temperature in the modified scenarios relative to the base case. These are summarized in Table 12 and show again the relative effectiveness of case22 versus case11.

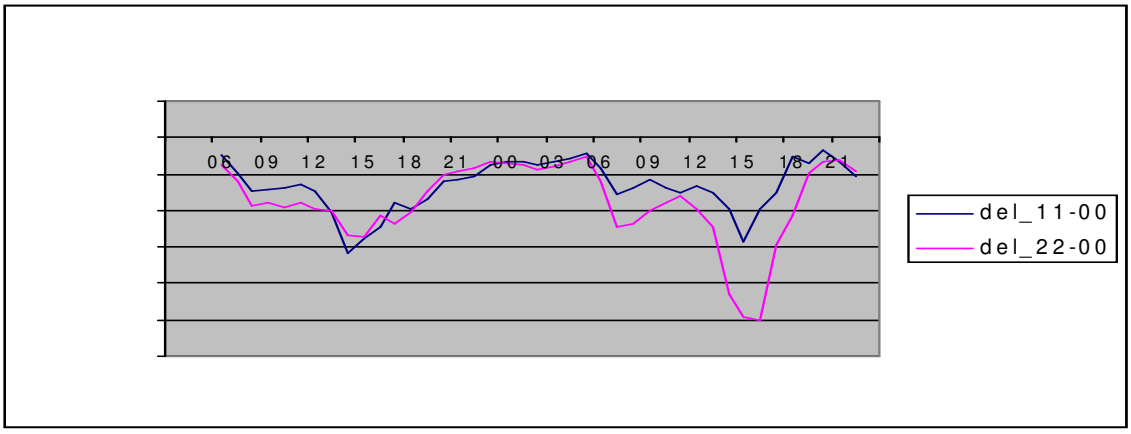

Figure 52. Temperature difference from base case for case11 and case22 for episode 1.

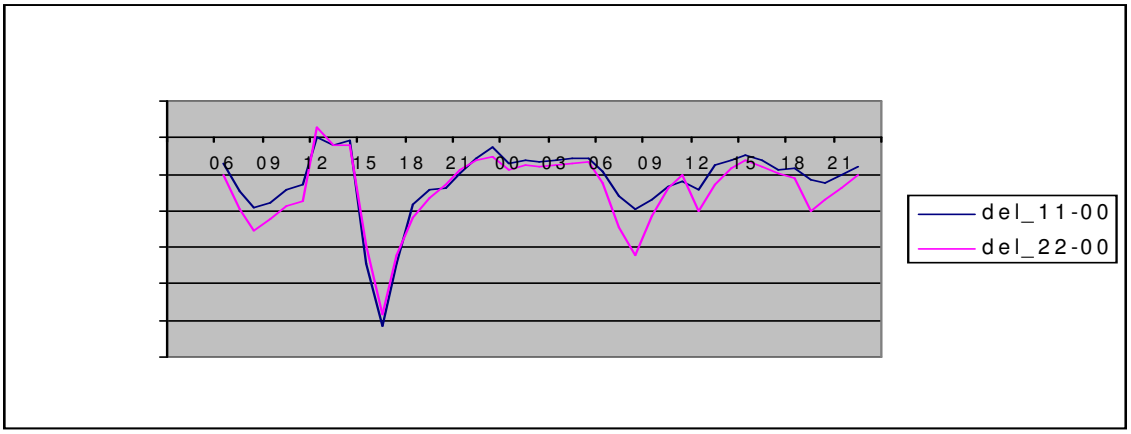

Figure 53. Temperature difference from base case for case11 and case22 for episode 2.

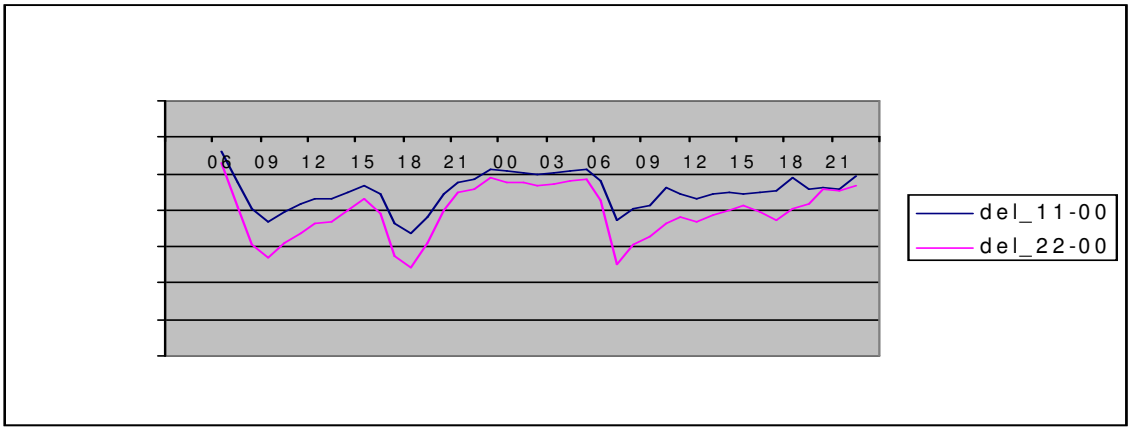

Figure 54. Temperature difference from base case for case11 and case22 for episode3.

Table 12. Degree-hours (DH/48hours) resulting from heat island control

	DH / 48 hours		
	Episode 1	Episode 2	Episode 3
Case11	-27.34	-24.84	-30.61
Case22	-36.39	-29.71	-42.14

Attachment 4. Summary of Training Materials

During the course of the project, LBNL and IIIT staff made several presentations at different sites in India. These presentations are listed below:

- "Urban Heat Islands and Mitigation Technologies" Indian Institute for Information Technologies, July 4, 2005; Hyderabad, India
- "Cool Roofs for Urban Heat Island Mitigation" FAPPCI Presentation, July 2, 2005; Hyderabad, India
- "Urban Heat Islands and Mitigation Technologies" Indian Institute of Technology, July 5, 2005; Mumbai, India
- "Urban Heat Islands and Mitigation Technologies" India Meteorological Department, January 12, 2006; New Delhi , India
- "Monitored Cool Roofs Energy Savings and Potentials in India" International Conference on Green Buildings, 13 & 14 October 2006, Hotel Grand Ashok, Bangalore
- "Heat Island Effects and Mitigation Techniques" International Conference on Green Buildings, 13 & 14 October 2006, Hotel Grand Ashok, Bangalore

Cool roofs session at the GBC-CII, Chennai conference: The outreach conference was intended to educate local manufacturers, architects, and building contractors and owners about the benefits of cool roofs. It was coordinated with the GBC-CII conference to take advantage of addressing a large group of participants. LBNL organized a 1.5 hours cool roofs special session at the conference in Chennai on 21 September 2007. The session consisted of talks by LBNL staff (Drs. Hashem Akbari and Jayant Sathaye), IIIT staff (Dr. Vishal Garg), and two industry experts.

The talks focused on

(1) Advances in cool roofs and cool colored roofs technologies,
(2) Cool roofing materials,
(3) Monitoring the energy and peak demand of two Satyam Computers Training Center buildings in Hyderabad, and
3) Programs and standards for cool roofing.

The purpose of the session was to inform conference participants of the urban heat island benefits of cool roofs, demonstrate their practical applications in India, including the choice of materials that are available in the US and in India, and to illustrate the benefits and costs of installing cool roofs on new and existing buildings.

Training Workshop on Cool Roofs: The purpose of the training workshop was to train as many as 20 counterpart institutions in the use of the monitoring instruments, the monitoring protocol, and the accompanying software. The half-day course focused on energy and environmental benefits of heat island mitigation technologies, and provided a guide for developing a successful implementation program. The LBNL-developed guidebook was used to provide the training.

With assistance from USAID's ECOIII program, LBNL organized a half-day training workshop on cool roofs in Delhi in September 2007. The course was conducted jointly with the building simulation course that was organized by the ECOIII project. The topics for this course included

- Advances in Cool Roofs and Cool Colored Roofs technologies

- Cool Roofing materials
- Building energy monitoring
- Monitoring the energy and peak demand of two buildings in Hyderabad
- Programs and Standards for Cool Roofing
- Cool surfaces and shade trees for heat island mitigation and outdoor air quality improvement in Hyderabad

In addition to the material on cool roofs that was presented at the conference session in Chennai, the training course focused on procedures and equipment used for measurement and monitoring of temperature, electricity use, heat fluxes, and weather, and on the modeling of urban meteorological conditions and air quality with a case study of Hyderabad.

Kiosk and brochure: LBNL and IIIT staff developed a brochure for distribution at the conference and the workshop. The brochure highlighted the benefits of cool roofs, provided information on the cool roofs, cool pavements, and vegetation planting programs, discussed the materials that are available for this purpose, and illustrated the electricity savings of cool roofs as demonstrated by the Hyderabad experiment.